REMARKS

Applicants would first like to thank Examiner Chen for the courtesy extended to attorney for Applicants, Dean L. Fanelli, during an October 23, 2007 telephone interview.

Claims 22, 24-32, and 33-34 are pending in this application for the Examiner's review and consideration upon entry of the amendments. Claims 22, 24 and 32 have been amended and new claims 33 and 34 have been added to more clearly recite the claimed invention. Support for the amendments can be found in the application as-filed. No new matter has been added by the amendments.

I. Interview Summary

Attorney for Applicants, Dean L. Fanelli, conducted an interview with the Examiner on October 23, 2007 to discuss the pending rejection. According to the Examiner, evidence supporting the biological activity of the claimed proteins is required to overcome the section 112, first paragraph, rejection.

II. The Rejections Under 35 U.S.C. § 112, First Paragraph

Claims 22 and 24-32 are rejected on pages 2-4 of the office action under 35 U.S.C. § 112, first paragraph, as allegedly failing to comply with the enablement requirement. According to the office action, the claim(s) contains subject matter, which was not described in the specification in such a way as to enable one skilled in the art to which it pertains, or with which it is most nearly connected, to make and/or use the invention.

Applicants have amended the claims to include MMP proteins and transforming growth factor-β ("TGF-β") type II. Applicants submit the following articles evidencing the biological activity of the claimed proteins:

(1) Siller-Lopez *et al., Treatment with Human Metalloproteinase-8 Gene Delivery Amerliorates Experimental Rat Liver Cirrhosis, Gastroenterology* (2004),126, 1122-1133 (attached as Exhibit A);

(2) Hernandez-Canaveral *et al., Amplified Expression of Dominant-Negative Transforming Growth Factor-Beta II Receptor Inhibits Collagen Type I Production Via Reduced SMAD-3 Activity, J. Gastroenterology and Hepatology* (2004), 19, 380-387 (attached as Exhibit B);

(3) Gonzalez-Cuevas *et al., Urokinase Plasminogen Activator Stimulates Function of Active Forms of Stromelysin and Gelatinases (MMP-2 and MMP-9) in Cirrhotic Tissue, J. Gastroenterology and Hepatology* (2006), unpublished proof (attached as Exhibit C);

(4) Miranda-Diaz *et al., Improved Effects of Viral Gene Delivery of Human uPA plus Biliodigestive Anastomosis Induce Recovery from Experimental Biliary Cirrhosis, Molecular Therapy* (2004), 9:1, 30-37 (attached as Exhibit D); and

(5) Garcia-Banuelos *et al., Cirrhotic Rat Livers With Extensive Fibrosis Can Be Safely Transduced with Clinical-Grade Adenoviral Vectors. Evidence of Cirrhosis Reversion, Gene Therapy* (2002) 9, 127-134 (attached as Exhibit E).

Applicants respectfully submit that the cited references adequately evidence the biological activity of the claimed proteins necessary to overcome the rejection under 35 U.S.C. § 112, first paragraph. Applicants respectfully that the rejection of claims 22 and 24-32 under 35 U.S.C. § 112, first paragraph, be reconsidered and withdrawn.

III. Conclusions

It is respectfully submitted that the rejections to the claims have been overcome. Should the Examiner disagree, Applicants respectfully request a telephonic or in-person interview with the undersigned attorney to discuss any remaining issues and to expedite the eventual allowance of the claims.

Except for issues payable under 37 C.F.R. § 1.18, the Commissioner is hereby authorized by this paper to charge any additional fees during the entire pendency of this application including fees due under 37 C.F.R. 1.16 and 1.17 which may be required, including any required extension of time fees, or credit any overpayment to Deposit Account 50-0310.

Respectfully submitted,
Morgan, Lewis & Bockius LLP

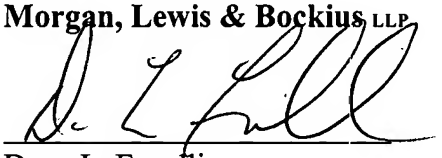

Dean L. Fanelli
Registration No. 48,907

Dated: October 31, 2007
Morgan, Lewis & Bockius LLP
Customer No. **09629**
1111 Pennsylvania Avenue, N.W.
Washington, D.C. 20004
202-739-3000

GASTROENTEROLOGY 2004;126:1122–1133

BASIC–LIVER, PANCREAS, AND BILIARY TRACT

Treatment With Human Metalloproteinase-8 Gene Delivery Ameliorates Experimental Rat Liver Cirrhosis

FERNANDO SILLER-LÓPEZ,* ANA SANDOVAL,* SILVIA SALGADO,* ADRIANA SALAZAR,* MIRIAM BUENO,* JESUS GARCIA,* JOSE VERA,* JAVIER GÁLVEZ,* IVÁN HERNÁNDEZ,* MARTHA RAMOS,* ESTUARDO AGUILAR-CORDOVA,† and JUAN ARMENDARIZ-BORUNDA*,§

*Institute for Molecular Biology in Medicine and Gene Therapy, Centro Universitario de Ciencias de la Salud, University of Guadalajara, Guadalajara, Mexico; †Advantagene, Inc., San Diego, California; and §Organismo Publico Descentralizado Hospital Civil Guadalajara, Guadalajara, Mexico

See editorial on page 1199.

Background & Aims: An extrahepatic human neutrophil collagenase complementary DNA (matrix metalloprotease-8) cloned in an adenovirus vector was used as a therapeutic agent in cirrhosis. *Methods:* A high titer of clinical-grade AdMMP8 was obtained. *Results:* HeLa cells transduced with AdMMP8 expressed recombinant matrix metalloprotease-8 messenger RNA and matrix metalloprotease-8 protein. Matrix metalloprotease-8 in culture sups showed enzymatic activity against native collagen type I, which was inhibited by ethylenediaminetetraacetic acid, 1,10-phenanthroline, and tissue inhibitor of metalloprotease-1. In vivo transduction showed matrix metalloprotease-8 activity, and studies to establish the efficacy of this characterized vector were performed in CCl_4 and bile duct–ligated cirrhotic rats. Transduction with 3×10^{11} viral particles per kilogram resulted in hepatic detection of both messenger RNA and protein matrix metalloprotease-8. A consistent response in fibrosis reversal was observed in CCl_4 rats. Liver fibrosis in bile duct–ligated cirrhotic animals was decreased in 45%, along with diminished hydroxyproline content, after AdMMP8 treatment. The expression of matrix metalloprotease-2 and matrix metalloprotease-3 was up-regulated in AdMMP8 rats. Free tissue inhibitor of metalloprotease-1, as an indirect measurement of active uncomplexed matrix metalloproteases, was also increased in the AdMMP8 groups. Transforming growth factor-β messenger RNA was diminished, and matrix metalloprotease-9 and hepatocyte growth factor increased. Treatment in both models correlated with improvements in ascites, functional hepatic tests, and gastric varices, indicating diminished intrahepatic blood pressure in animals injected with AdMMP8. *Conclusions:* Therefore, therapy with the matrix metalloprotease-8 gene is promising for use in a clinical setting.

Our research has been focused on the cellular and molecular mechanisms that govern the progression and potential reversion of fibrotic processes in both experimental and human cirrhosis. Liver cirrhosis is an irreversible end-stage disease and is the seventh leading cause of mortality worldwide. Generally, chronic consumption of alcohol is the main cause of cirrhosis, although chronic infection with viral hepatitis C is also a major cause.[1] Normally, the homeostatic hepatic cell/extracellular matrix (ECM) ratio is maintained in the liver by well-balanced synthesis and degradation of ECM components.[2] In cirrhotic liver, however, an altered balance takes place because of an excess in the synthesis and deposition of ECM proteins (fibrogenesis) and/or a reduction in the removal of this excess (fibrolysis), with the consequent onset of fibrotic scarring. The pathophysiology of ECM formation during hepatic fibrosis is multifaceted and complex. Fibrogenesis involves a change in the expression of ECM proteases (matrix metalloproteases; MMPs) or their inactivation by specific inhibitors (tissue inhibitors of metalloproteases; TIMPs)[3,4] and an increase in the synthesis of interstitial (types I and III) and basement membrane (type IV) collagens, fibronectin, and proteoglycans driven by signaling pathways mediated by proinflammatory cytokines such as transforming growth factor (TGF)-β, interleukin-1, and platelet-derived growth factor. These cytokines are produced mainly by activated Kupffer cells, which in turn activate

Abbreviations used in this paper: BDL, bile duct ligation; bp, base pair; ECM, extracellular matrix; ELISA, enzyme-linked immunosorbent assay; HGF, hepatocyte growth factor; HSC, hepatic stellate cell; MMP, matrix metalloprotease; PCR, polymerase chain reaction; PCNA, proliferating cell nuclear antigen; TGF, transforming growth factor; TIMP, tissue inhibitor of metalloprotease; VP, viral particle.

0016-5085/04/$30.00
doi:10.1053/j.gastro.2003.12.045

quiescent hepatic stellate cells (HSC), giving them a major role in scarring organ tissue.[2,5–7]

For this reason, conventional therapies seeking a cure for hepatic cirrhosis have mainly focused on preventing or reducing the biosynthesis of collagen and/or increasing the synthesis or activity of MMPs responsible for ECM degradation.[5,8] With the advent of gene therapy, novel approaches have been used to heal liver cirrhosis.[9,10] Our previous work with urokinase-plasminogen activator gene delivery has shown promise. Human urokinase-plasminogen activator treatment of cirrhotic rats resulted in reversion of liver fibrosis and in vigorous hepatic cell regeneration.[11]

This work focuses on restoration of normal liver architecture with consequent recovery of liver function of cirrhotic animals by adenoviral administration of a gene coding for MMP-8, a neutrophil collagenase whose preferential substrate is type I collagen.[12,13] The rationale for using MMP-8 consisted of promoting in situ degradation of ECM proteins, releasing hepatic growth factors, and freeing up space for hepatic cell proliferation. We constructed an adenovirus vector (AdMMP8) that has proven efficient transduction and induced MMP-8 production with properties of the naturally occurring protein, which degraded efficiently in vitro in collagen type I and was inhibited by ethylenediaminetetraacetic acid (EDTA), TIMP-1, and 1,10-phenanthroline. Furthermore, because we had shown that cirrhotic liver[11,14] transfection by adenovirus vectors was dose dependent and that dosing in the range of 10^{11} viral particles (VP) per kilogram was most effective in inducing a therapeutic effect, we decided to use a single application of 3×10^{11} VP per kilogram of AdMMP8 via the iliac vein in severely cirrhotic rats. This resulted in in situ production of the cognate protein effective against collagen type I and in amelioration of the cirrhotic process. We used 2 different experimental cirrhosis models to validate our proof of concept, and we provided mechanistic insights on the molecular action of MMP-8.

Materials and Methods

Recombinant Plasmid Adenoviral Construction

pAdHM2-MMP-8, an ΔE1 ΔE3 adenoviral plasmid vector expressing the proenzyme of human MMP-8 under the control of the cytomegalovirus promoter (pCMV) and with a simian virus 40 polyadenylation signal, was constructed by an in vitro ligation method according to the method described below.[15] The expression cassette coding for MMP-8 was excised with *NruI*/*ScaI* from plasmid pcDNA-MMP-8 and inserted into the *SmaI* site of the multiple cloning site of the shuttle plasmid pHM3, and the resulting plasmid, pHM3-MMP-8, was digested with I-*CeuI* and PI-*SceI*. The released fragment was ligated with the I-*CeuI*/PI-*SceI*–digested plasmid pAdHM2, which contains the ΔE1–ΔE3 adenovirus type 5 genome. The resulting ligation product was transformed into ultracompetent DH5a, and recombinant clones were isolated by ampicillin selection and screened by restriction analysis. Large-scale preparation of recombinant plasmid pAdHM2-MMP-8 was performed after positive identification.

Generation of Adenoviral Vector

AdMMP8, a replication-defective adenoviral vector, was obtained from pAdHM2-MMP8 by *PacI* digestion and transfected with lipofectamine into human kidney embryonic 293 cells seeded in a 6-well plate by following the manufacturer's instructions. Twenty-four hours later, cells were cultured in minimal essential medium/5% BCS or overlaid with 0.5% agarose/minimal essential medium/10% BCS. Ten days after transfection, plaques showing a cytopathic effect were isolated, and viruses were amplified by transduction of human kidney embryonic 293 cells seeded in a 100-mm dish. Recombinant viruses were harvested and plaque-purified twice and expanded in 293 cells for preparation of large-scale stocks. Polymerase chain reaction (PCR) was used for identification of AdMMP8 in every step of purification and for the final production. Vector production (including AdGFP as an irrelevant control vector) was performed under Good Laboratory Practice conditions by using standard methods as previously described.[16] Stocks were stored at −70°C and thawed immediately before use. Recombinant adenovirus was titered on 293 cells by end-point dilutions[16] and tested for replication deficiency by titration on nonpermissive HeLa cells.

Matrix Metalloprotease-8 Expression in HeLa Cells Infected With AdMMP8

Confluent HeLa cells obtained 24 hours after seeding in a 100-mm dish were incubated with AdMMP8 1×10^{10} VP per milliliter (2.7×10^9 IU/mL) in minimal essential medium/5% BCS, and medium was replaced with X-Vivo15 serum-free medium 24 hours later. Cellular lysate and supernatant serum-free medium were re-collected at 48 hours after transduction for successive analysis. Serum-free media supernatant was treated with 1 mmol/L phenylmethylsulfonyl fluoride, and 0.05% Brij35 and subsequently concentrated 5-fold on a Centricon-50. Protein content was determined by the Bradford method[17] and stored at −20°C until assay.

Gene Expression by Reverse-Transcription Polymerase Chain Reaction

A total of 2 μg of total RNA was incubated with 1 U of ribonuclease-free deoxyribonuclease I at 37°C for 30 minutes, and the reaction was terminated by the addition of 50 mmol/L EDTA and heating at 75°C for 10 minutes. Samples were incubated with 0.5 mg of oligo(dT)[18] primer at 70°C for 10 minutes and subjected to 100 U of Moloney murine leukemia virus reverse transcriptase (RT) for 50 minutes at

37°C; the same samples without RT were used as control. PCR amplification of the MMP-8 complementary DNA (cDNA) fragment corresponding to nucleotides 439–797 (358 base pairs [bp]) of the published human sequence (GenBank accession no. J05556) was performed as previously described[18] with Taq polymerase for 30 cycles (94°C for 1 minute, 56°C for 1 minute, and 72°C for 1 minute) by using sense primer complementary to base pairs 439–462 (5′-AGCTGTCAGAGGCTGAGGTAGAAA-3′) and antisense primer complementary to base pairs 774–797 (5′-CCTGAAAGCATAGTTGGGATACAT-3′). PCR for the constitutively expressed human housekeeping gene glyceraldehyde-3-phosphate dehydrogenase (GenBank accession no. X01677) was performed with Taq polymerase for 30 cycles (94°C for 1 minute, 69°C for 1 minute, and 72°C for 1 minute) by using sense primers complementary to base pairs 396–414 (5′-GCAGGGGGGAGCCAAAAGGG-3′) and antisense primer complementary to base pairs 942–961 (5′-TGCCAGCCCCAGCGTCAAAG-3′). The size of the expected product was 565 bp.[19]

Likewise, total RNA was extracted from livers of control and experimental animals to conduct RT-PCR for hypoxanthinephospho-ribosyltransferase and hepatocyte growth factor (HGF); collagen type I, III, and IV; TGF-β1; and MMP-9 to analyze hepatic regeneration and mechanisms induced by expression of MMP-8.

In Vitro and In Vivo Quantification of Matrix Metalloprotease-8 Secretion by Enzyme-Linked Immunosorbent Assay

Secretion of MMP-8 into the media supernatants and cell lysates from uninfected and infected cells was quantified by using a Biotrak enzyme-linked immunosorbent assay (ELISA) according to the manufacturer's instructions. Dilutions of the samples were effectuated to work within the standard range of the assay. For in vivo determination, liver extracts were obtained essentially as described previously[11] and assayed with the same human ELISA as described previously.

In Vitro and In Vivo Collagenase Activity Against Soluble Type I Collagen

Type I collagen proteolytic activity was analyzed as described elsewhere.[12,20] To activate the MMP-8 proenzyme, aliquots (10 μL) of the concentrated media supernatants were incubated for 4 hours at 25°C with 1 mmol/L APMA in a buffer containing 50 mmol/L Tris (pH 7.5), 0.2 mol/L NaCl, 10 mmol/L $CaCl_2$, 1 mmol/L $ZnCl_2$, 0.05% Brij35, and 100 mmol/L arginine. Pretreated samples were then incubated for 16 hours at 27°C with 10 μg of soluble calf skin type I collagen in the absence or presence of the MMP inhibitors 1,10-phenanthroline (2 mmol/L), EDTA (20 mmol/L), or TIMP-1 (200 nmol/L) in a final volume of 50 mL. For in vivo analysis, MMP-8 proteolytic activity was assessed in liver homogenates. Proteins were extracted with 6 mol/L of guanidine HCl for 3 days. Proteins were then dialyzed against phosphate-buffered saline for 2 hours, and sodium dodecyl sulfate was added to a final 1%. Protein concentrations were determined by the Bradford method.[17] A total of 500 μg of total protein was incubated for 4 hours at 25°C with same buffer as described previously and was then incubated for 16 hours under the same conditions.

The reaction products were analyzed on an 8% sodium dodecyl sulfate-polyacrylamide gel. The gel was stained with Coomassie Brilliant Blue R-250 and destained with 30% methanol and 10% acetic acid.

Animal Models of Cirrhosis

Basically, the regimen for CCl_4 intoxication was performed during 8 weeks, as described previously,[11] and all animal studies were performed on male Wistar rats in accordance with University of Guadalajara's animal experimentation guidelines. This experimental animal model closely resembles human alcohol-induced cirrhosis. Rats weighing 150–200 g were anesthetized with ethyl ether, and the common bile duct was exposed and ligated to induce fibrosis by total biliary obstruction (bile duct ligation; BDL) according to the method of Lee et al.[21] After surgery, rats were kept for 4 weeks and were given free access to food and water throughout the experiment. Five rats were sham-operated at the same time and used as controls. For the experiments aimed to show proof of concept on fibrosis reversion, at least 5 rats were used for each experiment. That is, 10 rats were ligated as described previously for 4 weeks, and a liver biopsy sample was obtained from each animal before and after the surgical procedure. Then, a biliodigestive anastomosis was established in each animal to re-establish bile flow to eliminate the injurious fibrogenic cause. Animals were left at this stage for 7 days, and a liver biopsy sample was also taken. At this point, 5 animals received 3×10^{11} VP per kilogram of either AdMMP8 or AdGFP and 10 days later were killed. The fourth and final liver biopsy sample was obtained for each animal. The fibrosis index in multiple liver biopsy samples from animals at different stages was then determined.

Quantitative Analyses of Fibrotic Index and Immunohistochemistry

Essentially, fibrotic index and immunohistochemistry were analyzed according to our previous reports, in which multiple 5-mm-thick liver sections from AdMMP8, AdGFP, and saline-treated rats were stained with Masson's dye and in which morphometric image analyses (20 different microscopic fields in each tissue section) were performed by a computer-assisted Image program (Qwin Leica).[11,22,23] Histological findings, cell necrosis, and hepatic rearrangement after treatment were confirmed independently by 2 pathologists blinded to the study.

Hepatic cell proliferation was determined with standard techniques by using a monoclonal anti–proliferating cell nuclear antigen (PCNA) antibody (Boehringer Mannheim, Mannheim, Germany) at a 1:20 dilution in phosphate-buffered saline and by registering the number of positive cells as described previously by using a computerized image program

and checking 20 random microscopic fields for each tissue section.

Biochemical Determinations of Hydroxyproline Content

Liver samples were obtained at the moment of death, and 150 mg was subjected to acid hydrolysis to determine the amount of hydroxyproline according to Rojkind and Gonzalez.[24]

Western Blot Analysis

The presence of MMP-2, MMP-3, and TIMP-1 in liver homogenates from treated rats was shown by Western blot analysis, as described previously.[25] Approximately 100 mg of control and experimental liver tissue was homogenized in lysis buffer (10 mmol/L HEPES [pH 7.9], 0.42 mol/L NaCl, 1.5 mmol/L of $MgCl_2$, 0.5 mmol/L dithiothreitol, 0.5% Nonidet P-40, and 25% glycerol) with a protease inhibitor cocktail from Roche (Summerville, NJ) at 4°C, followed by centrifugation for 30 minutes at 13,000 rpm. Supernatant was collected, and protein concentration was determined by the Bradford assay.[17] A total of 20 μg of protein for MMP-2 and MMP-3 and 300 μg for TIMP-1 was separated by electrophoresis on 10% acrylamide/sodium dodecyl sulfate gels and transferred to polyvinylidene difluoride membranes. Blots were blocked in 5% nonfat dry milk in Tris-buffered saline for 1.5 hours; incubated for 1.5 hours in primary antibody diluted 1:1000 for MMP-2, 1:5000 for MMP-3, and 1:500 for TIMP (polyclonal antibodies; Santa Cruz Biochemicals, Santa Cruz, CA) in 0.5% blocking buffer; and then incubated for 1 hour with horseradish peroxidase–conjugated polyclonal secondary antibody (from Sigma [St. Louis, MO] for the MMPs and from Roche for TIMP-1) diluted 1:5000 for MMP-2 and MMP-3 and 1:3000 for TIMP-1. Proteins were detected with enhanced chemiluminescence detection reagents.

Statistical Analysis

Results are expressed as mean ± SD. The Student *t* test was used. $P < 0.05$ was considered to indicate a significant difference between groups.

Results

The construction strategy for AdMMP8 cDNA consisted of cloning the MMP-8 expression cassette into the pHM3 shuttle plasmid, and the recombinant adenoviral plasmid pAdHM2-MMP-8 was generated by digestion of pHM3-MMP-8 and pAdHM2 with endonucleases I-*Ceu*I and PI-*Sce*I, as described by Mizuguchi and Kay.[15] The recombinant adenoviral vector AdMMP8 was generated after transfection of pAdHM2-MMP-8 into subconfluent 293 cells, and plaques from the first and second round of amplification and from the final characterized production were identified by the appearance of cytopathic effects and by PCR for the MMP-8 gene (data not shown).

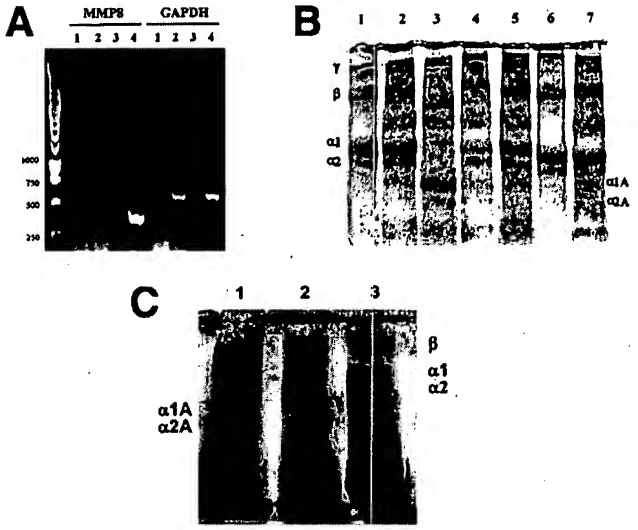

Figure 1. (*A*) PCR products of MMP-8 and glyceraldehyde-3-phosphate dehydrogenase (GAPDH) of total RNA extracted from control (*lanes 1* and *2*) and AdMMP8-transduced (*lanes 3* and *4*) HeLa cells, treated without (*lanes 1* and *3*) or with (*lanes 2* and *4*) Moloney murine leukemia virus reverse transcriptase. PCR was performed with specific primers for human MMP-8 and GAPDH. A DNA molecular 1-kilobase DNA ladder (Promega, Madison, WI) was used as a size marker. (*B*) Collagenolytic activity of culture supernatants from control and AdMMP8-transduced HeLa cells. Soluble native type I collagen was incubated alone (*lane 1*) or with media supernatant from AdMMP8-transduced HeLa cells pretreated without (*lane 2*) or with (*lanes 3–7*) 1 mmol/L APMA. Collagen was incubated in the presence of EDTA 20 mmol/L (*lane 4*), 1,10-phenanthroline 2 mmol/L (*lane 5*), and TIMP-1 50 nmol/L (*lane 6*) or 200 nmol/L (*lane 7*). (*C*) MMP-8 enzymatic activity in cirrhotic liver homogenates transduced with AdMMP8 3×10^{11} viral particles per kilogram (*lane 1*), administered with AdGFP (*lane 2*) and collagen type I (*lane 3*). Collagen dimers and monomers are depicted as α and β, α1A, and α2A and are the characteristic 3/4 and 1/4 products of the degradation of collagen chains α1 and α2, respectively.

Matrix Metalloprotease-8 Messenger RNA Expression in AdMMP8-Transduced HeLa Cells

HeLa cells were transduced with 1×10^{10} VP per milliliter AdMMP8, and 48 hours later cells were harvested for the analysis of MMP-8 messenger RNA (mRNA) expression by RT-PCR analysis by using a set of oligonucleotides specific for human neutrophil collagenase (Figure 1*A*). MMP-8 PCR product was absent in control cells, but mRNA for MMP-8 was constantly detected after AdMMP8 transduction. Expression of the housekeeping gene glyceraldehyde-3-phosphate dehydrogenase in nontransduced and transduced HeLa cells was constant and not affected by treatment (Table 1).

Expression of Matrix Metalloprotease-8 Protein in AdMMP8-Transduced HeLa Cells

The levels of MMP-8 protein expression and secretion in control and AdMMP8-transduced HeLa cells

Table 1. Primer Sequences and PCR Conditions for Genes Analyzed in Tissue Samples

Gene	Primer sense	Primer antisense	Product (*base pairs*)	Annealing (°C)	Cycles (n)
HPRT	5′-TCC CAG CGT CGT T TAG TG-3′	5′-GGC TTT TCC ACT TTC GCT GA-3′	618	60	30
HGF	5′-GCC ATG AAT TTG ACC TCT ATG AA-3′	5′-TTT AAT TGC ACA ATA CTC CCA AG-3′	518	60	30
COL I	5′-CAA GAA TGG CGA CCG TGG TGA-3′	5′-CTA CCG ACG TGC TCA GTG TGG-3′	1074	62	32
COL III	5′-AGA TGG ATC AAG TGG ACA-3′	5′-CAT GTT TCT CCG GTT TCC AT-3′	449	50	30
TGF-β	5′-GCC TCC GCA TCC CAC CTT TG-3′	5′-GCG GGT GAC TCT TTT GGC GT-3′	396	60	30
MMP-9	5′-TTG AGT CCG GCA GAC AAT CC-3′	5′-CCT TAT CCA CGC GAA TGA CG-3′	279	60	29

COL, collagen; HPRT, hypoxanthinephospho-ribosyltransferase.

were quantified by ELISA (Table 2) by using a polyclonal antibody against human neutrophil MMP-8 that does not cross-react with MMP-1, -2, -3, -7, -9, or -13 or MT1-MMP. Pro-MMP-8 and active MMP-8 (both free and TIMP complexed) can be detected by this ELISA system. There was a 1300-fold increase in the secretion of MMP-8 to the extracellular media after the infection of HeLa cells by AdMMP8 as compared with uninfected cells. Conversely, a 23-fold increase of intracellular MMP-8 was induced by adenoviral transduction.

Levels of MMP-8 in the filtrate (i.e., proteins <50 kilodaltons) after Centricon concentration of culture supernatants were negligible, and collagenolytic activity was not detected in this fraction (data not shown), which denotes the presence of MMP-8 in culture supernatants in the form of either latent (85 kilodaltons) or active (64–67 kilodaltons) form.

Collagenolytic Matrix Metalloprotease-8 Activity of Media Supernatant in AdMMP8-Transduced HeLa Cells

HeLa cells were transduced with AdMMP8 1×10^{10} VP per milliliter for 48 hours and 24-hour serum-free media supernatant was harvested for analysis of proteolytic activity against collagen type I.

AdMMP8 codes for the gene of latent MMP-8, which after expression requires the proteolytic (e.g., serine proteases or trypsin) or chemical (e.g., APMA or $HgCl_2$) removal of the pro-domain to become functionally active.

Table 2. MMP-8 Expression in Control and AdMMP8-Transduced HeLa Cells

	Levels of MMP8 (ng MMP-8/mg protein)		
Variable	Supernatant (S)	Cellular lysate (CL)	CL/S
Control	0.07 ± 0.04	13.7 ± 2.3	196
AdMMP8	97.0 ± 8.1	317.2 ± 14.9	3.3

NOTE. MMP-8 protein of culture supernatant and cell lysate of HeLa cells were measured by ELISA. Data represent the mean ± SEM of 4 replicates.

Nonetheless, it can be spontaneously activated in vivo by mechanisms not yet elucidated.[26]

Culture media from nontransduced HeLa cells showed the same pattern of protein fragments as those from AdMMP8-transduced HeLa cells without the organomercurial APMA preincubation (Figure 1*B*; lanes 1 and 2). APMA-preactivated supernatant efficiently degraded soluble native type I collagen into the characteristic α1A (3/4) and α2A (1/4) cleavage products (lane 3). The known chemical inhibitors EDTA (lane 4) and 1,10-phenanthroline (2 mmol/L; lane 5) strongly inhibited MMP-8 activity. The physiological inhibitor TIMP-1 showed a progressive decrease in the degradation of the substrate at increasing concentrations of TIMP-1: 50 nmol/L (lane 6) or 200 nmol/L (lane 7). Collagenolytic MMP-8 activity in the hepatic tissue of cirrhotic animals transduced with AdMMP8 is shown in Figure 1*C*.

Homogenates from hepatic tissue were analyzed for proteolytic activity against native collagen type I. Even though a pro–MMP-8–coding cDNA was administered, internal mechanisms not yet elucidated seem to be acting to convert it into active MMP-8. Figure 1*C* clearly shows how collagen I is degraded when it is incubated with samples from liver homogenates transduced with AdMMP8; this is not observed with the GFP-treated animals.

AdMMP8-Directed Matrix Metalloprotease-8 Gene Expression in Cirrhotic Rat Livers

Hepatic cirrhosis is characterized by an altered balance between synthesis and breakdown of ECM proteins, mostly collagen type I. To push the ECM degradation and free up space for hepatocyte cell expansion, we pursued the AdMMP8-driven degradation of exacerbated collagen deposited in animals with cirrhosis induced for 8 weeks with CCl_4.

We tested several doses and found that a single intravenous injection of 3×10^{11} VP per kilogram of AdMMP8 into 8-week-old CCl_4 cirrhotic animals pro-

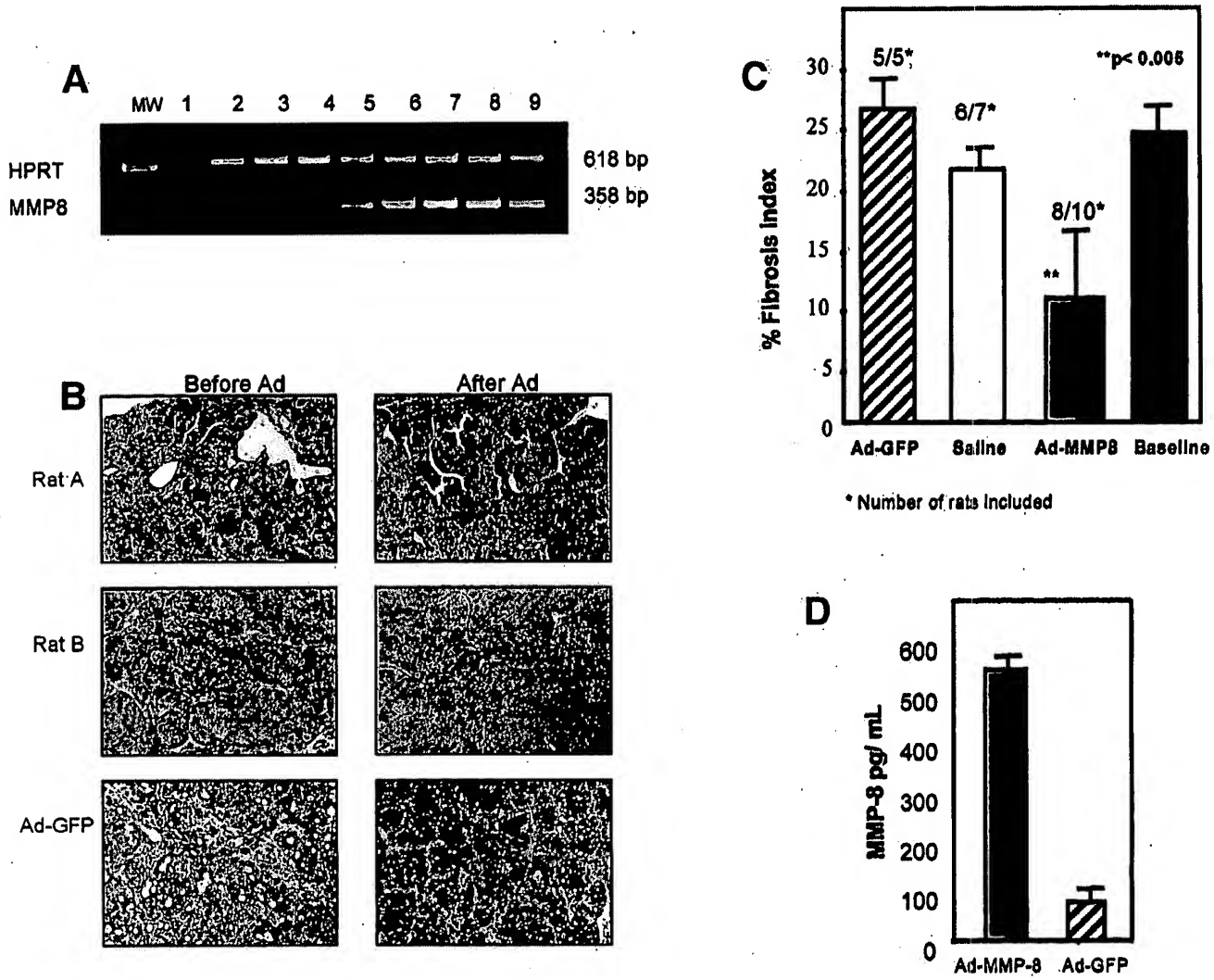

Figure 2. (*A*) PCR products of MMP-8 and hypoxanthinephospho-ribosyltransferase (HPRT) of total RNA extracted from livers of cirrhotic rats treated with AdGFP (*lanes 2–4*) or AdMMP8 (*lanes 5–9*) in the presence of Moloney murine leukemia virus reverse transcriptase. *Lane 1* shows a sample from AdMMP8-treated liver in the absence of Moloney murine leukemia virus reverse transcriptase in a complementary DNA reaction. PCR was performed with specific primers for human MMP-8 and HPRT. A DNA molecular 100-bp DNA ladder (Invitrogen, Carlsbad, CA) was used as a size marker. (*B*) Representative liver sections of cirrhotic rats after 8 weeks of CCl_4 administration and AdMMP8 (rats A and B) or AdGFP adenoviral vector injection. MEC was observed with Masson trichrome staining (50×). The change in the amount of extracellular matrix material is evident before and after 14 days of AdMMP8 treatment as compared with AdGFP-treated animals. (*C*) Quantitative measurement of fibrosis reversion. Twenty microscopic fields per liver biopsy sample from all animals were counted and analyzed with computerized Image program (Qwin Leica) to measure fibrosis. Statistical analysis was performed with 8 responding AdMMP8-treated animals (8 of 10). Significance was achieved in the MMP-8 group ($P < 0.005$) compared with nonresponding animals treated with AdGFP and saline. (*D*) Determination of matrix metalloproteinase-8 activity by a specific ELISA in liver homogenates of cirrhotic rats treated as indicated. Values indicate the mean of 3 determinations.

voked a substantial, albeit transient, expression of MMP-8 mRNA transcripts, which could be detected by RT-PCR. Hepatic levels of the AdMMP8-directed MMP-8 mRNA transcripts were measured at 7 days of transduction and varied between individual subjects (n = 10), but the same pattern of expression was observed repeatedly in various experiments (Figure 2*A*). Control cirrhotic animals injected with AdGFP did not express MMP-8 mRNA transcripts.

Reversion of CCl_4-Induced Cirrhosis by a Single AdMMP8 Injection via the Iliac Vein

Computer-assisted analyses showed that 8 of 10 AdMMP8-treated rats had a variable, yet remarkable, degree (30%–60%) of hepatic fibrosis resolution by day 14 after adenovirus vector administration (Figure 2*B* and *C*). It is worth mentioning that each animal was its own control. A liver biopsy sample was taken by laparotomy

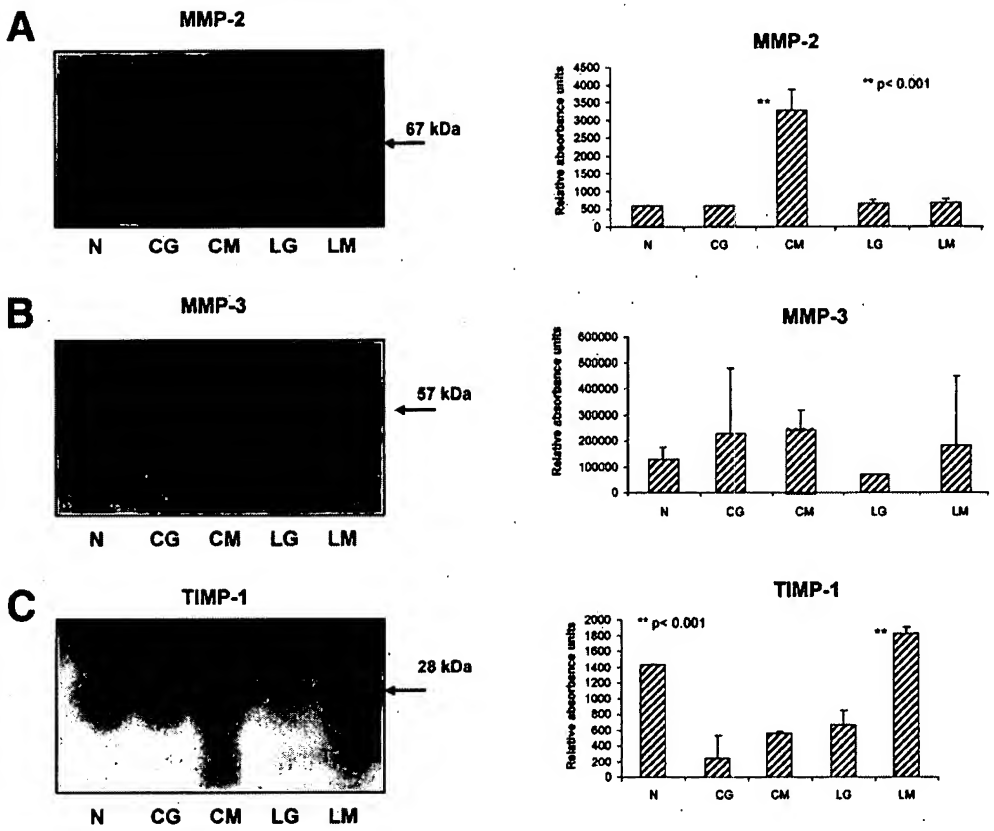

Figure 3. MMP and TIMP-1 Western blot analysis. Liver homogenates from control and experimental animals were analyzed for MMP-2, MMP-3, and free TIMP-1. Representative samples are shown. (*A*) MMP-2 shows a statistical increase ($P < 0.001$) in the CCl_4/MMP-8 group. (*B*) MMP-3 defined a marked augmenting tendency in the treated groups; however, no statistical significance was achieved in any group. (*C*) Free TIMP-1 increased in groups injected with AdMMP8 for both models of experimental cirrhosis. Statistical significance was present only for the BDL-MMP-8 group ($P < 0.001$). CM, CCl_4 group administered AdMMP8; CG, CCl_4 group with AdGFP; LM, BDL group treated with AdMMP8; LG, BDL group injected with AdGFP; N, normal rat.

at the moment of adenovirus infusion, and bleeding was stopped with Gel-Foam application. A second comparative biopsy sample from the same rat liver was obtained at the end of treatment, when all animals were killed. Quantitative data shown in Figure 2*C* show that animals injected with AdGFP (5 of 5) did not show a reduction in either liver fibrosis or cell necrosis. A characteristic chronic inflammatory stage was also present. Control cirrhotic animals given saline showed only a minor decrease in fibrosis, confirming our data on the specificity of collagenase activity on hepatic ECM degradation. Quantitative data gathered from animals that responded to treatment showed that results were statistically significant ($P < 0.005$). Furthermore, levels of MMP-8 protein expression were determined by ELISA and are shown in Figure 2*D*. Liver extracts from AdMMP8-transduced cirrhotic animals showed a mean value of approximately 550 pg/mL, whereas liver extracts from cirrhotic rats injected with the irrelevant adenovirus vector AdGFP contained negligible activity.

Degradation of fibrotic tissue could also be taking place via activation of latent tissue gelatinases (Figure 3). We measured the expression of MMP-2, MMP-3, and TIMP-1 in liver homogenates from rats made cirrhotic with chronic CCl_4 intoxication and BDL for 4 weeks after AdMMP8 iliac vein administration. MMP-2 specifically degrades collagen type IV, and other collagens to a lesser degree.[27,28] MMP-2 (Figure 3*A*) was clearly increased in both CCl_4-induced and BDL-induced experimental cirrhosis animals treated with AdMMP8. Nonetheless, only in the CCl_4 model was statistical significance achieved ($P < 0.001$). Although there was a small up-regulation in MMP-3 in AdMMP8-treated animals (Figure 3*B*), there was no statistical significance in any group. TIMP-1, which is known to impede MMP's activity, was augmented in its free form (28 kilodaltons) in liver extracts from rats of the experimental cirrhosis group and the AdMMP8-treated group, but not in the AdGFP group, displaying statistical significance in the BDL model ($P < 0.001$; Figure 3*C*).

We also provide mechanistic insights on gene expression for collagen I, III, and IV; TGF-β; and MMP-9. Liver samples from AdMMP8-treated BDL cirrhotic rats had collagen type I, III, and IV slightly decreased, but with no statistical significance. TGF-β was diminished, as opposed to MMP-9, which was increased. This is consistent with protein data obtained in the Western blot analysis (Figure 4).

Decreased fibrosis correlated with improvements in ascites and functional hepatic tests. Severe (>7% of body weight) accumulation of peritoneal fluid, an important clinical manifestation of advanced hepatic cirrhosis, was

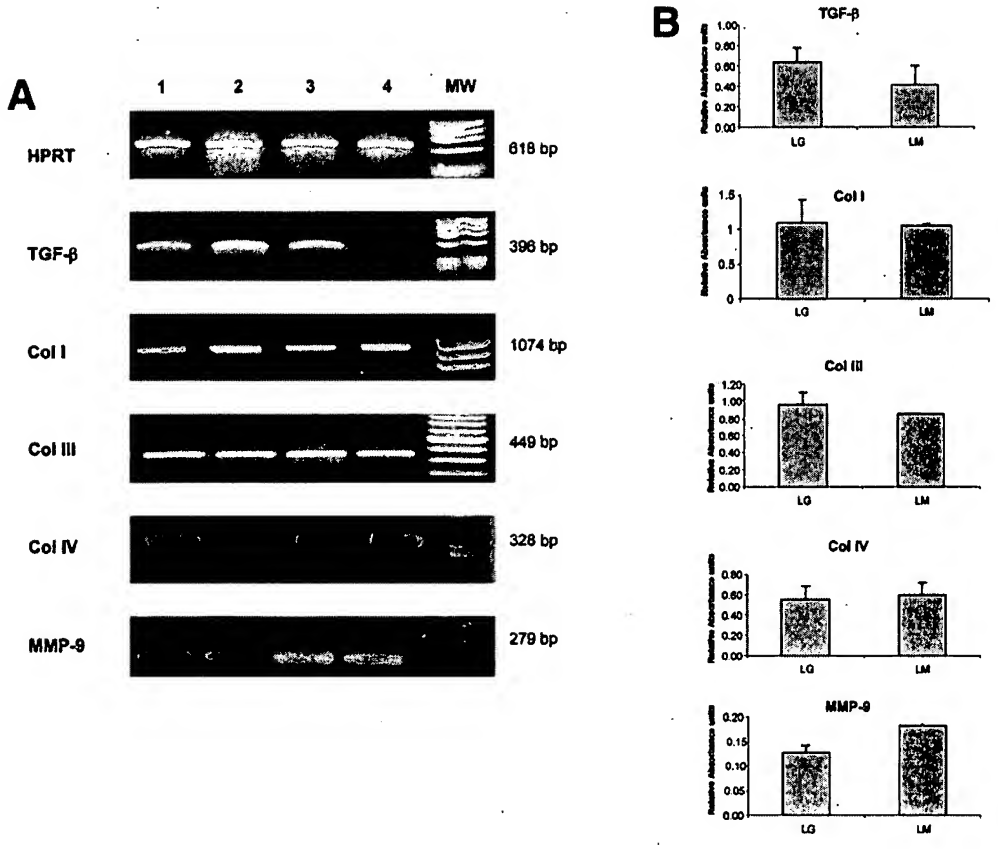

Figure 4. (*A*) Representative RT-PCR products of hypoxanthinephospho-ribosyltransferase and genes involved in ECM turnover from livers of LDB cirrhotic rats treated with AdGFP (LG; *lanes 1* and *2*) or AdMMP8 (LM; *lanes 3* and *4*). A 100-base pair (bp) DNA ladder or ϕX174 was used as a size marker (MW). (*B*) Densitometric data obtained from 3 different experiments are shown as mean ± SD. MMP-9 and TGF-β1 expression were inversely expressed after AdMMP8 treatment. HPRT, hypoxanthinephospho-ribosyltransferase; Col, collagen.

detected in all animals treated with AdGFP (5/5). Two cirrhotic animals out of 10 injected with AdMMP8 showed moderate ascites (<7% of body weight), whereas 6 had only trace amounts at the end of 14 days after AdMMP8. An important rearrangement of the hepatic parenchyma and hyperchromatic nuclei was also noted, reflecting a brisk liver cell regeneration that was confirmed with gene expression for HGF by RT-PCR analysis. Figure 5*A* shows that HGF gene expression was up-regulated in the cirrhotic rats treated with AdMMP8, but not in AdGFP-treated cirrhotic animals. These data correlate well with the immunohistochemical findings shown in Figure 5*B* with anti-PCNA antibody staining. Liver sections from AdGFP-treated animals did not show significant liver cell regeneration.

Reduction of hepatic fibrosis resulted in morphological improvement, as can be seen in Figure 5*C*, where a smooth hepatic texture in normal and AdMMP8-treated rat livers is conspicuous, as compared with the rough and granular liver surface from AdGFP-injected animals. Furthermore, these findings were accompanied by a clear improvement in collateral circulation and gastric varices (Figure 5*D*), suggesting diminished intrahepatic blood pressure in animals injected with AdMMP8.

We wanted to test our proof of concept in a different cirrhosis model that resembles human secondary biliary fibrosis. Thus, rats undergoing complete bile duct occlusion present progressive and aggressive fibrosis in the virtual absence of inflammation and necrosis. Ten rats were subjected to ligation and sectioning of the common bile duct, and liver biopsy samples were obtained from each rat before BDL ligation and at every step after ligation. At the end of BDL (4 weeks), all rats had a dramatic increase in liver fibrosis as compared with baseline fibrosis (Figure 6) and were subjected to a biliodigestive anastomosis to drain the clogged bile and eliminate the fibrogenic stimulus. Rats were left at this stage for 7 days. The hepatic fibrosis index, however, remained increased to a similar extent in all animals. Five rats were then injected via the iliac vein with 3×10^{11} VP per kilogram of AdMMP8, and 5 rats were injected with 3×10^{11} VP per kilogram of irrelevant adenoviral vector (AdGFP) as control. The 10 rats were kept under careful surveillance for 10 more days while they were monitored for overall health status, and they were then killed. A statistically significant decrease in fibrosis (45%; $P < 0.05$) was noted in rats injected with AdMMP8, but no decrease in the fibrosis index was observed in the 5 animals injected with AdGFP. The biochemical determinations of hydroxyproline correlated with the diminished fibrosis as measured by image morphometric analysis (Figure 6*B* and *C*).

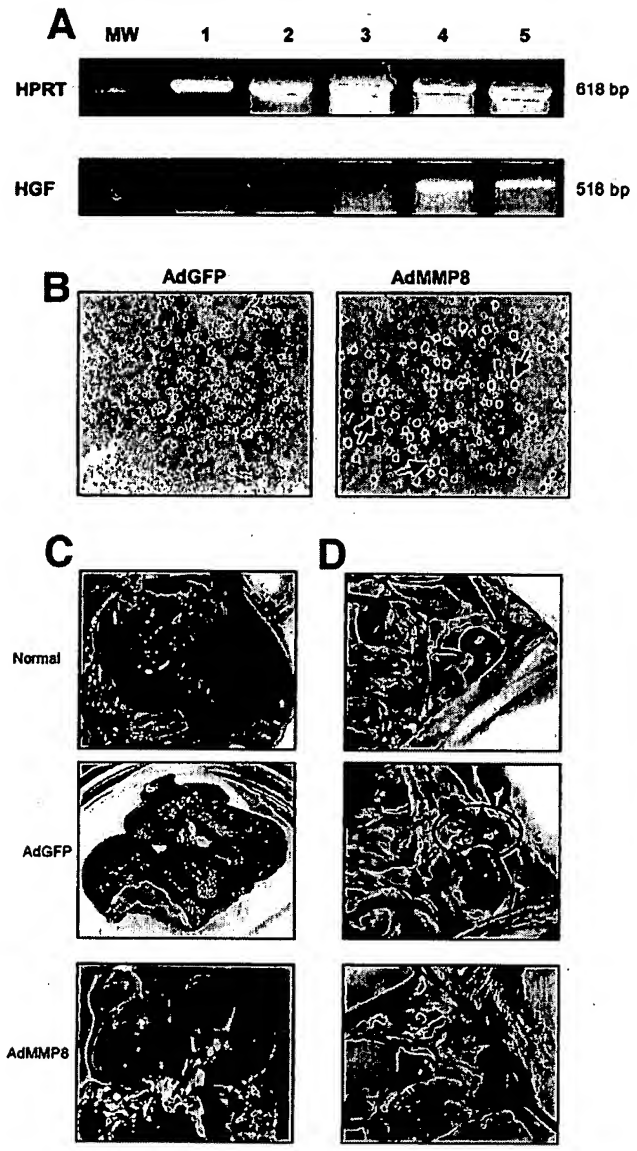

Figure 5. (*A*) RT-PCR from liver tissue for hypoxanthinephospho-ribosyltransferase (HPRT) and HGF. Representative samples from control and experimental groups were loaded in agarose gel. *Lane 1*: molecular marker ϕX174. *Lanes 2–4*: BDL rats with AdGFP. *Lanes 5* and *6*: BDL rats treated with AdMMP8. (*B*) Immunohistochemistry on liver slides from control and treated rats with anti-PCNA antibody was performed to determine hepatocyte proliferation. Hepatocytes with nuclear PCNA immunostaining after AdMMP8 treatment were more abundant as compared with livers from AdGFP-administered cirrhotic rats. (*C*) Macroscopic view of normal and AdGFP- and AdMMP8-treated cirrhotic rat livers 14 days after adenovirus administration. A smooth hepatic texture in normal and AdMMP8-treated rat livers is clearly seen, as compared with a rough and granular liver surface from AdGFP-injected animals. (*D*) A notable improvement in collateral circulation and gastric varices is present (*circle*).

Discussion

A recent growing body of evidence suggests that gene therapy with adenovectors as gene carriers may be used efficiently and safely in rats, even in the presence of severe liver disease.[11,29,30] The toxicity of adenovirus vectors injected into cirrhotic rats is an issue we have addressed before. We have previously reported that doses in the order of 10^{12} VP per kilogram are highly toxic for cirrhotic rats, but cirrhotic rats could tolerate doses in the range of 10^{11} VP per kilogram.[14] Thus, a dose of 3×10^{11} VP per kilogram was selected to conduct these experiments. Obviously, we do not intend to use this shuttle vector to carry genes in human cirrhotic livers in light of all the findings and reports, specifically the Jesse Gelsinger affair. However, we think we have proven our point: that is, we have established our proof of concept in 2 experimental models resembling human cirrhosis.

For clinical scenario application, it must be considered that most of the human population has been exposed to wild-type adenovirus (especially the Ad2 and Ad5 serotypes used for gene therapy vectors). In patients, the magnitude of the immune response is determined by preexisting antibody titers and is modified by the route of administration, but it is not dose-response dependent.[31] A preexisting immune response is expected to diminish adenovector transduction and to produce an increased immune response that must be considered. It is obvious, then, that a more suitable and safe vector must be designed and developed for use in this particular human disease.

Even so, we have shown that a single dose of a first-generation recombinant adenoviral vector carrying a gene for a collagen-degrading enzyme (MMP-8) reversed extensive liver fibrosis, stimulated liver cell proliferation, and resulted in stabilized functional hepatic tests and the disappearance of abnormal gastric circulation and ascites. In this article, we have confirmed and extended previous observations, including ours,[11,29,30] in the sense that systemic administration of adenoviral vectors preferentially targets livers, even functionally damaged livers, and that doses in the order of 10^{11} VP per kilogram are well tolerated by cirrhotic rats.[14] Thus, we have shown that enough healthy tissue is available for vector transduction that sufficed to induce a repairing response. In this study, we observed that regardless of the onset of a chronic liver disease in cirrhotic animals at the moment of "therapeutic" vector administration, MMP-8 transgene expression was effective and significant. These results, along with increasing compelling evidence,[11,29,30] imply that transient or regulated expression of a gene therapy targeted to the hepatic gland may be useful as a therapeutic strategy even in the presence of severe, lingering hepatic disease.

The discovery of processes that regulate the extent of fibrogenesis and the mechanisms governing ECM degra-

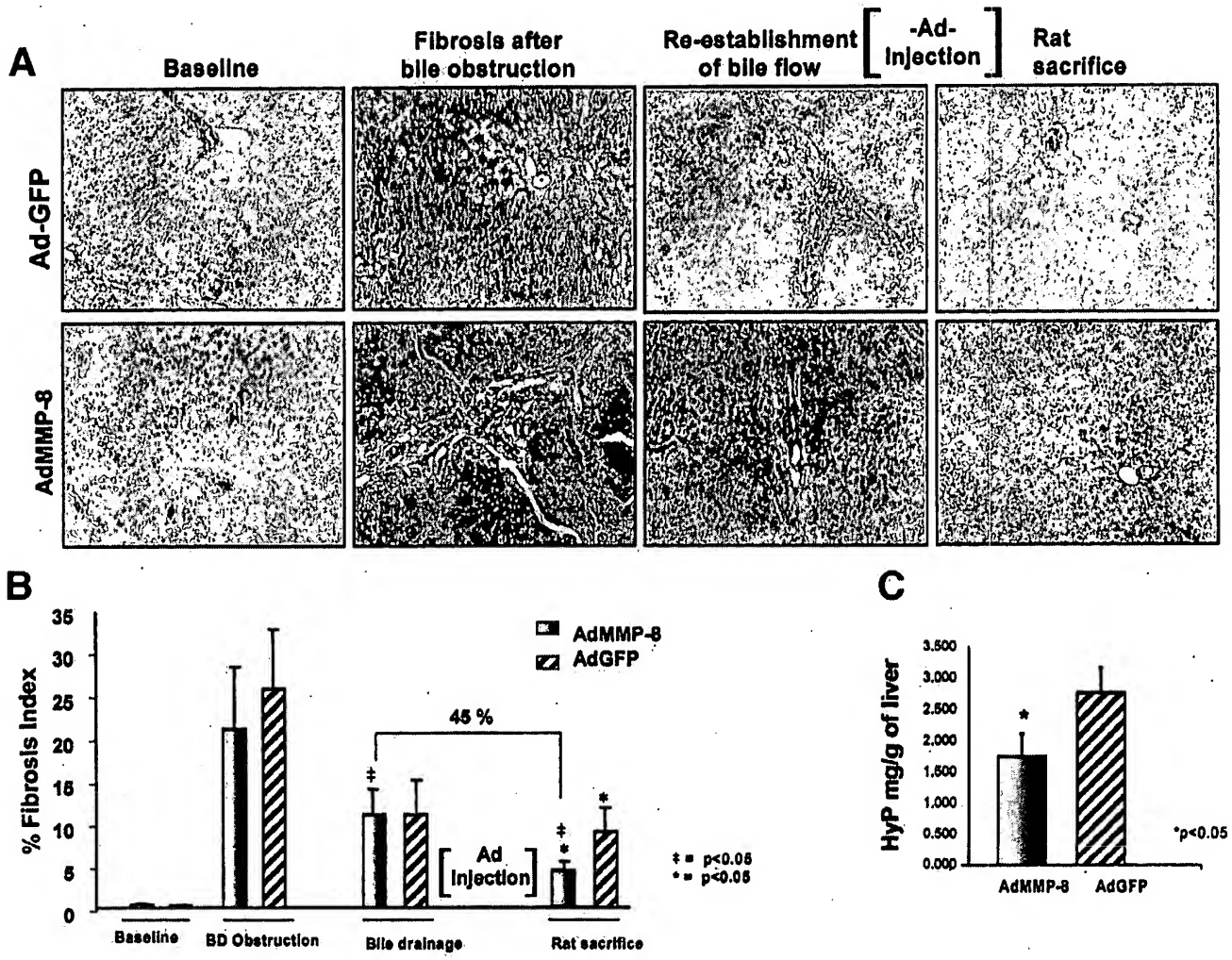

Figure 6. Induction of fibrosis reversion by 3×10^{11} viral AdMMP8 particles per kilogram in rat cirrhosis after prolonged bile obstruction. (*A*) Liver sections of cirrhotic rats after bile duct ligation, bile drainage by biliodigestive anastomosis, and AdMMP8 or AdGFP adenoviral vector injection. Masson trichrome staining (100×) shows cirrhotic nodules surrounded by thick fibrotic bands (*blue*) even at the end of treatment with AdGFP. However, animals treated with AdMMP8 showed only thin fibrous bands consisting of connective tissue proteins. (*B*) Percentages of fibrous tissue deposition at every step and after AdGFP or AdMMP8 adenoviral vector infusion. Determinations of fibrous tissue were performed in 20 random fields by an automated image analyzer. Values are presented as mean ± SD. (*C*) Biochemical determination of hydroxyproline (HyP) in liver tissue at the end of treatment ($P < 0.05$). Ad, adenovirus; BD, bile duct.

dation have been slow to emerge. Impairment of an organ's ability to repair itself after a trauma or a sustained injury will determine the onset of a fibrogenic response, invariably leading to abated functioning.[32]

Several mechanisms control ECM synthesis and ECM degradation. Degradation of ECM proteins is mainly mediated by MMPs, which represent a proteinase family that requires zinc ions for activity. MMPs are synthesized on demand and secreted, in most cases, as nonactive proenzymes that are in turn activated by various proteases, such as plasmin[11,33,34] and stromelysin.[35] In this article, we found by Western blot analysis an increase in the production of MMP-2, MMP-3, and free TIMP-1 in liver extracts from cirrhotic rats treated with AdMMP8. Free TIMP-1 was determined as an indirect measurement of active uncomplexed MMPs. Mechanisms other than proteolysis can render MMPs activation; it has been shown that stoichiometric activation of human skin fibroblast procollagenase can be performed by factors present in human skin and rat uterus.[36] In this study, we achieved high AdMMP8-driven MMP-8 collagenase production. Such an enzyme had a biochemical performance as the naturally occurring protein and induced a decrease in liver fibrosis in 2 different experimental cirrhosis models. The higher concentration of MMP-8 inside the cell as compared with the extracellular culture media might indicate that MMP-8 could be stored in specific granules within the transduced cells, similarly to the

naturally occurring storage of MMP-8 in neutrophil leukocytes. Furthermore, consistent with previous findings with COS cells transfected with an MMP-8 plasmid, there was also a significant and constitutive secretion of MMP-8 into the culture supernatant.[13] The level of glycosylation of MMP-8 has been associated with the intracellular storage or release of the enzyme to the extracellular compartment. In neutrophils, MMP-8 is highly glycosylated and remains stored in intracellular granules, whereas poorly glycosylated recombinant MMP-8 from plasmid-transfected COS cells is released to the culture supernatant.[13,37] The specific intracellular localization of MMP-8 in HeLa-transduced cells and the degree of glycosylation of the recombinant protein that is produced remains to be elucidated.

Furthermore, our data suggest that MMP-8 is efficiently converted to a functional collagenase in vivo, regardless of the unelucidated mechanism. This is evident from the collagenolytic activity assay, in which type I collagen is degraded in the absence of APMA (Figure 1*C*).

Administration of the MMP-8 cognate gene in cirrhotic animals induced amelioration of hepatic cirrhosis. Remodeling of ECM excessively deposited in cirrhotic livers is performed by a tilted positive balance of artificially driven MMP-8 getting activated inside the fibrotic liver. This is enhanced by naturally occurring MMP-2 and MMP-3, which seem to be up-regulated by MMP-8 treatment. Nonetheless, other fibrinolytic mechanisms might also be taking place. Alteration of MMP expression plays a major role in liver fibrogenesis and cirrhosis. Furthermore, another level of control of MMP activity is achieved through its physiological inhibitors (TIMPs) by stabilizing the proenzyme and inhibition of the active species.[38,39] TIMP-1 is able to block every MMP. The TIMP-1 increase we found in its free form suggests that a pool of metalloproteases (other than MMP-8) were rendered active and were ready to degrade the fibrotic scar.

The fact that we found increased liver cell proliferation (i.e., abundant hyperchromatic nuclei, and then measured by immunohistochemistry with the proliferation marker [PCNA] dispersed throughout the hepatic parenchyma and gene expression of HGF in MMP-8 treated rats) suggests that a change—not only in the amount, but also in the nature—of the ECM is ongoing. Collagen I decreases have been shown to enhance liver restoration by inducing HSC apoptosis and hepatocyte regeneration. Type I collagen perpetuates or promotes the activated phenotype of HSC.[40] Besides, direct contact of epithelial cells with collagen type I takes them out of the cell cycle; however, once they contact partially degraded collagen I mediated by $\alpha v\beta_3$, integrin reenters the cell cycle. Because collagen type I is the main MMP-8 substrate, its degradation represents a favorable event that contributes to restitution of hepatic cell population, as corroborated by our findings. Also, it has been shown in liver-regenerated rats after partial hepatectomy that the synthesis of ECM might play an important role in reestablishing the quiescent and differentiated phenotype of hepatocytes.[41] Several in vitro studies showed that ECM[39] modulates the phenotype of hepatocytes. Therefore, the notion that in AdMMP8-treated animals a different kind of ECM is present and the reasoning that potent growth factors are released in situ (such as HGF), resulting in cell proliferation, seem plausible. In this line of evidence, HGF was mainly embedded in the ECM of liver, spleen, and kidney bound to matrix proteins including heparan sulfate, thrombospondin, and collagen types I, III, IV, V, and VI.[42]

The effect of ECM remodeling phenomena on the overall clinical status of AdMMP8-treated cirrhotic animals deserves further consideration. It is clear that liver internal mechanisms caused improved hepatic synthetic functioning, as reflected in the disappearance of ascites and the reestablishment of transaminases (alanine aminotransferase and aspartate aminotransferase).

In addition, more compelling evidence of liver function improvement was a notable decrease of collateral gastric varices, which is equal to restored intrahepatic blood pressure in animals treated with the therapeutic AdMMP8 vector. Effective therapies for alcohol-induced liver cirrhosis and cirrhosis resulting from bile obstructive disorders are lacking, and the disease is increasing; therefore, a gene therapy approach is attractive. We believe that therapy with the MMP-8 gene holds promise for use in a clinical setting.

References

1. Diehl MA. Alcohol and liver regeneration. Clin Liver Dis 1998;2:1–10.
2. Friedman SL. Molecular regulation of hepatic fibrosis, an integrated cellular response to tissue injury. J Biol Chem 2000;275:2247–2250.
3. Okinawa T, Freeman M, Lo W, Vaughan DE, Fogo A. Modulation of plasminogen activator inhibitor-1 in vivo: a new mechanism for the anti-fibrotic effect of renin-angiotensin inhibition. Kidney Int 1997;51:164–172.
4. Tremble PR, Lane TF, Sage EH, Werb Z. SPARC, a secreted protein associated with morphogenesis and tissue remodeling, induces expression of matrix metalloproteinases in fibroblasts through a novel extracellular matrix-dependent pathway. J Cell Biol 1993;121:1433–1444.
5. Schuppan D, Cho JJ, Jia JD, Hahn EG. Interplay of matrix and myofibroblasts during hepatic fibrogenesis. Curr Top Pathol 1999;93:205–218.
6. Armendariz-Borunda J, Roy N, Simkewich C, Raghow R, Seyer JM, Kang AH. Activation of Ito cells involves regulation of AP-1 binding

proteins and induction of type I collagen gene expression. Biochem J 1994;304:817–824.
7. Armendariz-Borunda J, Seyer JM, Postlehwaite AE, Kang AH. Kupffer cells from carbon tetrachloride-injured rat livers produce chemotactic factors for fibroblast and monocytes: the role of tumor necrosis factor α. Hepatology 1991;14:895–900.
8. Wu J, Danielsson A. Inhibition of hepatic fibrogenesis: a review of pharmacological candidates. Scand J Gastroenterol 1994;29: 385–391.
9. Ueki T, Kaneda Y, Tsuitsui H, Nakanishi K, Sawa Y, Morishita R, Matsumoto K, Nakamura T, Takahashi H, Okamoto E, Fujimoto J. Hepatocyte growth factor gene therapy of liver cirrhosis in rats. Nat Med 1999;5:226–230.
10. Rudolph KL, Chang S, Millard M, Schreiber-Agus N, DePinho RA. Inhibition of experimental liver cirrhosis in mice by telomerase gene delivery. Science 2000;287:1253–1258.
11. Salgado S, Garcia J, Vera J, Siller F, Bueno M, Miranda A, Segura A, Grijalva G, Segura J, Orozco H, Hernandez-Pando R, Fafutis M, Aguilar LK, Aguilar-Cordova E, Armendariz-Borunda J. Liver cirrhosis is reverted by urokinase-type plasminogen activator gene therapy. Mol Ther 2000;2:545–551.
12. Hasty KA, Jeffrey JJ, Hibss MS, Welgus HG. The collagen substrate specificity of human neutrophil collagenase. J Biol Chem 1987;262:10048–10052.
13. Hasty KA, Pourmotabbed F, Goldberg GI, Thompson JP, Nelson RL, Spinella D, Mainardi CL. Human neutrophil collagenase: a distinct gene product with homology to other matrix metalloproteinases. J Biol Chem 1990;265:11421–11424.
14. García-Bañuelos J, Siller-López F, Miranda A, Aguilar LK, Aguilar-Cordova E, Armendariz-Borunda J. Cirrhotic rat livers with extensive fibrosis can be safely transduced with clinical-grade adenoviral vectors. Evidence of cirrhosis reversion. Gene Ther 2002;9:127–134.
15. Mizuguchi H, Kay MA. Efficient construction of a recombinant adenovirus vector by an improved in vitro ligation method. Hum Gene Ther 1998;9:2577–2583.
16. Nyberg-Hoffman C, Shabram P, Li W, Giroux D, Aguilar-Cordova E. Sensitivity and reproducibility in adenoviral infectious titer determination. Nat Med 1997;3:808–811.
17. Bradford MM. A rapid and sensitive method for quantitation of microgram quantities of protein utilising the principle of protein-dye binding. Anal Biochem 1976;72:248–254.
18. Chubinskaya S, Huccch K, Mikecz K, Cs-Szabo G, Hasty KA. Chondrocyte matrix metalloproteinase-8: up-regulation of neutrophil collagenase by interleukin-1b in human cartilage from knee and ankle joints. Lab Invest 1996;74:232–240.
19. Platzer C, Ofe-Hakim S, Reinke P, Decke WD, Ewart R, Volk HD. Quantitative PCR analysis of cytokine transcription patterns in peripheral mononuclear cells after anti-CD3 rejection therapy using two novel multispecific competition fragments. Transplantation 1994;58:264–268.
20. Tschesche H. Human neutrophil collagenase. Methods Enzymol 1995;248:431–449.
21. Lee SS, Girod C, Braillon A, Hadengue A, Lebrec D. Hemodynamic characterization of chronic bile duct-ligated rats: effect of pentobarbital sodium. Am J Physiol 1986;251:G176–G180.
22. Pilette C, Rousselet MR, Bedossa P, Chappard D, Oberti F, Rifflet H, Maïga MY, Gallois Y, Calés P. Histopathological evaluation of liver fibrosis: quantitative image analysis vs semi-quantitative scores. J Hepatol 1998;28:439–446.
23. Kage M, Shimamatu K, Nakashima E, Kojiro M, Inove O, Yano M. Long-term evolution of fibrosis from chronic hepatitis to cirrhosis in patients with hepatitis C: morphometric analysis of repeated biopsies. Hepatology 1997;25:1028–1031.
24. Rojkind M, Gonzalez E. An improved method for determining special radioactivities of proline and hydroxyproline. Anal Biochem 1974;57:1–7.
25. Diehl AM, Yin M, Fleckenstein J, Yang SQ, Lin HZ, Brenner DA, Westwick J, Badgy G, Nelson S. Tumor necrosis factor-alpha induces c-jun during the regenerative response to liver injury. Am J Physiol 1994;267:G552–G561.
26. Nagase H, Woessner JF Jr. Matrix metalloproteinases. J Biol Chem 1999;274:21491–21494.
27. Corcoran ML, Hewitt RE, Kleiner DE Jr, Stetler-Stevenson WG. MMP2: expression, activation and inhibition. Enzyme Protein 1996;49:7–19.
28. Nagase H, Ogata Y, Suzuki K, Enghild JJ, Salvensen G. Substrate specific and activation mechanisms of matrix metalloproteinases. Biochem Soc Trans 1991;19:715–718.
29. Hecht N, Pappo O, Shouval D, Rose-John S, Galun E, Axelrod JH. Hyper-IL-6 gene therapy reverses fulminant hepatic failure. Mol Ther 2001;3:683–687.
30. Nakatani T, Kuriyama S, Tominaga K, Tsujimoto T, Mitoro A, Yamazaki M, Tsujinoue H, Yoshiji H, Nagao S, Fukui H. Assessment of efficiency and safety of adenovirus mediated gene transfer into normal and damaged murine livers. Gut 2000;47:563–570.
31. Harvey B, Hackett N, Sawy T, Rosengart T, Hirschowitz E, Lieberman M, Lesser M, Crystal R. Variability of human systemic humoral immune response to adenovirus gene transfer vectors administered to different organs. J Virol 1999;73:6729–6742.
32. Iwano M, Fisher A, Okada H, Plieth D, Xue C, Danoff TM, Neilson EG. Conditional abatement of tissue fibrosis using nucleoside analogs to selectively corrupt DNA replication in transgenic fibroblasts. Mol Ther 2001;3:149–159.
33. Yong V, Krekoski C, Forsyth P, Bell R, Edwards D. Matrix metalloproteinases and diseases of the CNS. Trends Neurosci 1998; 21:75–80.
34. Nagase H. Activation mechanisms of matrix metalloproteinases. Biol Chem 1997;378:151–160.
35. Vater CA, Nagase H, Harris ED Jr. Purification of an endogenous activator of procollagenase from rabbit synovial fibroblast culture medium. J Biol Chem 1983;258:9374–9382.
36. Tyree B, Seltzer JL, Halme J, Jeffrey JJ, Eisen AZ. The stoichiometric activation of human skin fibroblast pro-collagenase by factors present in human skin and rat uterus. Arch Biochem Biophys 1981;208:440–443.
37. Smith GN Jr, Brandt KD, Hasty KA. Procollagenase is reduced to inactive fragments upon activation in the presence of doxycycline. Ann N Y Acad Sci 1994;732:436–438.
38. Cawszon TE, Galloway A, Mercer E, Murphy G, Reynolds JJ. Purification of rabbit bone inhibitor of collagenase. J Biochem 1981;195:159–165.
39. Stetler-Stevenson WG, Krutzsch HC, Liotta LA. Tissue inhibitor of metalloproteinase-2 (TIMP-2). A new member of metalloproteinase inhibitor family. J Biol Chem 1998;264:17374–17378.
40. Issa R, Zhou X, Trim N, Sadler-Millward H, Krane S, Benyon C, Iredale J. Mutation in collagen-I that confers resistance to the action of collagenase results in failure of recovery from CCl4-induced liver fibrosis, persistence of activated hepatic stellate cells, and diminished hepatocyte regeneration. FASEB J 2003; 17:47–49.
41. Rudolph KL, Trautwein C, Kubicka S, Rakemann T, Bahr MJ, Sedlaczek N, Schuppan D, Manns MP. Differential regulation of extracellular matrix synthesis during liver regeneration after partial hepatectomy in rats. Hepatology 1999;30:1159–1166.
42. Kim T-H, Mars WM, Stolz DB, Michalopoulos GK. Expression and activation of pro-MMP2 and pro-MMP9 during rat liver regeneration. Hepatology 2000;30:75–80.

Received December 19, 2001. Accepted December 18, 2003.

Address requests for reprints to: Juan Armendariz-Borunda, M.D., Institute for Molecular Biology in Medicine and Gene Therapy, CUCS, University of Guadalajara, Apdo. Postal 2-123, Guadalajara, Jal 44281, Mexico. e-mail: armendbo@cucs.udg.mx; fax: (52) 33-3618-7473.

Journal of Gastroenterology and Hepatology (2004) **19**, 380–387

HEPATOLOGY

Amplified expression of dominant-negative transforming growth factor-beta type II receptor inhibits collagen type I production via reduced Smad-3 activity

IVAN HERNANDEZ-CAÑAVERAL,* JAIME GONZÁLEZ,* FERNANDO LÓPEZ-CASILLAS† AND JUAN ARMENDARIZ-BORUNDA*

**Institute for Molecular Biology in Medicine and Gene Therapy, Centro Universitario de Ciencias de la Salud, University of Guadalajara, Guadalajara, Jal, and †Institute of Physiology, Universidad Autonoma de Mexico, Mexico*

Abstract

Background and Aim: As a pleiotropic protein, transforming growth factor (TGF)-β induces its effects by binding to its Ser/Thr kinase receptor type II and then recruiting and activating receptor type I, which is phosphorylated and activates Smads that transduce the signal to the nucleus.

Methods: In this work, the authors blocked TGF-β1 signal transduction pathway via delivery of a dominant-negative receptor-II (ΔCyTbRII)-cDNA lacking Ser/Thr kinase intracytoplasmic domain activity. Thus, Cos-1 and hepatic stellate cells were cotransfected with pCMV5-ΔCyTbRII and pAdTrack-green fluorescent protein using lipofectamine.

Results: Fluorescence microscopy demonstrated an average 10% transfection efficiency. Radiolabeled ^{125}I-TGF-β was bound mostly by cell membrane-expressed truncated receptor-II rather than wild-type receptor type II. Electrophoretic mobility shift assays were performed using consensus Smad-2 and -3 sequences rendering a three-fold decrease in DNA-binding activity, reflecting a down-activation in Smad complexes in pCMV5-ΔCyTbRII-transfected cells, but not in mock-transfected cells. The identity of these transcriptional factors was confirmed using irrelevant double-stranded oligonucleotides and specific antibodies to compete for DNA binding. Also, collagen I mRNA expression showed a five-fold decrease, which was reflected at the protein level as a diminished collagen type I production in pCMV5-ΔCyTbRII-transfected Cos-1 cells as measured by [^{3}H]proline incorporation and sodium dodecyl sulfate–polyacrylamide gel electrophoresis.

Conclusion: Thus, this could be a useful strategy to downregulate or prevent exacerbated synthesis and deposition of extracellular matrix in a given fibrotic process.

Key words: collagen I, dominant-negative, signal transduction, Smad, transforming growth factor-β.

INTRODUCTION

Transforming growth factor (TGF)-β is a member of a prominent family of growth factors whose biological functions are multiple, such as cell differentiation, embryogenesis, immune response, inflammation, and tissue repair, and dependent on the target cell on which they act.[1,2] Modulation of TGF-β and binding of its receptor, along with intracellular signaling molecules, have been linked to numerous disease states, including cancer, hereditary hemorrhagic telangiectasia, atherosclerosis, and fibrotic diseases of the kidney, liver, and lung.[3–5]

Transforming growth factor-β has five isoforms and TGF-β 1, 2 and 3 are present in most species, including all mammals; TGF-β 4 and 5 have been found in birds and amphibians, respectively. Transforming growth factor-β is constitutively synthesized and secreted in a

Correspondence: Dr Juan Armendariz-Borunda, Institute for Molecular Biology in Medicine and Gene Therapy, CUCS, University of Guadalajara, Apdo. Postal 2-123, Guadalajara, Jal, Mexico 44281. Email: armendbo@cucs.udg.mx

Accepted for publication 11 July 2003.

biological latent form needing to be activated before binding to specific intracellular signaling receptors.[6] *In vivo*, TGF-β is activated by, among others, plasmin and thrombospondin-1 by structural modification of the inactive complex.[7] The active form of TGF-β is a 25-kDa homodimer protein, which initiates a transduction signal pathway when is bound to its receptor. Transforming growth factor-β receptors are virtually present in all cells of the body and can bind only the active form of TGF-β. Three different receptors to TGF-β have been reported. Receptors type I and II are involved in signal transduction; TGF-β binds directly to receptor II (TRII), which is a constitutively active kinase. Then, receptor I (TRI) is immediately recruited into the complex and becomes phosphorylated by TRII, which allows TRI to propagate the signal to downstream substrates.[8] Receptor II has an intracytoplasmic domain with serine/threonine kinase activity that functions like a switch to propagate the signal.[9]

Elegant studies with cloned TGF-β and TRI have confirmed the inability to bind ligand in the absence of TRII.[10,11] Additional studies have shown that truncated TRII that is lacking the cytoplasmic domain still binds TGF-β, recruits TRI, and form a complex. However, TGF-β binding to TRI facilitated by this truncated TRII fails to inhibit epithelial cell proliferation and other effects of TGF-β. Activated TRI by TRII is able to activate proteins in cytoplasm to transduce the signal to nuclei. Such proteins, called Smads, are transcriptional activators of TGF-β response.

Nine different Smads have been reported, and Smad-2 and -3 are c-terminally phosphorylated and activated by TGF-β receptors.[12,13] These have been shown to act as transcriptional factors through their ability to directly bind DNA and induce transcriptional response, alone or in collaboration with other transcription factors.[14] Optimal DNA sequence polymerase chain reaction (PCR)-based techniques have led to the definition of the Smad-3 and -4 consensus sequence. This consensus 'Smad-binding element' is GTCTA GAC, a palindromic sequence with two copies of GTCT and its reverse complementary AGAC sequence in the opposite DNA strand.[15] Major advances in the understanding of the intimate mechanisms of TGF-β signaling through the Smad pathway have been made, using cDNA microarrays and the promoter transactivation approach. Direct target genes, like *COL1a2*, *COL3a1*, *COL6a1*, *COL6a3*, *TIMP-1* and *PAI-1* have been identified.[16,17] In the present paper, the authors used TGF-β-truncated receptor-II cDNA as a transfected agent, which was over-expressed in the cell membrane and was able to obliterate and block the signal transduction pathway, otherwise originated by the binding of nearby TGF-β 1 to a wild-type receptor. Although the present findings have been demonstrated *in vitro* so far, the authors believe that this strategy can be used to potentially deliver this pharmacological weapon to prevent the evolution of fibrosis in experimental animal models, as previously shown by others.[18,19] Then it might be possible to eventually use this approach to bridge the gap between the laboratory bench and the clinical scenario, and treat patients with hepatic fibrosis.

METHODS

Plasmid constructs

The pCMV5-ΔCytTβRII construct was verified using endonucleases restriction analysis and sequentiation with a sequenase kit (Promega, Madison, WI, USA). ΔCytTβRII was constructed by introducing a stop codon and a BamHI site after nt 597 in the cDNA of TRII to TGF-β, then subcloned in KpnI and BamHI into pCMV5.[10]

Cell culture

Hepatic stellate cells (HSC) were established as cell lines according to methodology described in the authors' previous papers.[17,20] Briefly, activated HSC were routinely used while they were in subculture 20–25th. Thus, subcultured cells were grown in a 5% CO_2 : 95% O_2 atmosphere in Dulbecco's modified Eagle's medium (DMEM; Gibco, Rockville, MD) supplemented with 10% fetal bovine serum, 100 IU/mL penicillin, 100 μg/mL streptomycin and 2 mM L-glutamine (complete medium). Cos-1 were obtained from the American Type Tissue Collection (Manassas, VA, USA) and kept under appropriate cell culture conditions until used.

Transfection and reporter gene assay

Subcultured HSC and Cos-1 cells were transiently cotransfected with indicated construct and internal control pAdTrack-green fluorescent protein (GFP) using Lipofectamine (Gibco). At 48 h post transfection the cells were exposed to fluorescence stereoscopic Olympus SZX12 microscopy (Olympus, Tokyo, Japan) to validate GFP emission and thereby quantitative transfection efficiency. For some cell transfection experiments, mock constructs were used.

Receptor affinity labeling

The receptor affinity labeling was carried out as previously described.[11] Briefly, recombinant TGF-β1 (Promega, Madison, WI, USA) was ^{125}I-labeled, HSC and Cos-1 cells were transfected with 10 μg of control and pCMV5-ΔCytTβRII; 48 h post transfection, cells were washed with sterile phosphate-buffered saline (PBS) and replenished with fresh medium containing 10% fetal calf serum. Cells were sequentially incubated with 150 pM ^{125}I-TGF-β1 and 10 mg/mL disuccinilmydil suberate. Cell lysates were subjected to 9% sodium dodecyl sulfate–polyacrylamide gel electrophoresis (SDS–PAGE) and autoradiography. Proper molecular weight controls were included to verify species of receptors.

Reverse transcription–polymerase chain reaction for procollagen-α1 mRNA levels and cognate protein synthesis

Total cellular RNA was extracted according to Chomczynski and Sacchi.[21] At 48 h post-transfection with control pAdTrack and pCMV5-ΔCytTβRII, HSC and Cos-1 cells were washed twice with PBS and left overnight in serum-free DMEM. Serum-starved subconfluent cell cultures were treated with recombinant TGF-β1 (5 ng/mL) in serum-free medium for an additional 20 h, then washed twice with PBS and recollected with Trizol (Gibco). The aqueous phase containing RNA was precipitated with isopropanol at 4°C overnight. The quantity and intactness of RNA were routinely tested by determining optical density readings and the ethidium bromide fluorescence of RNA electrophoresed in 1% agarose gel. Two micrograms of RNA were reverse-transcribed into cDNA by using M-MLV reverse transcriptase (Gibco) according to the manufacturer's instructions, and the cDNA was amplified using PCR. The upstream primer was 5′-CAAGAATGGCGAC CGTGGTGA-3′, which encompasses to nucleotides 393–373, while the downstream primer was 5′-GGT GTGACTCGTGCAGCCATC-3′; by using these primers a PCR product of 1074 bp was obtained.[22]

The assay to estimate collagen I production was carried out 48 h post transfection of the cells. Hepatic stellate cells and Cos-1 cells were incubated in serum-free conditions as described before. Transforming growth factor-β1 (5 ng/mL) was added for 20 h in culture, and its effect on collagen synthesis was determined by using [^{3}H]proline [42 Ci/mmol] for the last 4 h of culture. Thus, cells were incubated in 35-mm dishes with 1 mL of DMEM with 15 μCi [^{3}H]proline (Sigma, St Louis, MO, USA) supplemented with fresh ascorbate (50 μg/mL) and b-aminopropionitrile (80 μg/mL). The medium was harvested into a solution containing protease inhibitors (0.2 mM phenyl-methyl-sulfonyl-fluoride [PMSF], 10 Mm *N*-ethylmaleimide, leupeptin 1 μg/mL, pepstatin 1 μg/mL, and 2.5 mM ethylenediamine tetraacetic acid [EDTA], final concentration). Collagen was precipitated by adding ethanol (33% final concentration). Samples for electrophoresis were dissolved in a sample buffer containing 10% glycerol and 5% SDS. Seven per cent SDS-PAGE was carried out on slab gels with 3% stacking gels and run at 16°C, as described by Laemmli.[23] The gels were dried, applied to Kodak XAS-1 film (Kodak, New York, NY, USA) and exposed for several hours at −70°C. Fluorograms were quantitated by scanning the autoradiographic bands with Kodak 1D software.

Nuclear extract preparation and electrophoretic mobility shift assays

Preparation of nuclear extracts was carried out according to a modification of the Dignam method described by Andrews and Faller.[24] Briefly, 1–10 million each of HSC and Cos-1 cells were harvested and washed twice with 15 mL of sterile PBS. The cell pellet was resuspended in 0.4 mL of cold buffer A (10 mM HEPES-KOH pH 7.9, 1.5 mM $MgCl_2$,10 mM KCl, 0.5 mM DTT, and 0.2 mM PMSF) and allowed to swell on ice for 10 min. Then vortexing was applied, the pellets were spun in a microfuge, the supernatants were discarded, and the pellets were resuspended in 20–100 μL of cold buffer C (20 mM HEPES-KOH pH 7.9, 25% glycerol, 420 mM NaCl, 1.5 mM $MgCl_2$ 0.2 EDTA, 0.5 mM DTT, 0.2 mM PMSF) and incubated on ice for 20 min. Samples were spun at 10 000 r.p.m. for 2 min at 4°C. The supernatants (containing DNA-binding proteins), were transferred to a new tube and protein concentrations were determined using the Bradford method.[25] Nuclear extracts were stored at −70°C.

Sequence-specific double-stranded oligonucleotides were end-labeled with [^{32}P]dATP using T4-kinase. Binding reactions containing 10 μg of nuclear extracts and 30 000 c.p.m. of labeled oligonucleotides were carried out for 20 min at 37°C in 40 μL of binding buffer. Protein–DNA complexes were resolved in 6% polyacrylamide gels containing 0.5× Tris-Borate-EDTA (TBE). The sequence of the double-stranded oligonucleotides used as a probe was: 5′-TCG AGA GCC AGA CAA AAA GCC AGA CAT TTA GCC AGA CAC-3′ 3′-GTG TCT GGC TAA ATG TCT GGC TTT TTG TCT GGC TCT CGA-5′.[15]

RESULTS

Transfection efficiency

In order to standardize and quantitatively determine the ratio of transfected cells between different experiments, HSC and Cos-1 cells were routinely cotransfected with plasmid containing the cDNA of a dominant-negative TGF-βTRII pCMV5-ΔCyTβRII and a control plasmid carrying pAdTrack-GFP. Figure 1a is a representative example of the results that were routinely obtained for the efficiency of transfection. Co-transfection was validated with the emission of GFP from the control plasmid, consistently obtaining approximately 10% of transfection efficiency, as is comparatively seen in Figure 1a.[20] Figure 1ai (light microscopy) shows the actual cell number in a given microscopy field, while Figure 1aii depicts the successful GFP-displaying cells in the same field. Although there were some minor differences between the efficiencies of transfection among individual cell culture dishes, they were negligible. The typical morphological features of HSC are clearly noticeable.

Overexpression of dominant-negative receptor type II

The Δ-CytTbRII construct was transiently transfected using lipofectamine as indicated in the Methods section and its cognate protein expression was unraveled using affinity labeling of the cells with ^{125}I-TGF-β1. The transfected cells with ΔCytTbRII construct yielded a TGF-β1 labeled product of approximately 50 kDa

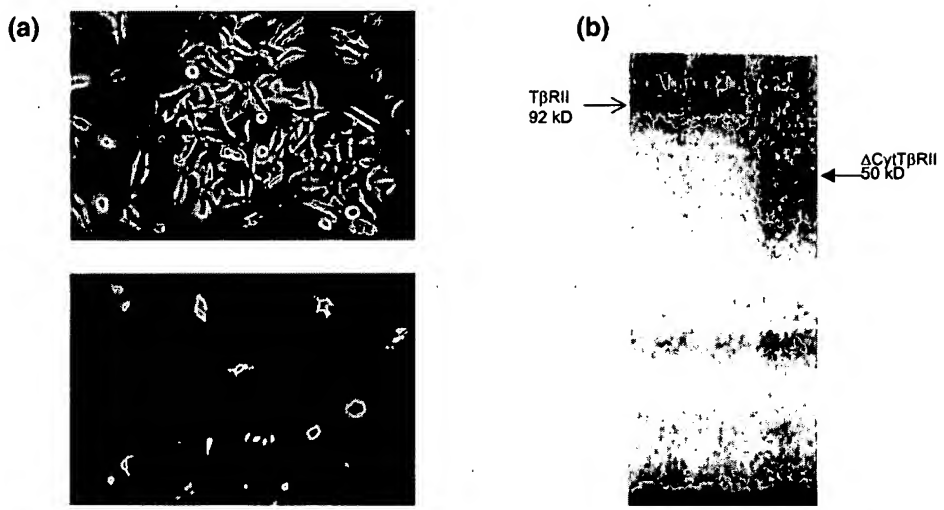

Figure 1 (a) Expression of green fluorescent protein (GFP) in hepatic stellate cells (HSC) cotransfected with pCMV5ΔCytTbRII and pAdTrack-GFP to validate the transfection efficiency using lipofectamine. (ai) Cell number and morphology were evaluated using light microscopy and (aii) GFP-transfected cells were observed by means of an Olympus fluorescent stereoscopic microscope. Transfection efficiency in HSC was similar to that in Cos-1 cells. (b) Affinity labeling experiments were performed using radiolabeled transforming growth factor (TGF)-β1 as indicated in the methods section. The HSC and Cos-1 cells were cultured in 10% fetal bovine serum-supplemented Dulbecco's modified Eagle's medium. Control and dominant-negative receptor II-transfected cells were affinity labeled using sequential incubation in fresh media with 150 pM ^{125}I-TGF-β1 and 10 mg/mL disuccinilmydil-suberate. Cell lysates were subjected to 9% sodium dodecyl sulfate–polyacrylamide gel electrophoresis and autoradiography. Lane 1, non-transfected control cells; lane 2, mock-transfected cells, lane 3, pCMV5-ΔCytTbRII-transfected cells.

(Fig. 1b), which coincided with the predicted size of the truncated receptor as has been previously reported.[11] This piece of data indicated to the authors that the cytoplasmic domain of TRII is dispensable for ligand binding. The ability of ΔCytTbRII to bind TGF-β1, generating an inactive complex, raised the possibility that ΔCytTbRII could act in a dominant-negative fashion over wild-type receptors, diminishing the response to TGF-β1 in the cells. After exposure to radiolabeled TGF-β1, cells transfected with mock constructs and cells incubated with media only showed an intense band of approximately 92 kDa, corresponding to wild-type TGF-β TRII.

Transfection with pCMV5-ΔCytTbRII results in obliterated expression of the collagen I gene

To confirm that ΔCytTbRII acted in a dominant-negative fashion on expression of specific pro-fibrogenic target genes, the HSC and Cos-1 cells were transiently cotransfected with ΔCytTbRII and control plasmid, and total RNA was extracted. Reverse transcription–polymerase chain reaction assays were set up in order to elucidate whether the steady-state levels of collagen type I were modified. Figure 2a shows representative experiments where cultured cells constitutively expressed collagen I mRNA at some level, which was potentiated by the addition of recombinant TGF-β1 (5 ng/mL). In contrast, collagen I mRNA showed a decrease of approximately five-fold as measured by Kodak gel analysis software in TGF-β1-stimulated cells transfected with ΔCytTbRII (Fig. 2a). Histograms shown in Figure 2b quantitatively confirmed the authors' observations.

Diminution of the activation of Smad by dominant-negative receptor type II

It has shown before that TGF-β1 may upregulate the transcriptional activity of the collagen type I gene, through modulating the concentration of AP-1 *trans*-acting factors that bind with high affinity to the enhancer-spanning DNA fragment.[20] However, different TGF-β-inducible genes may be activated by multiple mechanisms. Therefore, the following experiments were aimed at discovering whether TGF-β intracellular signaling was mediated via Smad-2/3 activation in this system.

In order to elucidate the mechanisms regulating the decrease in collagen I mRNA expression, the authors focused on the potential obliteration of the Smad activation pathway. Thus, gel retardation experiments (electrophoretic mobility shift assays [EMSA]) using a Smad-2/3 radioprobe were carried out. Because the authors wanted to identify and quantify these transcriptional factors, EMSA assays were carried out using synthetic double-stranded oligonucleotides bearing the Smad-2 and Smad-3 consensus sequence. A radiolabeled nuclear factor kappa B (NFκB) probe was used as

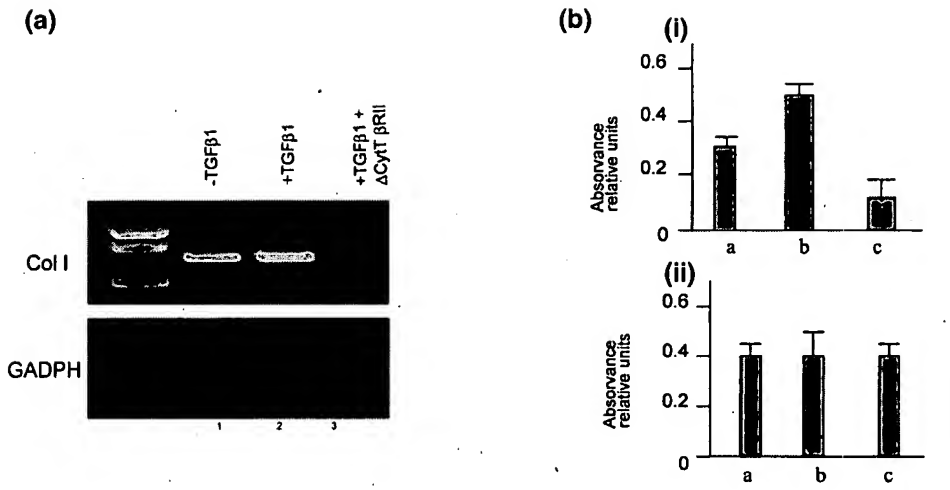

Figure 2 Determination of collagen gene expression by semiquantitative reverse transcription–polymerase chain reaction (RT–PCR). (a) Total RNA was extracted from cells and cDNA was obtained. Standardization of constitutive gene expression was accomplished with the glyceraldehyde-phosphate dehydrogenase (GAPDH) gene. Lane 1, molecular weight ladder; lane 2, control cells non-treated with transforming growth factor (TGF)-β1; lane 3, mock-transfected and TGF-β1-treated cells; lane 4, TGF-β1-treated cells transfected with pCMV5-ΔCytTbRII. Assays were performed in triplicate. (b) (bi) Histograms show the intensity of multiple-photographed bands, which was recorded with a digital camera and quantified with a computer program to find the average levels of collagen I mRNA transcripts. (bii) In order to rule out experimental caveats, final RT–PCR determinations were carried out between the linear range and then standardization of each cDNA was accomplished with the GAPDH gene as a constitutively expressed gene.

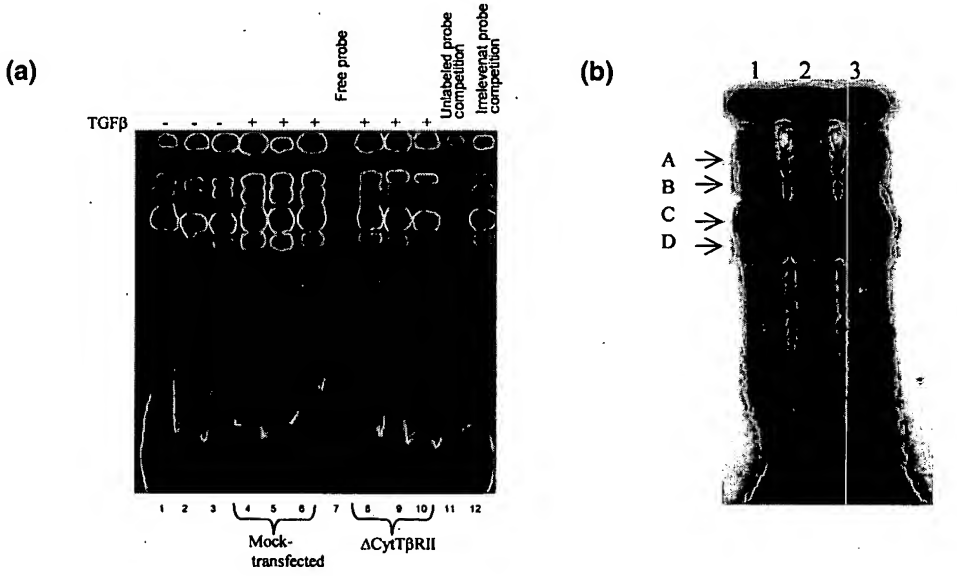

Figure 3 Electrophoretic mobility shift assays were performed as described in the experimental procedure section. (a) Lanes 1–3, The 5′-end radiolabeled Smad-2/3 probe was incubated with 3 μg of nuclear extracts hepatic stellate cells and Cos-1 cells without transforming growth factor (TGF)-β stimulation; lanes 4–6 and 8–11, 3 μg of nuclear extracts from TGF-β1-treated cells were incubated with radiolabeled probe; moreover lanes 8–10 were previously pCMV5-ΔCytTbRII-transfected cells. Free probe is shown in lane 7. Lane 11 shows competition with a 200-fold molar excess of unlabeled probe. Lane 12 depicts competition with synthetic nuclear factor kappa B-irrelevant probe. (b) Pre-incubation of nuclear extracts from TGF-β1-treated cells with (lane 2) anti-Smad-2 (2 μg) and (lane 3) anti-Smad-3 antibodies (2 μg). A, B, C, and D indicate the different Smad complexes. Fixed amounts of nuclear proteins (3 mg) were used. Lane 1 represents incubation of nuclear proteins with antibody-resuspending buffer.

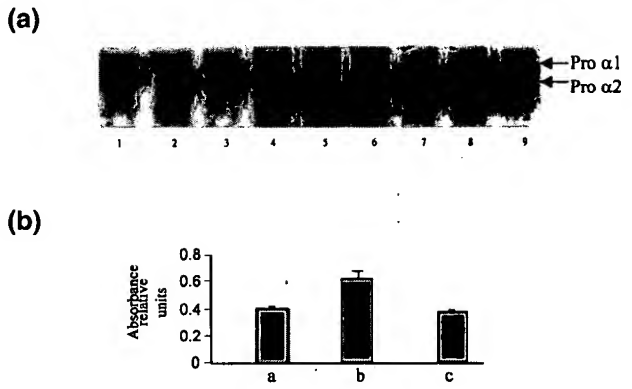

Figure 4 Collagen synthesis decrease in pCMV5-ΔCytTbRII-transfected Cos-1 and hepatic stellate cells. (a) Control and transfected cells were overnight incubated with transforming growth factor (TGF)-β1 (5 ng/mL). Cell cultures were supplemented with ascorbate (50 μg/mL) and b-aminopropionitrile (80 μg/mL). [^{3}H]proline (15 μCi/mL) was added for the last 4 h of incubation. 1 mL of media was recollected and total protein was precipitated using absolute ethanol. Protein pellets were dissolved in gel-sample buffer and extracellular proteins were size-fractionated on 7% sodium dodecyl sulfate–polyacrylamide gel electrophoresis detected by autoradiography. Lanes 1–3, Proa1(I) and Proa2(I) chain synthesis of control Cos-1 cells non-treated with TGF-β1; lanes 4–6, mock-transfected and TGF-β1-treated cells; lanes 7–9, the Proa1(I) and Proa2(I) chain synthesis of TGF-β1-treated cells transfected with pCMV5-ΔCytTbRII. (b) Quantitative data resulting from three different experiments. (bi) Collagen synthesis of control cells non-treated with TGF-β1; (bii) mock-transfected and TGF-β1-treated cells; (biii) TGF-β1-treated cells transfected with pCMV5-ΔCytTbRII ($P < 0.05$). Hepatic stellate cells rendered an identical pattern of collagen synthesis.

a competitor-irrelevant probe. These probes were used in assays containing nuclear proteins obtained and isolated from Cos-1 cells and HSC treated or not treated with TGF-β and mock-transfected or transfected with ΔCytTbRII. The protein concentration was determined and adjusted to equal concentration for either cell type as described in the legend for Figure 3. Figure 3a shows that nuclear extracts from TGF-β1-treated, mock-transfected cells contained five-fold more Smad-2/3 binding proteins as compared with their non-treated counterparts (Fig. 3a, lanes 1–3), reflecting the increased activity of these transcriptional mediators. Cells transfected with 10 μg of pCMV5-ΔCytTbRII and stimulated with 5 ng of TGF-β1 showed a clear decrease (three-fold) in the concentration of Smad-2/3 binding proteins (Fig. 3a, lanes 8–10). This fact suggests that TGF-β-induced intracellular signaling is modulated by intracellular concentrations of such DNA-binding proteins. Competition with the cold Smad-2/3 DNA consensus sequence demonstrated the specificity of the binding assay (Fig. 3a, lane 11). Also, competition with an irrelevant competitor (the NFkB consensus sequence), using concentrations as high as 200-fold molar excess, failed to compete out the binding.

Treatment of cell nuclear extracts with monoclonal antibody anti-Smad-3 diminishes its binding to a specific consensus sequence

Smad-2 and -3 are transcriptional factors that are stimulated by TGF-β1. Thus, in order to verify and extend previous observations, the authors designed experiments using monoclonal antibodies against Smad-2 and -3 to elucidate the nature of active transcriptional factors in the present system. Therefore, the authors addressed the question of whether antibodies against Smad-2 and -3, could compete for the binding to the target DNA. Figure 3b shows a representative picture of three different experiments when nuclear extracts from TGF-β1-treated cells were preincubated with corresponding antibodies, and subjected to standard EMSA assays. When nuclear proteins were separately preincubated with anti-Smad-2 and anti-Smad-3 antibodies, it was found that mostly the latter antibody was able to reduce the binding for the target DNA. Specifically, complex A disappeared and complex B intensity decreased substantially. These data confirm that the Smad-2/3 DNA probe-bound nuclear factors are Smad-3.

Transfection with ΔCytTbRII results in decreased collagen synthesis

After determining that pCMV5-ΔCytTbRII-transfected cells showed decreased collagen I mRNA steady-state levels and diminished Smad-2/3 binding activity, the authors wanted to elucidate whether these phenomena were reflected in alterations in collagen I synthesis. It was found that TGF-β1 stimulated pro-collagen I synthesis approximately 2.5-fold at 5 ng/mL TGF-β1 as measured using [^{3}H]-proline incorporation assays (Fig. 4). In general, these results are in agreement with the authors' previous and others observations.[17,26,27] However, when the cells were transfected with the dominant-negative receptor and challenged with

TGF-β1 (5 ng/mL), they did not respond to this cytokine fibrogenic stimuli; suggesting that overexpression of the truncated TGF-β1-receptor results in obliteration of signal transduction.

DISCUSSION

Transforming growth factor-β1 is thought to be an important cytokine in regulating the production, degradation and accumulation of extracellular matrix (ECM) proteins, and it plays a pivotal role in fibroproliferative changes that occur following tissue damage in multiple organs, including the liver.[28] Mesenchymal and infiltrating cells have been suggested as potential sources of TGF-β in several tissues. Given the heterogeneity of the cellular source, the general consensus is that no definitive therapy has been implemented to ameliorate a given fibroproliferative process. Consequently, a promising target for this purpose is to neutralize the fibrogenic cytokine, TGF-β1. The authors' previous results have demonstrated that excessive production of TGF-β1 in activated Kupffer cells from cirrhotic rat livers can be obliterated by using an antisense technology. Thus, the authors were able to show that the use of antisense S-oligodeoxynucleotides targeted against the translational initiation site of TGF-β resulted in decreased TGF-β1 production as measured with a mink lung cells proliferation assay.[29] In contrast, a plausible strategy would also consist in the use of a decoy or a dominant-negative receptor. The receptor's activation in response to ligand is well known, but the intracellular events involved in signal transduction in response to TGF-β is currently a motive of intensive investigation and Smad-2 and Smad-3 have been reported in other systems to be mostly transducers in response to TGF-β.[8,12-14]. These two proteins can form complexes with Smad-4 and translocate into the nucleus, where they act as transcriptional modulators on TGF-β-responsive gene promoters, for example those for plasminogen activator inhibitor 1 (*PAI-1*) and the alpha chains of collagen I, which both play a central role in the progression of fibrosis in several tissues. As collagen I is a major ECM component involved in the process of fibrogenesis, the specific inhibition of the intracellular actions of TGF-β ligand seems to be a promising target for antifibrotic therapy, that is, reversion of hepatic fibrosis. However, the underlying molecular mechanisms of the profibrogenic effects of TGF-β1 are still the focus of intense investigations. Furthermore, similar strategies to that presented here have been reported. Nonetheless, the authors communicate in this paper detailed molecular mechanisms of action. Recently, potential gene therapies using dominant-negative or soluble TGF-β receptors have been described[18,19] and another strategy has been based on the reduced generation of active TGF-β1 by the effect of protease inhibitors such as camostat mesilate.[30] Although the central focus of those investigations has consisted in the prevention of fibrosis, data was lacking concerning the intracellular mechanism of inhibition in the progression of fibrosis.

In the present study, the authors show that overexpression in the cell membrane of a dominant-negative type II TGF-b1 receptor results in the inhibition of the steady-state levels of collagen type I mRNA in a quantifiable fashion, a fact that is reflected in collagen I protein production by cultured cells.

The present findings suggest that a diminished activation of Smad-3 in HSC and Cos-1 cells is a key step in the further downregulation of collagen I gene expression. This is in agreement with reports of constitutive phosphorylation and nuclear localization of Smad-3 being correlated with increased collagen gene transcription in activated HSC.[31] In addition, Smad-3 has been shown to be an important mediator in the activation of HSC.[32] Taken all together, these reports support the present data that sheds light on the molecular mechanisms involved.

ACKNOWLEDGMENTS

This work was supported by CONACYT grant #28832 to J Armendariz-Borunda and by PIHCSA Medica, SA de CV. The authors appreciate the technical support of Vidal Delgado.

REFERENCES

1 Letterio JJ, Roberts AB. Regulation of immune responses by TGF-beta. *Ann. Rev. Immunol.* 1998; **16**: 137–61.
2 Clark DA, Coker R. Transforming growth factor-beta. *Int. J. Biochem. Cell Biol.* 1998; **30**: 293–8.
3 Blobe GC, Schiemann WP, Lodish HF. Role of transforming growth factor β in human disease. *N. Engl. J. Med.* 2000; **342**: 1350–8.
4 Olaso E, Friedman S. Molecular regulation of hepatic fibrogenesis. *J. Hepatol.* 1998; **29**: 836–47.
5 Armendariz-Borunda J, Seyer JM, Kang AH, Raghow R. Regulation of TGF-β gene expression in rat liver intoxicated with carbon tetrachloride. *FASEB J.* 1990; **4**: 215–21.
6 Piek E, Heldin CH, Ten Dijke P. Specificity, diversity, and regulation in TGF-β superfamily signaling. *FASEB J.* 1999; **13**: 2105–24.
7 Khalil N. TGF-β: from latent to active. *Microbes Infect.* 1999; **1**: 1255–63.
8 Massagué J. TGF-β signal transduction. *Ann. Rev. Biochem.* 1998; **67**: 753–91.
9 Wrana JL, Attisano L, Wieser R, Ventura F, Massagué J. Mechanism of activation of the TGF-β receptor. *Nature* 1994; **370**: 341–6.
10 Attisano L, Carcamo J, Ventura F, Weis FM, Massague J, Wrana JL. Identification of human activin and TGF beta type I receptors that form heteromeric kinase complexes with type II receptors. *Cell* 1993; **75**: 671–80.
11 Wieser R, Attisano L, Wrana JL, Massagué J. Signaling activity of transforming growth factor β type receptors lacking specific domains in the cytoplasmic region. *Mol. Cell Biol.* 1993; **13**: 7329–247.
12 Padgett RW, Cho SH, Evangelista C. Smads are the central component in transforming growth factor-β signaling. *Pharmacol. Ther.* 1998; **78**: 47–52.

13 Massage J, Wotton D. Transcriptional control by the TGF-β/Smad signaling system. *EMBO J.* 2000; **19**: 1745–54.
14 Attisano L, Wrana JL. Smads as transcriptional co-modulators. *Curr. Opin. Cell Biol.* 2000; **12**: 235–43.
15 Dennler S, Itoh S, Vivien D, Dijke PT, Huet S, Gauthier JM. Direct binding of Smad3 and Smad4 to critical TGF-β-inducible elements in the promoter of human plasminogen activator inhibitor-type 1 gene. *EMBO J.* 1998; **17**: 3091–100.
16 Verrecchia F, Chu ML, Mauviel A. Identification of novel TGF-β/Smad gene targets in dermal fibroblasts using a combined cDNA microarray/promoter transactivation approach. *J. Biol. Chem.* 2001; **276**: 17058–62.
17 Armendariz-Borunda J, Katayama K, Seyer J. Transcriptional mechanism of type I collagen I gene expression are differentially regulated by interleukin-1β, tumor necrosis factor α, and transforming growth factor β in Ito cells. *J. Biol. Chem.* 1992; **267**: 14316–21.
18 Qi Z, Atsuchi N, Ooshima A, Takeshita A, Ueno H. Blockade of type β transforming growth factor prevents liver fibrosis and dysfunction in the rat. *Proc. Natl Acad. Sci. USA* 1999; **96**: 2345–9.
19 Ueno H, Sakamoto T, Nakamura T *et al.* A soluble transforming growth factor beta receptor expressed in muscle prevents liver fibrosis and dysfunction in rats. *Hum. Gene Ther.* 2000; **11**: 33–42.
20 Armendariz-Borunda J, Simkevich CP, Roy N, Raghow R, Kang AH, Seyer J. Activation of ito cells involves regulation of AP-1 binding proteins and induction of type I collagen gene expression. *Biochem. J.* 1994; **304**: 817–24.
21 Chomczynski P, Sacchi N. Single step method of RNA isolation by guanidinium thiocyanate-phenol-cloroformo extraction. *Anal. Biochem.* 1987; **162**: 156–9.
22 Armstrong LC, Watkins K, Pinkerton KE, Last JA. Collagen mRNA content and distribution in the lungs of rats exposed to ozone. *Am. J. Respir. Cell Mol. Biol.* 1994; **11**: 25–34.
23 Laemmli UK, Beguin F, Gujer-Kellenberger G. A factor preventing the major head protein of bacteriophage T4 from random aggregation. *J. Mol. Biol.* 1970; **47**: 69–85.
24 Andrews CN, Faller VD. A rapid micropreparation technique for extraction of DNA-binding proteins from limiting numbers of mammalian cells. *Nucl. Acid Res.* 1991; **19**: 2499.
25 Bradford MM. A rapid sensitive method for the quantification of microgram quantities of protein utilizing the principle of protein-dye binding. *Anal. Biochem.* 1976; **72**: 248–54.
26 Weiner FR, Giambrone NA, Czaja MJ *et al.* Ito-cell gene expression and collagen regulation. *Hepatology* 1990; **11**: 111–17.
27 Davis BH. Transforming growth factor beta responsiveness is modulated by the extracellular collagen matrix during hepatic ito cell culture. *J. Cell Physiol.* 1988; **136**: 547–53.
28 Border WA, Noble NA. Transforming growth factor β in tissue fibrosis. *N. Engl. J. Med.* 1994; **331**: 1286–92.
29 Armendariz-Borunda J, LeGros L Jr,, Campollo O, Panduro A, Rincon AR. Antisense S-oligodeoxynucleotides down-regulate TGF-β-production by Kupffer cells from CCl_4-injured rat livers. *Biochem. Biophys. Acta* 1997; **1353**: 241–52.
30 Okuno M, Akita K, Moriwaki H *et al.* Prevention of rat hepatic fibrosis by the protease inhibitor, camostat mesilate, via reduced generation of active TGF-β. *Gastroenterology* 2001; **120**: 1784–800.
31 Inagaki Y, Mamura M, Kanamaru Y *et al.* Constitutive phosphorylation and nuclear localization of Smad3 are correlated with increased collagen gene transcription in activated hepatic stellate cells. *J. Cell Physiol.* 2001; **187**: 117–23.
32 Schnabl B, Kweon YO, Frederick JP, Wang XF, Rippe RA, Brenner DA. The role of Smad3 in mediating mouse hepatic stellate cell activation. *Hepatology* 2001; **34**: 89–100.

doi:10.1111/j.1440-1746.2006.04398.x

HEPATOLOGY

Urokinase plasminogen activator stimulates function of active forms of stromelysin and gelatinases (MMP-2 AND MMP-9) in cirrhotic tissue

Jaime González-Cuevas,* Miriam Bueno-Topete* and Juan Armendariz-Borunda*,†

*Institute for Molecular Biology in Medicine and Gene Therapy, CUCS, University of Guadalajara and †OPD Civil Hospital of Guadalajara, Guadalajara, Jalisco, Mexico

Key words
carbon tetrachloride, cirrhosis, collagens, hepatic stellate cells, metalloproteinases, urokinase plasminogen activator.

Accepted for publication 28 October 2005.

Correspondence
Dr Juan Armendariz-Borunda, Institute for Molecular Biology in Medicine and Gene Therapy, CUCS, University of Guadalajara, Apdo. Postal 2-123, Guadalajara, Jalisco 44281, México. Email: armendbo@cucs.udg.mx

Abstract

Background: The authors' previous data support the notion that adenoviral-driven urokinase plasminogen activator (u-PA) expression results in reversion of experimental liver cirrhosis. The specific aim of the present study was to decipher the mechanisms involved in the regulation by endogenous/gene-delivered u-PA of matrix metalloproteinases (MMP) and related proteins engaged in degradation of excessive hepatic connective tissue.

Methods: Tissue slices from cirrhotic rat livers were incubated with u-PA-rich supernatants from 24-h-cultured hepatic stellate cells (HSC). Matrix metalloproteinase-2, -9 and tissue inhibitor of metalloproteinases-1 (TIMP-1) were detected by western blot and biologic activity. The HSC that discontinued u-PA production were transfected with the adenovector Adu-PA and serum-free supernatants evaluated for proteolytic activity by MMP-3, MMP-2 and MMP-9. Collagen I, transforming growth factor-β1 (TGF-β1), plasminogen activator inhibitor-1 (PAI-1) and TIMP-1 mRNA levels were also evaluated.

Results and Conclusion: Endogenous u-PA from cultured HSC significantly induced the active forms of MMP-2 (68 kDa) and MMP-9 (78 kDa) in cirrhotic tissue slices. The TIMP-1 molecular forms demonstrated that u-PA pushed the presence of 'free' TIMP-1 (not complexed with MMP; 71%) in cirrhotic tissue. When non-producing u-PA-HSC were transfected with adenoviral vector coding for the functional human protein u-PA (Adhu-PA), an overactivation of MMP-3, MMP-2 and MMP-9 (800%, 48% and 100%, respectively) was found as compared with HSC transfected with control adenovirus encoding green fluorescent protein (Ad-GFP). Finally, gene expression of collagen I, TGF-β1, PAI-1 and TIMP-1 were downregulated by Adhu-PA action as well.

Introduction

Common causes of liver fibrosis and cirrhosis include mostly hepatitis B and C virus and chronic intake of alcohol, representing an enormous worldwide health-care burden.[1,2] It has been well-established at the physiopathological level that during chronic liver injury, a shift occurs in the delicate balance between the deposition and degradation of extracellular matrix (EMC) as a consequence of the relative overabundance and function of fibrogenic factors, tilting the balance towards the development of liver fibrosis and eventual cirrhosis.[3]

Among the multiple factors engaged in these complex, yet coordinated processes, plasminogen activators are well-characterized serine proteases that catalyze the conversion of plasminogen to the broad-spectrum protease plasmin. Urokinase plasminogen activator (u-PA) is a 54-kDa glycoprotein composed by an epiderman growth factor (EGF) domain, a kringle domain and a catalytic domain responsible for the conversion of plasminogen into plasmin. The EGF domain is responsible for u-PA binding with its cognate receptor (u-PAR), which is present in a wide variety of cells including hepatic stellate cells (HSC), macrophages, fibroblasts, monocytes, and endothelial cells. In contrast, u-PA is synthesized by renal parenchymal cells, fibroblasts, epithelial cells, neumocytes and HSC.[4,5] Urokinase plasminogen activator, either directly or through the production of plasmin, can cleave fibronectin and laminin. Plasmin is a protease that degrades fibrin and several other extracellular matrix proteins including fibronectin, laminin, proteoglycans and collagen type IV. In addition, plasmin plays an important role in the activation of different matrix metalloproteinases (MMP), that is, pro-MMP1, pro-MMP-3, pro-MMP-9 and pro-MMP-2, via membrane type (MT)-MMP1 and transforming growth factor-β (TGF-β). The final outcome in the

plasmin production will depend on the net balance between u-PA and plasminogen activator inhibitors (PAI)-1 and PAI-2.[6]

The implications raised by the system plasminogen activators/plasmin are growing in importance and relevance regarding the pathophysiology of extracellular matrix degradation/remodeling in several organs undergoing fibrosis.

Thus, our group has been involved in the design of experimental approaches using strategies of gene therapy/genomic medicine, specifically delivering adenoviral vectors containing u-PA cDNAs to the liver of cirrhotic rats, in order to induce reversion of hepatic fibrosis.

By means of adenoviral vectors (Ad-vectors) we were able to demonstrate that adenoviral vector coding for the functional human protein u-PA (Adhu-PA)-driven expression of u-PA rendered two major important effects: induction of extracellular matrix degradation (i.e. decrease of fibrosis index in 85%) and stimulation of hepatocyte regeneration through hepatocyte growth factor (HGF) and c-met upregulation.[7,8]

Worthwile mentioning, u-PA regulation has been well-studied in carcinogenesis,[9] fibrinolysis[10] and wound healing.[6] In liver, few reports have focused on the role of u-PA.[11–13] Thus, Bezerra *et al.* used u-PA (-/-) and/or t-PA (-/-)-deficient transgenic mice, and investigated the mechanisms involved after performing partial hepatectomy on uPA-non-expressing mice.[13] In contrast, Pérez-Liz *et al.* used HSC to show that TGF-β may regulate gene expression, production and u-PA activity on the HSC surface, but it decreases u-PA secretion to the extracellular space.[14] Therefore, TGF-β might be clocking specific matrix degradation mechanism through the plasminogen activator system. To our knowledge, and with the exception of our previous work,[7,8] there is no published work in the area of liver cirrhosis regarding uPA relevance and influence on MMP activation, as well as on the regulation of fibrogenic molecules involved in TGF-β signaling. Likewise, at the time of writing there was no report on the use of uPA-transfected HSC, either human or rat, in order to unravel the cascade of events involved in MMP activation.

Therefore, in the present paper we focused on the elucidation of collagenolytic mechanisms triggered by u-PA, either endogenously produced by cultured HSC or generated by transfection with Adhu-PA.

Methods

Animals

Male Wistar rats were rendered cirrhotic by chronic administration of CCl_4 during 8 weeks in an animal model that closely resembles human hepatic cirrhosis induced by alcohol abuse or chronic infection with hepatitis C virus.[15] Briefly, animals weighing 80 g received three doses i.p. per week of CCl_4 and mineral oil in a ratio of 1:6 for the first week, 1:5 the second week, 1:4 the third week, and 1:3 for the fourth through eighth weeks. Normal rats were pair-fed and injected with vehicle only. All animal studies were performed in accordance with the University of Guadalajara's animal guidelines. Five male rats were used for each group.

Liver tissue slices from CCl_4-induced cirrhotic and normal animals (400 mg), were incubated according to Cerbon *et al.*[16] in Hank's solution during 3 h at 37°C in an O_2–CO_2 (5%–95%) humid atmosphere at 25 r.p.m. shaking under different stimuli represented by cultured u-PA-containing HSC supernatants (80 μg). In some experiments these supernatants were treated with penicilloic acid to inactivate u-PA enzymatic activity. After these treatments, proteins were extracted from the liver slices and subjected to different analyzes: western blots for tissue inhibitor of metalloproteinases (TIMP)-1, MMP-2 and MMP-9 and zymograms for MMP-2, MMP-9 and MMP-3.

Liver homogenates

Liver slices (400 mg) were minced in protein extraction buffer containing 50 mmol/L Tris-HCl (pH 8.0), 150 mmol/L NaCl, 0.02% sodium azide, 100 μL/mL aprotinin, 1% Triton X-100, 1% phenylmethylsulphonylfluoride, 10 μL/mL aprotinin and 1 μL/mL Statin using a Politron (Brinkman, Switzerland).[17] The homogenate was centrifuged at 12 000 *g* for 30 min at 4°C and supernatant was transferred to a clean tube and stored at −80°C. Protein concentration of each extract was measured according to Bradford.[18]

Western blot for u-PA and TIMP-I, MMP-2 and MMP-9

Increasing amounts of protein from each sample (30, 50 and 80 μg) were boiled for 3 min in the presence of sodium dodecylsulfate (SDS) gel-loading buffer with 10% β-mercaptoethanol and electrophoresed in 12% SDS-polyacrylamide gel electrophoresis (PAGE). The gel was run at 75 mA at room temperature, proteins were transferred to nitrocellulose blocked with 5% non-fat milk in Tris-buffered saline, and incubated with 1:10 000 of polyclonal goat antiuPA (Sigma, St Louis, MO, USA), in 0.5% blocking buffer for 1 h at room temperature. After washing, the blots were incubated with secondary antigoat antibody–horseradish peroxidase conjugate: (1:10 000; Sigma-Aldrich, St Louis, MO, USA) for 30 min at room temperature. After repeated washes, the membranes were incubated in equal volumes of detection reagents 1 and 2 (BM chemiluminescence western blotting kit, Roche, Mannheim, Germany) for 1 h at room temperature and immediately exposed to X-ray film (X O-MAT 1651454 Kodak, Rochester, NY, USA). The same electrophoresis and blotting conditions were used for TIMP-1, MMP-2 and MMP-9 with the exception in the amount of protein loaded. For TIMP-1, 80 μg total protein was used and 350 μg for the rest of the MMP. Primary antibodies were monoclonal antimouse TIMP-1 diluted 1:1000 (Oncogene, Carpinteria, CA, USA) or polyclonal antigoat MMP-2 1:1000 (Santa Cruz Biotechnology, Santa Cruz, CA, USA) or MMP-9 polyclonal antigoat 1:1000 (Santa Cruz Biotechnology). Then, horseradish peroxidase antibodies (40 mU/mL antimouse IgG-peroxidase-labeled [IgG-POD]/antirabbit IgG-POD or antigoat IgG-POD; Roche) were used to develop further with the substrate diacylhydrazide-like luminol.

Assay with cultured hepatic stellate cells

Hepatic stellate cell line and determination of urokinase plasminogen activator

The cell line used in these studies is of human origin (HSC 180) and strongly positive for α-smooth muscle actin (α-SMA).

These cells are high producers of u-PA during the first days of culture. Therefore, cells were grown in 100-mm tissue culture dishes with Dulbecco's Modified Eagle Medium (D-MEM) supplemented with 10% fetal calf serum (FCS), 1% antibiotic–antimycotic solution, and 1% non-essential amino acids for 48 h to reach 80% confluency. Cells were then thoroughly washed with phosphate-buffered saline (PBS) to remove any traces of FCS and incubated for 24 h in serum-free D-MEM, and supernatants were recollected and centrifuged at 330 *g* at 4°C for 5 min. Proteins were determined according to Bradford. Different amounts of proteins were run in 12% SDS-PAGE, and western blots for u-PA were carried out as described earlier.

Urokinase plasminogen activator enzymatic kinetics in cultured hepatic stellate cells

The HSC were grown in 100-mm tissue culture dishes with D-MEM supplemented with 10% FCS, 1% antibiotic–antimycotic solution, and 1% non-essential amino acids for 48 h to reach 80% confluency. Cells were thoroughly washed with PBS to remove any traces of FCS and incubated for 24 h. In additional experiments cells were grown for 5, 7, 14 and 21 days and the serum-free supernatants were recollected and centrifuged at 330 *g* at 4°C for 5 min. Proteins were determined according to Bradford and used for zymography assays.

Urokinase plasminogen activator zymography

A total of 80 µg of total protein supernatants were electrophoresed in a 10% SDS-PAGE containing 1 mg/mL gelatin and 12.5 µg/mL plasmin-free plasminogen. After washing with 2.5 Triton X-100, the gel was incubated at 37°C for 48 h in 100 mmol/L glycine, 20 mmol/L ethylenediamine tetra-acetic acid (EDTA) pH 8.3. The gel was finally stained with 0.5% Coomassie blue. Proteolytic activity of u-PA (54 kDa) was detected as a white zone in a dark field.[19]

Inhibition of urokinase plasminogen activator enzymatic activity

Urokinase plasminogen activator inhibition was carried out with penicilloic acid as described by Higazi and Mayer, based on the fact that when penicillin is subjected to an alkaline medium pH 10, it is hydrolyzed into penicilloic acid.[20] Thus, we used Penicillin G (Pengesod, Mexico) subjected to hydrolysis by 1 mol/L NaOH 1 mol/L (500 mg/4.75 mL) to obtain a final concentration of 1 mol/L penicilloic acid.[21] Supernatants from cultured HSC were mixed with 6, 12 and 48 mmol/L penicilloic acid for 3 h at room temperature and u-PA activity was detected by zymography as previously described. Because the highest inhibition of u-PA was achieved with 48 mmol/L Penicilloic acid, we labeled this as the negative or inhibition control.

Transfection of cultured hepatic stellate cells with Adhu-PA

The natural/spontaneous u-PA production by HSC declines speedily after 24 h of culture. Therefore, we investigated whether transfection of HSC with an adenoviral vector containing the cDNA for u-PA (Adhu-PA) resulted in induced de novo expression of the functional protein.

Thus, cells were grown in 100-mm tissue culture dishes with D-MEM supplemented with 10% FCS, 1% antibiotic–antimycotic solution, and 1% non-essential amino acids for 48 h to reach 80% confluency. Then, cells were thoroughly washed with PBS to remove any traces of FCS and incubated for 5 or 7 days in serum-free D-MEM, transfected with 9×10^8 viral particles/mL of either Adhu-PA[7,22] or an irrelevant vector represented by adenovirus encoding green fluorescent protein (Ad-GFP). Forty-eight hours after transfection, supernatants were recollected and used for detection of enzymatic activity of MMP-2, MMP-9 and MMP-3 by zymography.

The production of Adhu-PA and Ad-GFP, replication-defective adenovirus vectors, has been previously described.[7,23] The vectors were prepared under good laboratory practice conditions, titered, characterized and had a vector particles (vp) to infection units (IU) ratio of <30.

Zymography for detecting MMP-9 MMP-2 and MMP-3

A total of 30 µg from cell culture supernatants was loaded onto 10% SDS-PAGE gel containing either 1 mg/mL gelatin (Bio-Rad Laboratories, Hercules, CA, USA) or casein 2 mg/mL diluted in PBS; after electrophoresis, SDS was removed from the gel by incubation in 2.5% Triton X-100 at room temperature with gentle shaking. The gel was washed with distilled water to remove detergent and incubated at 37°C for 48 h in a developing buffer containing 50 mmol/L Tris-HCL at pH 7.6, 0.2 mol/L NaCl, 5 mmol/L $CaCl_2$, and 0.02% BRIJ35 (Sigma-Aldrich).[24] Whenever casein was used as a substrate for MMP-3, the developing buffer contained 0.1 mol/L glycine pH 8.3.[25] The gel was then stained with a solution of 30% methanol, 10% glacial acetic acid, and 0.5 Coomassie Blue G-250, followed by destaining in the same solution without dye. Proteinase activity was detected as unstained bands on blue background representing areas of gelatin digestion, the activities in the gel slabs were quantified (arbitrary units) using an image analysis program. Degradation bands were observed at 66 kDa (MMP-2), 80 kDa (MMP-9), and 55 kDa (MMP-3).

Analysis of collagen I, TGF-β1, PAI-I and TIMP-1 gene expression by reverse transcriptase–polymerase chain reaction

Isolation of RNA from HSC transfected with adenovirus vectors was carried out according to the method described by Chommczynsky and Sacchi.[26] We then used reverse transcriptase–polymerase chain reaction (RT-PCR) according to previously described methodology.[27] Target genes were detected using oligonucleotide primers and conditions shown in Table 1. The RNA from HSC was isolated with Trizol, and 2 µg of total RNA were reverse transcribed in 0.05 mol/L Tris –HCl pH 8.3, 40 mmol/L KCL, 7 mmol/L $MgCl_2$ buffer containing 0.05 µg/µL random hexamers, 1 mmol/L dinucleotide triphosphate (dNTPS) mix, 0.05 U/µL RNase inhibitor and 200 U/µL Moloney murine leukemia virus (M-MLV) reverse transcriptase. Samples were incubated for 10 min at 70°C and then 60 min at 37.5°C. Reverse transcriptase was further inactivated by heating the sample tubes at 95°C for

10 min. The cDNAs obtained in this way were used immediately for reaction or were stored at −20°C until use. The levels of expression of all transcripts were normalized against expression of glyceraldehyde-3-phosphate-dehydrogenase (GAPDH) mRNA in the same tissue sample. Gene product amplification was performed in a PCR buffer of 50 mmol/L Tris-HCL pH 9.0 and 50 mmol/L NaCl containing a mix of 100 µmol/L dNTPs and 1 U of Taq DNA polymerase. Amplification reactions were overlaid with a light mineral oil and held at 95°C for 'hot start' PCR for 5 min and run in an automated thermal cycle for the number of cycles specified in Table 1.[28] and for annealing conditions show in Table 1.

Photographic and densitometric scanning

The densitometric analyses of the PCR products were performed in a DU series Beckman spectrophotometer using a gel scan area program. Samples prepared by electrophoresis were photographed with 665 polaroid film while being exposed to UV light and the negative of the film containing the dark bands was scanned by the instrument. After the scan was complete, the area corresponding to amplified PCR products was automatically calculated and normalized against the area represented by the expression of the constitutive gene (*GAPDH*). The results were then expressed as arbitrary absorbance units. Levels of significance were determined by Student's *t*-test.

Statistical analysis

All results are expressed as mean ± SD. Results were analyzed by the Student's *t*-test. $P < 0.05$ was considered statistically significant.

Results and discussion

Urokinase plasminogen activator secretion by hepatic stellate cells

The characterization of the HSC cell line used here demonstrated the functionality of several molecules involved in the plasminogen activator pathway. When supernatants from HSC in cultured XXX were analyzed, we found that 24-h culture supernatants contained the highest levels of u-PA as demonstrated by western blot (Fig. 1a). The kinetics of u-PA proteolytic activity was analyzed by a zymography assay. Supernatants from HSC cultured at different times were re-collected, and the highest level of enzymatic activity for endogenous u-PA was found in the 24 h supernatants, declining thereafter and being undetectable from the 5th to 21th day of culture (Fig. 1b).

These results coincide with previous reports in which rat HSC was shown to have a similar behavior concerning expression and production of u-PA, because rat HSC cells dramatically decreased their u-PA production after 7 days in culture, a time-frame were these cells entered the well-described 'activation process'.[5]

The cell line used in ongoing experiments in the authors' laboratory (HSC 180) was initially derived from a cirrhotic liver, suggesting that these cells are already in advanced activated status. Our findings are in good and clear correlation with a previous study by Sancho-Bru *et al.*, in which freshly isolated HSC from human cirrhotic livers were seen to have morphological and immunophenotypical features of myofibroblast-like cells as early as 24 h in culture.[29] Also, these cirrhotic human HSC markedly expressed genes involved in fibrogenesis, inflammation and apoptosis. Specifically, gene expression determination by microarray analysis showed that u-PA gene expression in freshly isolated HSC from cirrhotic livers dropped ninefold (from 27.6 to 3.4 relative units) after 7 days in culture. Concerning this issue, we are in the process of evaluating and analyzing in our HSC 180 the presence of transcriptional factors responsible for induction/downregulation of u-PA promoter (Ets-1, nuclear factor [NF]-κB, AP-1, and Rel).[30,31] This will shed light on how this loss of uPA production takes place.

Furthermore, and in order to verify the specificity of our functional assay, we conducted experiments with polyacrylamide gels containing the substrate gelatin in the presence or absence of plasminogen. As can readily be appreciated in Fig. 1(c), the degradation band corresponding to u-PA (54 kDa) was not detected when plasminogen was not included in the gel, thereby ratifying the specificity of the proteolytic enzyme for its substrate.

A control representing the inactivation of u-PA function was required. Therefore, the inhibition of u-PA enzymatic activity was carried out by means of penicilloic acid according to previous reports using an *in vitro* model of thrombolysis by Higazi and Mayer,[20] where 6 mmol/L penicilloic acid was sufficient to inactivate u-PA. The inhibition was found to be competitive and dose-dependent, and is due to the interaction of the hydrophobic side of

Table 1 Oligonucleotides sequences used for RT-PCR

Genes	Tm (°C)	No. cycles	Primers	Sequence	Size (bp)
Collagen 1	70	29	Sense	5'AGA TGG ATC AAG TGG ACA TC-3'	449
			Antisense	3' CAT GTT TCT CCG GTT TCC AT5'	
PAI-1	61	30	Sense	5'-CCA ACA GAG GAC TTCT TGG TCT 3'	808
			Antisense	3' CAC AGA GAG AGT CTG GCC ACG T 5'	
TGF-β	60	28	Sense	5'-GAA ACC CAC AAC GAA ATC TAT G-3'	295
			Antisense	3' CCT CCA CGG CTC AAC CAC-3'	
TIMP-1	65	32	Sense	5'-GAC CTG GTC ATA AGG GCT AAA3'	551
			Antisense	3' GCC CGT GAT GAG AAA CTC TTC ACT5'	
GAPDH	60	30	Sense	5'-GCA GGG GGG AGC CAA AAG GG3'	567
			Antisense	3' TGC CAG CCC CAG CGT CAA AG-3'	

GAPDH, glyceraldehyde-3-phosphate-dehydrogenase; PAI-I, plasminogen activator inhibitor-1; RT-PCR, by reverse transcriptase-polimerase chain reaction; TGF-β, transforming growth factor β; TIMP-1, tissue inhibitor of metalloproteinases; Tm, annealing temperature.

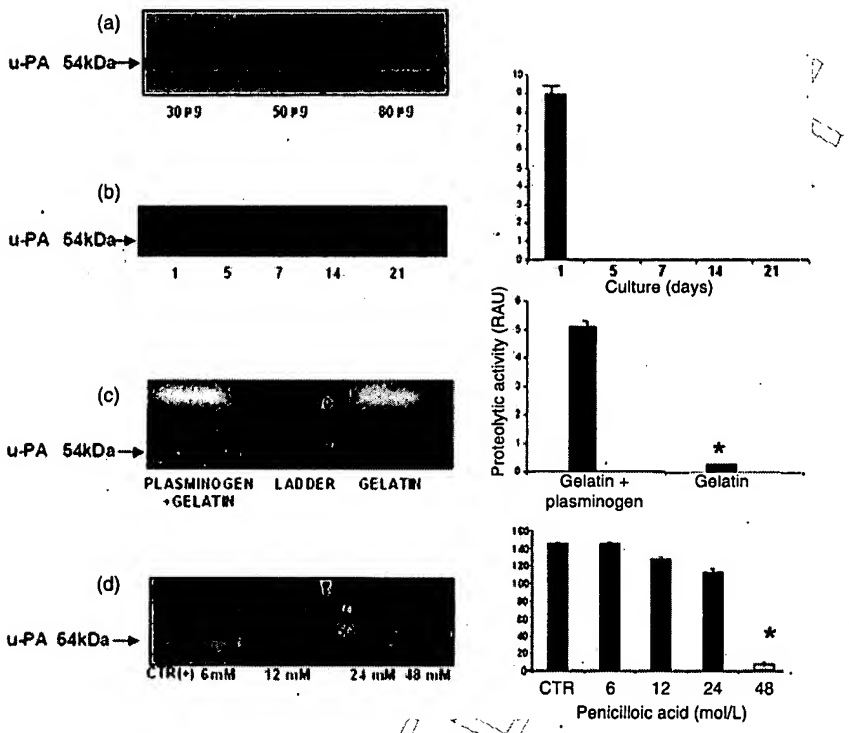

Figure 1 Urokinase plasminogen activator (u-PA) expression by hepatic stellate cells (HSC) in culture. The HSC were cultured for different periods (1, 5, 7, 14 and 21 days) in which only the last 24 h in each case, were cultured in serum-free D-MEM. Then, serum-free supernatant were re-collected. (a) Western blot in which increasing amounts of total proteins were separated in 12% sodium dodecylsulfate–polyacrylamide gel electrophoresis (SDS-PAGE), transferred to polyvinylidene fluoride (PVDF) membranes and incubated with a goat antihuman-u-PA monoclonal antibody and then with a secondary antigoat–horseradish peroxidase conjugate for developing. Band corresponding to u-PA was localized at 54 kDa. Data shown correspond to supernatants obtained at 1 day of culture where the maximum endogenous u-PA expression was found. (b) Maximum u-PA enzymatic activity in 1-day supernatants; 30 µg of total protein were separated in a 12% SDS-PAGE in the presence of gelatin (1 mg/mL) and 12.5 µg/mL plasminogen. Gels were incubated for 48 h and stained with Coomassie Blue. Clear bands representing substrate degradation were corroborated by means of molecular weight markers and quantified by densitometric scan using an EDAS-KODAK program. (c) Specificity of u-PA proteolytic activity assay; 80 µg of total protein were separated in a 12% SDS-PAGE in the presence or absence of 12.5 µg/mL plasminogen. Gels were incubated for 48 h and stained with Coomassie Blue. Clear bands representing substrate degradation were corroborated by means of molecular weight markers and quantified by densitometric scan using an EDAS-KODAK program. $*P < 0.005$. (d) Inhibition of u-PA enzymatic activity; 80 µg of protein from 24-h supernatants from cultured HSC were incubated for 3 h with different molarities of penicilloic acid at room temperature. Then, samples were subjected to electrophoresis under non-reducing conditions, suplementing the acrylamide with gelatin and plasminogen. Clear bands representing substrate degradation were corroborated by means of molecular weight markers and quantified by densitometric scan using an EDAS-KODAK program. $*P < 0.005$. RAU, relative absorbance units.

the chain of the penicillins with the active site of urokinase. Because the present experimental conditions are different, we produced a dose–response curve and found that as much as 48 mmol/L penicilloic acid was necessary to achieve a 90% reduction in u-PA activity (Fig. 1d), indicating that high concentrations of u-PA are present in the supernatants of the present cultured HSC.

Urokinase plasminogen activator-rich supernatants from hepatic stellate cells influence TIMP-1, MMP-2 and MMP-9 levels in cirrhotic liver tissue slices

One of our major objectives has been to elucidate the mechanisms by which u-PA is inducing reversion of liver fibrosis and hepatic regeneration. Thus, in previous reports from our laboratory at the Institute of Molecular Biology in Medicine and Gene Therapy, Guadalajara, we showed an increased expression of different MMP in cascade, driven by the influence of an Ad-vector containing u-PA cDNA.[7,8] Regardless of the high specificity of the antibodies used in those previous assays, we could not be sure of the actual bio-functionality of these proteins. Here, we have shown increased expression and bio-activity of MMP and we have extended in the mechanisms by describing the involvement of increased amounts of free-TIMP. Our reasoning for these experiments was based on the assumption that regulation of MMP activity takes place, in part through its coupling and inactivation of the MMP catalytic site by TIMP, and that the finding of more species of free-TIMP is indicative of more active MMP. Thus, we designed experiments in which liver slices from cirrhotic rat livers

were incubated in an appropriate atmosphere with supernatants rich in u-PA coming from HSC cultured at different times, to identify the predominant form of TIMP in the tissue slices. Towards that end, we made use of a monoclonal antibody against free TIMP-1 and/or complexed with MMP TIMP-1. According to different reports our results demonstrated no detectable levels of free TIMP-1 in cirrhotic livers when incubated with u-PA-free supernatant.[32] Nonetheless, parallel cirrhotic livers contained increased amounts of free-TIMP-1 (71%) after incubation with u-PA-rich supernatants, as can be appreciated by the western blot shown in Fig. 2. In order to verify the specificity of this experimental approach, u-PA-rich supernatants were first inactivated with penicilloic acid and then put in contact with liver slices from cirrhotic livers for 3 h; proteins were extracted and the western blot assays demonstrated a negligible expression of free TIMP-1, significant data as compared with the other two experimental conditions ($P < 0.005$; Fig. 2a). Determination of the complexed TIMP-1–MMP showed no significant differences amid the different groups (data not shown), probably as a consequence of protein saturation in the assay, given the amount of protein we used in order to pick up the free form of TIMP-1. It is known that in cirrhosis, the prevalent form of TIMP-1 is represented by complexes inhibiting extracellular matrix degradation/remodeling.[32] These new findings confirm and extend our previous reports.[7,8]

The task of interstitial collagenases is crucial in the initiation of collagen breakdown. Then, the downstream function of gelatinases plays a key role in finishing the complete degradation of collagen molecules. Therefore, we set up the assay for detecting expression of the two MMP-2 and MMP-9 gelatinases. Figure 2(b,c) clearly shows that active MMP-2 and MMP-9 (68 kDa and 78 kDa, respectively) are the predominant species of these two collagenases in cirrhotic liver slices incubated with HSC supernatants rich in u-PA. Meanwhile in the control groups (i.e. cirrhotic liver slices incubated with u-PA-free supernatants) only latent forms of MMP-2 and MMP-9 were detectable as 72 kDa and 92 kDa pro-metalloproteinases, respectively. Although several previous papers have attempted to describe the specific role of u-PA in other systems,[33,34] to our knowledge this is the first report describing the central role of u-PA in hepatic tissue regarding mechanisms activating and triggering fibrinolytic mechanisms on one side, and impeding the inactivation of MMP on the other, key events in the precise and coordinated process of experimental liver cirrhosis reversion.

Effect of transduction of cultured hepatic stellate cells with the adenoviral vector Adhu-PA

We used cell cultures of HSC at 5 and 7 days, because by this time the endogenous and spontaneous u-PA production had ceased. Therefore, efficiency of transfection was first evaluated by means of Ad-GFP adenovirus and the consequent green fluorescent protein expression as a reporter system. We achieved 100% transfection efficiency with a dose of 9×10^8 vp/mL (Fig. 3a). Our results are in agreement with previous reports by Weiskirchen *et al.* in cultured HSC and myofibroblasts, in which they compared the use of a similar Ad system driven by the promoter of cytomegalovirus and found a 100% efficiency of transfection as compared with only a 6% efficiency when using liposomes as a carrier for transfecting DNA.[35] Concurrent with the reporter gene data, 9×10^8 vp/mL of Adhu-PA significantly stimulated u-PA-induced production ($P < 0.005$) as determined by zymography at day 5 (eightfold) and

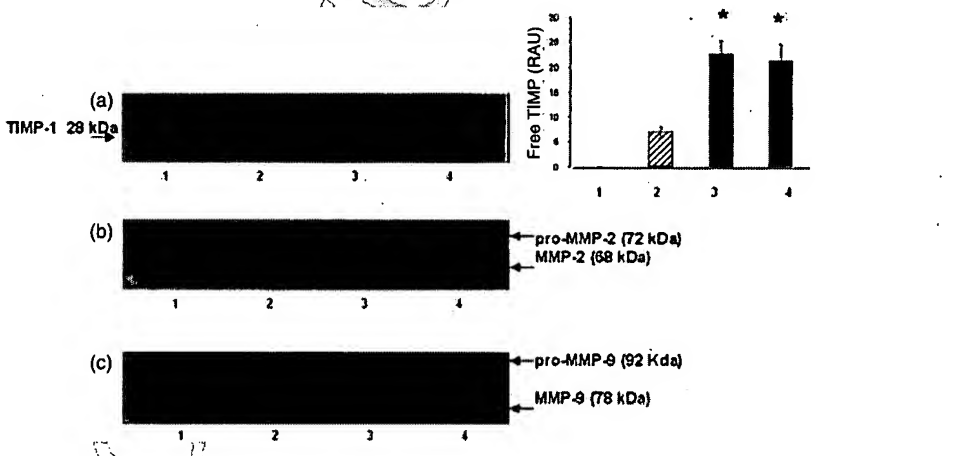

Figure 2 Expression of tissue inhibitor of metalloproteinases-1 (TIMP-1), matrix metalloproteinase (MMP)-2 and MMP-9 in cirrhotic tissue stimulated with hepatic stellate cell (HSC) supernatants. Cirrhotic tissue slices were incubated with urokinase plasminogen activator (u-PA)-rich supernatants from cultured HSC, proteins were extracted and run in a 12% odium dodecylsulfate–polyacrylamide gel electrophoresis (SDS-PAGE), transferred to polyvinylidene fluoride (PVDF) membranes and incubated separately with a monoclonal antimouse TIMP-1 antibody, polyclonal antigoat MMP-2 (1:1000; Santa Cruz Biotechnology) or polyclonal antigoat MMP-9 (1:1000; Santa Cruz Biotechnology) and developed using a secondary antibody–horseradish peroxidase conjugate and a chemiluminescence system. Corresponding bands for free TIMP-1 were quantified via densitometric scan using an EDAS-KODAK program. Values for each graph represent the mean ± SD of three different determinations. Lane 1, cirrhotic tissue incubated with plain D-MEM; lane 2, cirrhotic tissue incubated with u-PA-rich supernatants inactivated with penicilloic acid; lanes 3 and 4, cirrhotic tissue incubated with u-PA-rich supernatants from cultured HSC. RAU, relative absorbance units; *$P < 0.05$ (2 vs 3 and 4).

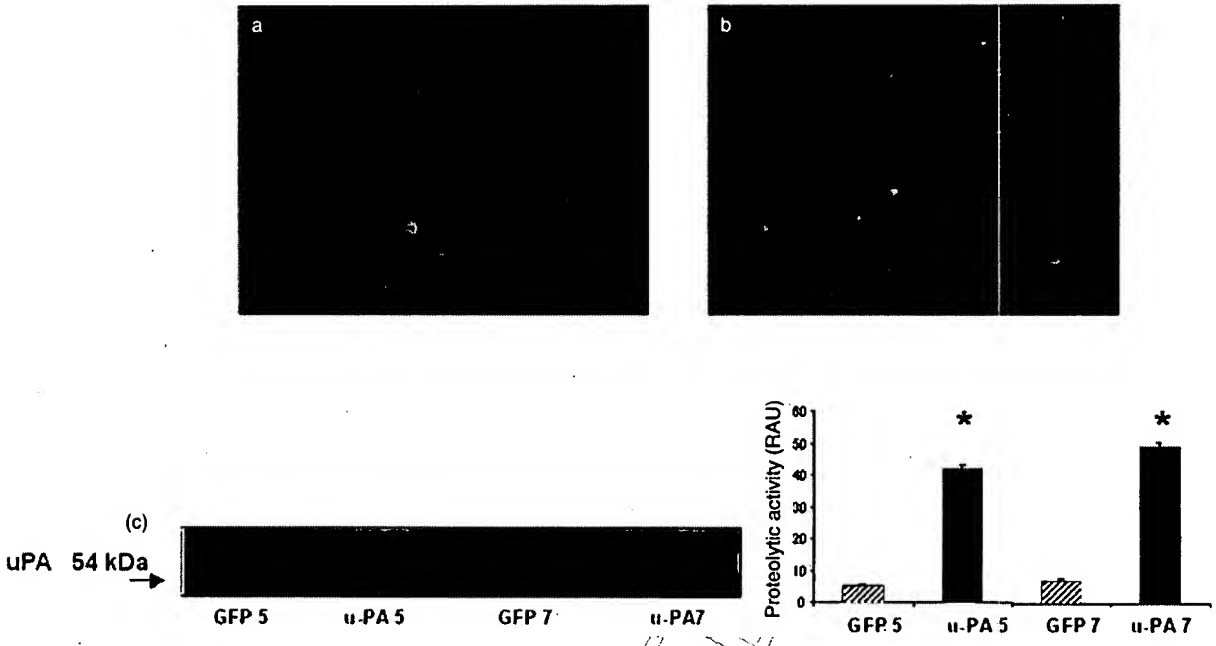

Figure 3 Transfection of hepatic stellate cells (HSC) with adenoviral vector coding for the functional human protein u-PA (Adhu-PA) and adenovirus encoding green fluorescent protein (Ad-GFP). The HSC, which stopped producing urokinase plasminogen activator (u-PA; 5th and 7th day of culture), were transfected with Adhu-PA and Ad-GFP. After 48 h in culture, cells were stimulated with fluorescent light at 520 nm to check for efficiency of transfection and 100% of the cells were successfully transfected (a, ×400; b, ×100). (c) Supernatants were re-collected, total proteins determined and separated by electrophoresis copolymerizing acrylamide with gelatin (1 mg/mL) plus plasminogen (12.5 μg/mL) to detect u-PA proteolytic activity by zymography. Clear bands were scanned and quantified using automated software EDAS-KODAK. Values for each graph represent the mean ± SD of three different determinations. GFP, transfected cells with irrelevant vector; u-PA, cells transfected with Adhu-PA. *$P < 0.005$ (u-PA 5 vs GFP 5 and u-PA 7 vs GFP7).

at day 7 (9.5-fold; Fig. 3b). Worth mentioning, HSC 180 cells used here displayed a characteristic u-PA pattern of expression: peaking in the first 24 h of culture and quickly declining thereafter (Fig. 1b). Results shown in Fig. 3 highlight the efficiency of transfection and reinforce the importance of u-PA action in our experimental strategy in mediating the triggering of antifibrogenic mechanisms.

Efficient transfection of hepatic stellate cells with adenovector Adhu-PA results in upregulation of MMP-3, MMP-2 and MMP-9 activities

As shown in Fig. 3, Adhu-PA-driven u-PA production can be efficiently accomplished once the endogenous u-PA production by HSC has ceased, and this fact allowed us to demonstrate additional roles on the antifibrogenic and fibrinolytic mechanisms involved in fibrotic material remodelling. The Adhu-PA transfection produced a significant increase in enzymatic activity of metalloproteinases using ad hoc substrates chosen for MMP specificity. By zymography, bio-activity of MMP-3 (stromelysin-1) was found to be increased eightfold over control Ad-GFP-transfected HSC cells at both 5 and 7 days after culture (Fig. 4a). The substrate used in this assay was casein. Furthermore, we also found a good correlation of protein induced by Adhu-PA transfection, which resulted in an increased amount of protein stromelysin-1 as determined by western blot, but far less MMP-3 was produced by HSC transfected with Ad-GFP ($P < 0.05$; Fig. 4b).

Figure 5(a) shows overexpression of MMP-2 (48%) and MMP-9 (100%) proteolytic activity in HSC under the influence of Adhu-PA as compared with their counterpart cells transfected with the irrelevant Ad-GFP ad-vector used as control ($P < 0.005$). This pattern was constant throughout the 5th and 7th day of culture (Fig. 5).

Cultured HSC have been long recognized as a suitable experimental model resembling *in vivo* liver fibrosis, given their specialized cellular and molecular characteristics,[3] changing from a quiescent, vitamin A-rich, non-proliferative cell to a highly contractile, proliferative and collagen I-, III- and IV-producing cell. Classic studies performed by several groups on kinetics of different MMP expression by cultured HSC, have demonstrated decreased MMP-3 expression and bio-activity in cultured HSC.[34,36,37] The present results correlate well with those previous reports and highlight the relevance of Adhu-PA-driven induced MMP-3 enzymatic activity in the context of the hepatic fibrosis process. Along these lines, it is well known that MMP-3 possesses a wide range of extracellular matrix component degradation, that is, fibronectin, laminin, elastin, proteoglycans, and collagens IV,V, IX, X. Furthermore, MMP-3 plays a role in the direct activation process of several latent metalloproteinases such as pro-MMP-1,

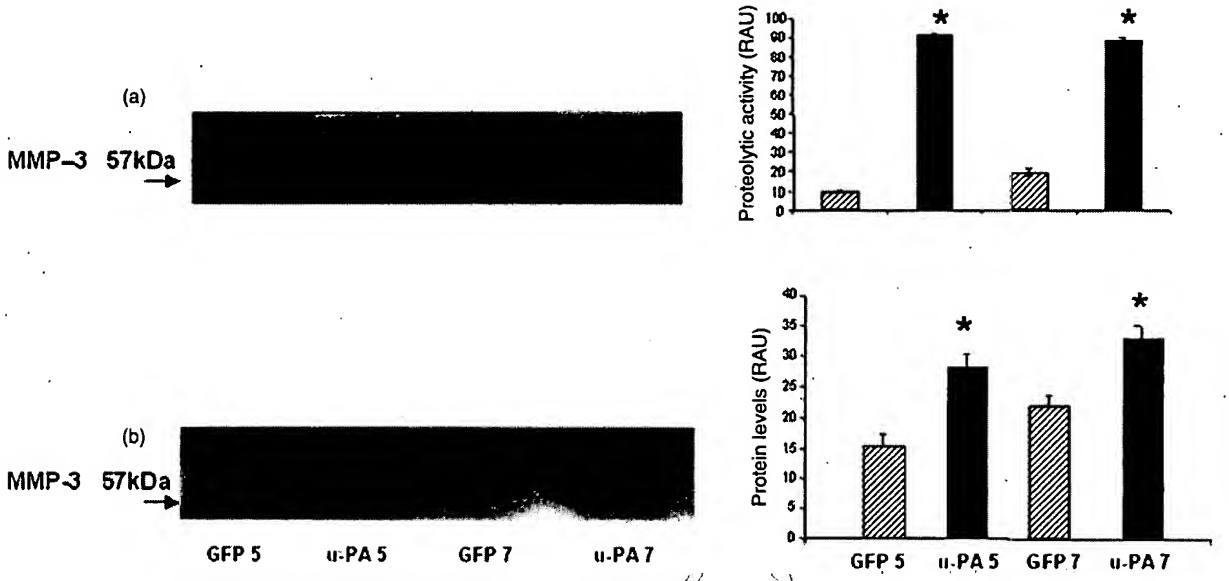

Figure 4 Expression of matrix metalloproteinase (MMP)-3 in adenoviral vector coding for the functional human protein u-PA (Adhu-PA)-transfected hepatic stellate cells (HSC). (a) Zymography demonstrating MMP-3 enzymatic activity. Polyacrylamide gels were copolymerized with casein (2 mg/mL). GFP 5,7, HSC transfected with adenovirus encoding green fluorescent protein (Ad-GFP) at 5th and 7th day of culture; u-PA 5,7, HSC transfected with Adhu-PA at 5th and 7th day of culture. $^*P < 0.005$ (u-PA 5 vs GFP 5). (b) Proteins were extracted from Adhu-PA and Ad-GFP-transfected cells, run in 12% electrophoresis, and transferred to polyvinylidene fluoride (PVDF) membranes. MMP-3 protein was detected with a goat polyclonal anti-MMP-3 antibody (1:800) and a secondary antigoat IgG-POD developed with chemiluminiscence. Values for each graph represent the mean ± SD of three different determinations. $^*P < 0.005$ (u-PA 7 vs GFP 7). RAU, relative absorbance units.

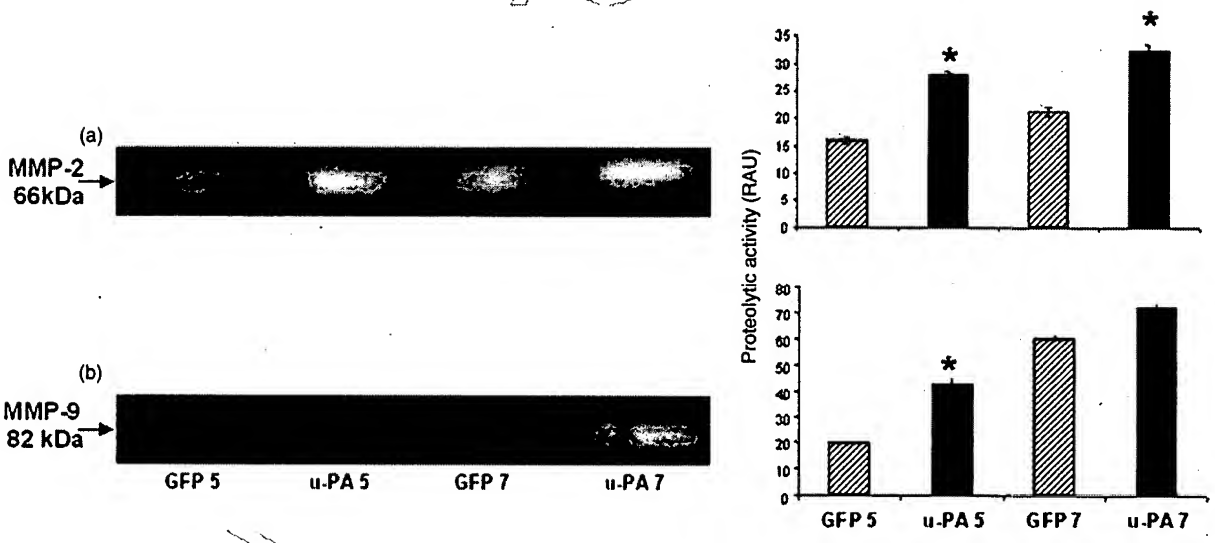

Figure 5 Biologic activity of active matrix metalloproteinase (MMP)-2 and active MMP-9 in hepatic stellate cells (HSC) transfected with adenoviral vector coding for the functional human protein u-PA (Adhú-PA). (a,b) Zymography showing the enzymatic activity of (a) MMP-2 and (b) MMP-9. Polyacrylamide gels were copolymerized with gelatin (2 mg/mL). GFP 5,7, HSC transfected with adenovirus encoding green fluorescent protein (Ad-GFP) at 5th and 7th day of culture; u-PA 5,7, HSC transfected with Adhu-PA at 5th and 7th day of culture. Values for each graph represent the mean ± SD of three different determinations. $^*P < 0.005$ (u-PA 5 vs GFP 5 and u-PA 7 vs GFP7). RAU, relative absorbance units.

-7, -8, -9, and -13.[38] All these data together, indicate that MMP-3 is a key element in the triggering of the extracellular matrix degradation cascade.

The MMP-1 and MMP-8 antifibrotic role has been documented in experimental models of liver cirrhosis by using targeted gene delivery.[39] However, MMP-8 is produced by cells outside the liver and therefore it was not detected in the present study. In contrast, the role of MMP-1 is currently being determined.

Transfection of hepatic stellate cells with Adhu-PA produces downregulation of pro-fibrogenic genes involved in liver fibrosis

The role of u-PA in the onset and progression of hepatic fibrosis was evaluated by means of semiquantitative RT-PCR. Four key molecules were studied and their steady-state levels decreased importantly after transfection with Adhu-PA in HSC cultured for 5 and 7 days. Hence, collagen type I (twofold), TGF-β (twofold), PAI-1 (threefold) and TIMP-1 (fourfold) mRNAs were shown to be significantly decreased as compared with the HSC transfected with the control Ad-vector Ad-GFP (Fig. 6). Worth mentioning, the drop in mRNA expression was more evident on the 5th day of HSC culture, suggesting that at the 7th day of culture the mechanisms of HSC activation were working more efficiently, which is reflected in higher transcription/expression of the key molecules studied. Of those, TGF-β deserves special consideration.

Transforming growth factor-β is a pleiotropic protein that plays a central role in almost every fibrogenic process described to date. Thus, TGF-β is implicated in fibrosis occurring in lung, kidney, heart, liver and skin (hypertrophic scars and queloids).[40] It is well-established that TGF-β stimulates extracellular matrix production as well as protease inhibitors (PAI-1, TIMP-1).[41]

Our results clearly demonstrate in HSC, which have ceased u-PA production, that Adhu-PA transfection is sufficient to induce (in a novel fashion) the synthesis and expression of the corresponding protein u-PA. Consequently, Adhu-PA transfection results in a highly specific decrease of TGF-β expression, and at the same time of genes such as PAI-1, TIMP-1, and collagen type I, which respond to intracellular signals generated by TGF-β and are involved in perpetuation of fibrogenesis.[42]

In correlation with our results, the role of u-PA in converting latent pro-MMP-9 into its active form has been demonstrated in different systems. Thus, it has been recently described that osteopontin, a sialic acid-rich, non-collagenic phosphoglycoprotein, generates NF-κb-inducing kinase (NIK)-dependent NF-κB activation through extracellular signal regulated kinase (ERK)/IKKβ/β-mediated pathways. The phosphorylation NF-κB inhibitor inducing its degradation to let NF-κB migrate to the nucleus and stimulate u-PA gene expression. In that paper Rangaswami *et al.* used cells from murine melanoma and an experimental murine model of tumors to show how osteopontin induced significant u-PA activation, resulting in conversion of pro-MMP-9 to active MMP-9.[43]

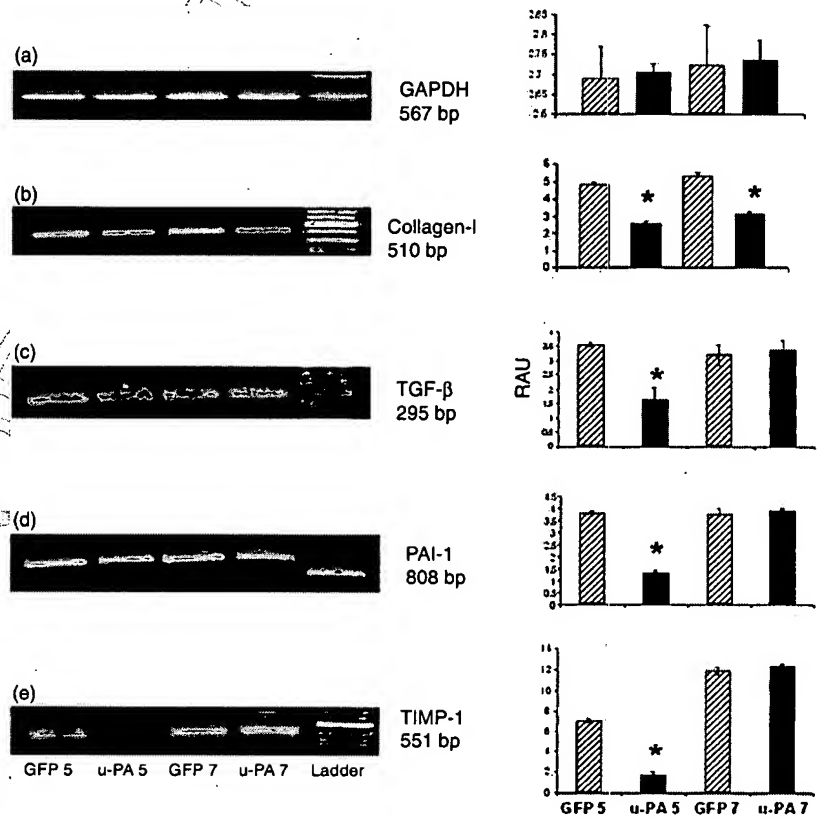

Figure 6 Gene expression for transforming growth factor-β (TGF-β), plasminogen activator inhibitor-1 (PAI-1), collagen-1 and tissue inhibitor of metalloproteinases-1 (TIMP-1) determined by semiquantitative reverse transcriptase–polymerase chain reaction (RT-PCR). Total RNA was extracted from hepatic stellate cells (HSC) cultured for 5 and 7 days and transfected with adenoviral vector coding for the functional human protein u-PA (Adhu-PA) and adenovirus encoding green fluorescent protein (Ad-GFP). Histograms are shown in the right panel where intensity of multiple photographed bands were recorded with a digital camera and quantified with a computer program to average levels of mRNA transcripts for the specified genes. In order to rule out experimental caveats, final RT-PCR determinations were carried out between the linear range and then standardization of each cDNA was accomplished with glyceraldehyde-3-phosphate-dehydrogenase (GAPDH) gene as the constitutively expressed gene. The RT-PCR reactions were routinely performed from 30 to 35 cycles using oligonucleotides primer show in Table 1. GFP 5,7, HSC transfected with Ad-GFP at 5th and 7th day of culture; u-PA 5,7, HSC transfected with Adhu-PA at 5th and 7th day of culture. *All P were <0.05 except for TIMP-1, which was <0.005 (u-PA 5 vs GFP 5 and u-PA 7 vs GFP 7). RAU, relative absorbance units.

As has been shown before, metabolism of MMP-9 is considered to be one of the more complex among the family of MMP, and the majority of the cells studied to date do not constitutively express the active form of MMP-9, but instead require several stimuli in order to produce it.[44,45]

Contrary to what has been shown with cultured cells (MDA-MB 231) derived from human mammary carcinoma and the data described here, MDA-MB 231 cells do not produce enough endogenous u-PA to activate MMP-9. Instead, activation by MMP-3 of pro-MMP-9 to the 82-kDa active form is an efficient mechanism.[46] These data clearly indicate the different types of u-PA production by HSC cells used in the present system.

Taking all these data together, our results suggest that the present activated HSC produce u-PA that stimulates, on one side, activation of key MMP in extracellular matrix degradation, such as MMP-3, MMP-2 and MMP-9. In contrast, u-PA is also involved in the gene downregulation of key pro-fibrogenic molecules, that is, TGF-β, PAI-1, TIMP-1 and collagen type I.

Acknowledgment

This work was supported by the Consejo Estatal de Ciencia y Tecnología de Jalisco, Project No. 08-2004.

References

1 Chief Medical Officer. *Annual Report of the Chief Medical Officer 2001. Liver Cirrhosis: Starting to Strike at Younger Ages.* XXX: Department of Health, XXX. Available from: http://www.doh.gov.uk/cmo/annual [Accessed XX XXX XXXX] report 2001/livercirrhosis.htm

2 Day CP. Non-alcoholic steatohepatitis (NASH): where are we now and where are going? *Gut* 2002; 50: 585–5.

3 Friedman SL. The cellular basis of hepatic fibrosis: mechanisms and treatment strategies. *N. Engl. J. Med.* 1993; 328: 1828–35.

4 Darras V. Measurement of urokinase-type plasminogen activator (u-PA) with an enzyme-linked immunosorbent assay (ELISA) based on three murine monoclonal antibodies. *Thromb. Haemost.* 1986; 56: 411–14.

5 Leyland H, Gentry J, Arthur M, Benyon R. The plasminogen-activating system in hepatic stellate cells. *Hepatology* 1996; 24: 1172–8.

6 Way-yee LI, Chong SSN, Huang EY, Tuan T-L. Plasminogen activator/plasmin system: a major player in wound healing? *Wound Repair Regen.* 2003; 11: 239–47.

7 Salgado S, Garcia J, Vera J *et al.* Cirrosis is reverted by urokinase-type plasminogen activator gene therapy. *Mol. Ther.* 2000; 2: 545–51.

8 Miranda-Diaz A, Rincon AR, Salgado S *et al.* Improved effects of viral gene delivery of human uPA plus biliodigestive anastomosis induce recovery from experimental biliary cirrhosis. *Mol. Ther.* 2004; 9: 30–7.

9 Choong P, Faorth A, Nadesapillai A. Urokinase plasminogen activator system. *Clin. Orthop.* 2003; 415S: S46–S48.

10 Mondino A, Blasi F. uPA and uPAR in fibrinolysis, immunity and pathology. *Trends Immunol.* 2004; 25: 450–6.

11 Carmeliet P, Schoonjans L, Kieckens L *et al.* Physiological consequences of loss of plasminogen activator gene function in mice. *Nature* 1994; 368: 419–24.

12 Carmeliet P, Bouche A, De Clerq C *et al.* Biological effects of disruption of the tissue type plasminogen activator, urokinase-type plasminogen activator, and plasminogen activator inhibitor-1 genes in mice. *Ann. N.Y. Acad. Sci.* 1995; 748: 367–81.

13 Bezerra JA, Currier AR, Melin-Aldana H *et al.* Plasminogen activators direct reorganization of the liver lobule after acute injure. *Am. J. Pathol.* 2001; 158: 921–9.

14 Pérez-Liz G, Flores-Hernández J, Arias-Montaño JA, Reyes-Esparza JA, Rodríguez-Fragozo L. Modulation of urokinase-type plasminogen activator by transforming growth factor beta1 in acetaldehyde-activated hepatic stellate cells.. *Pharmacology* 2005; 73: 23–30.

15 Armendàriz-Borunda J, Seyer JM, Kang AH, Raghow R. Regulation of TGFβ gene expression in rat liver intoxicated with carbon tetrachloride. *FASEB J.* 1990; 4: 215–21.

16 Cerbon Ambriz J, Gonzalez E, Rojkind M. Lactate and piruvate increase the incorporation of (^{3}H) proline into collagen (^{3}H) hydroxyproline in liver slices of CCL4 cirrhotic rats. *Lab. Invest.* 1987; 57: 392.

17 Sambrook J, Fritsch EF, Maniatis T, eds. *Molecular Cloning: A Laboratory Manual*, 2nd edn. New York: Cold Spring Harbor Laboratory Press, 1989.

18 Bradford MM. A rapid and sensitive method for the quantitation of proteing utilizing the principle of protein-dye binding. *Annal. Biochem.* 1976; 72: 248–54.

19 Monvosin A, Neaud V, De Ledinghen V *et al.* Direct evidence that hepatocyte growth factor-induced invasion of hepatocellular carcinoma cells is mediated by urokinase. *J. Hepatol.* 1999; 30: 511–18.

20 Higazi A-R, Mayer M. In vitro inhibition of urokinase by penicicillins. *Thromb. Haemost.* 1988; 60: 305–7.

21 Chain Ernest B. *The Chemical Structure of the Penicillins.* Nobel Lecture, March 20, 1946. Available from: http://nobelprize.org/medicine/laureates/1945/chain-lecture.pdf [Accessed XX XXX XXXX].

22 Lieber A, Vrancken PM-J, Gown A, Perkins J, Kay MA. A modified urokinase plasminogen activator induces liver regeneration without bleeding. *Hum. Gene Ther.* 1995; 6: 1029–37.

23 Nyberg-Hoffman C, Shabram P, Li W, Giroux D, Aguilar-Cordova E. Sensitivity and reproducibility in adenoviral infectious titer determination. *Nat. Med.* 1997; 3: 808–11.

24 Kenagy RD, Nikkari ST, Welgus HG, Clowes AW. Heparin inhibits the induction of three matrix metalloproteinases (stromelysin, 92-kD gelatinase, and collagenase) in primate arterial smoth muscle cells. *J. Clin. Invest.* 1994; 93: 1987–93.

25 Roche PC, Campeau JD, Shaw STJ. Comparative electrophoretic analysis of human and plasminogen activators in SDS polyacrylamide gels containing plasminogen and casein. *Biochim. Biophys. Acta* 1983; 745: 82–9.

26 Chommczynsky P, Sacchi N. Single-step method of RNA isolation by acid guanidinium thiocyanate-phenol cloroform extration. *Annal. Biochem.* 1987; 162: 156–9.

27 Delgado RV, Salazar A, Panduro A, Armendariz-Borunda J. Treatment with anti-transforming growth factor b antibodies influences an altered pattern of cytokines expresion in injured rat liver. *Biochim. Biophys. Acta* 1998; 1442: 20–7.

28 Bueno MR, Daneri A, Armendariz-Borunda J. Cholestasis-induced fibrosis is reduced by interferon α-2a and is associated with elevated liver metalloprotease activity. *J. Hepatol.* 2000; 33: 915–25.

29 Sancho-Bru P, Bataller R, Gasull X *et al.* Genomic and functional characterization of stellate cells isolated from human cirrhotic livers. *J. Hepatol.* 2005; 43: 272–82.

30 Czuwara J, Sementchenko V, Watson D, Trojanowska M. Ets-1 is an effector of the transforming growth factor β (TGFβ) signaling pathway and an antagonist of the profibrotic effects of TGFβ. *J. Biol. Chem.* 2002; 277: 20 399–498.

31 Reuninig U, Guerrini L, Nishiguchi T *et al.* Rel transcription factors contribute to elevated urokinase expression in human ovarian carcinoma cells. *Eur. J. Biochem.* 1999; 259: 143–8.

32 Kossakowska A, Lee S, Urbanski L *et al.* Altered balance between matrix metalloproteinases and their inhibitors in experimental biliary fibrosis. *Am. J. Pathol.* 1998; 153: 1895–902.

33 Zhou X, Murphy FR, Gehdu N, Zhang J, Iredale JP, Benyon C. Engagement of a b integrin regulates proliferation and apoptosis of hepatic stellate cells. *J. Biol. Chem.* 2004; **279**: 23 996–4006.
34 Von Bredow DC, Crees AE, Howard EW, Bowden GT, Nagle RB. Activation of gelatinase-tissue-inhibitors-of-metalloproteinase complexes by matrilysin. *Biochem. J.* 1998; **331**: 965–72.
35 Weiskirchen R, Kneifel J, Weiskirchen S *et al.* Cytokine regulation of matrix metalloproteinase activity and its regulatory dysfunction in disease. *Biol. Chem. Hoppe Seyler* 1995; **376**: 345–55.
36 Knittel T, Aurisch S, Neubauer K, Eichhorst S, Ramadori G. Cell type specific expression of neural cell adhesion molecule (N-CAM) in ITO cells of rat liver: upregulation during in vitro activation and in hepatic tissue repair. *Am. J. Pathol.* 1996; **149**: 449–62.
37 Myahara T, Schrum L, Rippem R *et al.* Peroxisome proliferator-activated receptors and hepatic stellate cell activation. *J. Biol. Chem.* 1999; **275**: 35 715–22.
38 Lijnen HR, Arza B, Van Hoef B, Collen D, Declerck P. Inactivation of plasminogen activator inhibitor-1 by specific proteolysis with stromelysin-1 (MMP-3). *J. Biol. Chem.* 2000; **276**: 37645–50.
39 Siller-Lopez F, Sandoval A, Salgado S *et al.* Treatment with human metalloproteinase-8 gene delivery ameliorates experimental rat liver cirrhosis. *Gastroenterology* 2004; **126**: 1122–33.
40 Powell DW, Mifflin RC, Valentich JD *et al.* Paracrine cells important in health and disease. *Am. J. Physiol.* 1999; **277**: 1–19.
41 Sawdey M, Podor JT, Loskutoff DJ. Regulation of type 1 plasminogen activator inhibitor gene expression in cultured bovine aortic endothelial cells. *J. Biol. Chem.* 1989; **264**: 10 396–401.
42 Smith AN, Carter QL, Kniss DA, Brown TL. Characterization of TGFbeta-responsive human trophoblast derived cell line. *Placenta* 2001; **22**: 425–31.
43 Rangaswami H, Bulbule A, Kundu G. Nuclear factor inducing kinase plays a crucial role in osteopontin-induced MAPK/I kinase-dependent nuclear factor kB-mediated promatrix metalloproteinase-9 activation. *J. Biol. Chem.* 2004; **279**: 38 921–35.
44 Dubois B, Massure S, Hurtenbach U *et al.* Resistance of young gelatinase B-deficent mice to experimental autoimmune encephalomyelitis and necrotizing tail lesions. *J. Clin. Invest.* 1999; **104**: 1507–15.
45 Houde M, de Bruyne G, Bracke M *et al.* Differential regulation of gelatinase B and tissue-type plasmin activator expression in human bowes melanoma cells. *Int. J. Cancer* 1993; **1**: 395–400.
46 Ramos-DeSimone N, Hahn-Dantona E, Sipley J, Nagase H, French DL, Quigley James P. Activation of metalloproteinase-9 (MMP-9) via a converging plasmin/stromelysin-1 cascade enhances tumor cell invasion. *J. Biol. Chem.* 1999; **274**: 13 066–76.

15

ARTICLE

doi:10.1016/j.ymthe.2003.09.015

Improved Effects of Viral Gene Delivery of Human uPA plus Biliodigestive Anastomosis Induce Recovery from Experimental Biliary Cirrhosis

Alejandra Miranda-Díaz,[1] Ana Rosa Rincón,[1] Silvia Salgado,[1] José Vera-Cruz,[1] Javier Gálvez,[1] Ma Cristina Islas,[1] Jaime Berumen,[2] Estuardo Aguilar-Cordova,[3] and Juan Armendáriz-Borunda[1,4,*]

[1] *Institute of Molecular Biology in Medicine and Gene Therapy, CUCS, University of Guadalajara, Apartado Postal 2-123, 44281 Guadalajara, Jalisco, Mexico*
[2] *Hospital General de Mexico, Mexico*
[3] *Advantagene, Inc., San Diego, California 92024, USA*
[4] *OPD Hospital Civil Guadalajara, Guadalajara, Mexico*

To whom correspondence and reprint requests should be addressed at the Institute for Molecular Biology in Medicine and Gene Therapy, Apartado Postal 2-123, 44281 Guadalajara, Jalisco, Mexico. Fax: (52)-33-3617-4159. E-mail: armendbo@cucs.udg.mx.

Gene therapy may represent a new avenue for the development of multimodal treatment for diverse forms of cirrhosis. This study explores the potential benefits of combining adenovirus-mediated human urokinase-plasminogen activator (AdHuPA) gene delivery and biliodigestive anastomosis to enhance the therapeutic efficacy of each treatment alone for cholestatic disorders resulting in secondary biliary cirrhosis. In an experimental model of secondary biliary cirrhosis, application of 6×10^{11} vp/kg AdHuPA adenovirus vector resulted in 25.8% liver fibrosis reduction and some improvement in liver histology. The relief of bile cholestasis by a surgical procedure (biliodigestive anastomosis) combined with AdHuPA hepatic gene delivery rendered a synergistic effect, with a substantial 56.9 to 42.9% fibrosis decrease. AdHuPA transduction resulted in clear-cut expression of human uPA protein detected by immunohistochemistry and induction of up-regulation in the expression of metalloproteinases MMP-3, MMP-9, and MMP-2. Importantly, functional hepatic tests, specifically direct bilirubin, were improved. Also, hepatic cell regeneration, rearrangement of hepatic architecture, ascites, and gastric varices improved in cirrhotic rats treated with AdHuPA but not in counterpart AdGFP cirrhotic animals. We believe this might represent a novel therapeutic strategy for human cholestatic diseases.

Key Words: bile-duct injury, fibrosis reversion, coadjuvant gene therapy

INTRODUCTION

Chronic obstruction of the common bile duct may cause hepatic fibrosis and secondary biliary cirrhosis. Thus, chronic cholestatic liver diseases are a leading indication for liver transplantation in adult and pediatric patients [1,2]. Among the most prominent cholestatic disorders are primary biliary cirrhosis, secondary biliary cirrhosis, primary sclerosing cholangitis, and extrahepatic biliary atresia [3]. Even when the underlying cause is treated or removed, it is usually thought that end-stage cirrhosis is an irreversible process [4]. Secondary biliary cirrhosis (SBC) onset is a consequence of congenital defects like biliary atresia, which is a devastating infant disease. Also, SBC is the result of biliary obstruction after iatrogenic cholecystectomies. Laparoscopic cholecystectomy remains the only treatment for symptomatic gallbladder stones and is the most prominent source of biliary injuries. Unfortunately, in some cases the surgery is complicated by vasculobiliary injury. Iatrogenic injury of the biliary tract represents a complex problem for surgeon and patient [5]. Reconstruction consists in performing a biliodigestive anastomosis (BDA), but it represents a surgical challenge. On the other hand, patients with primary biliary cirrhosis have experienced some relief when treated with ursodiol [6] or methotrexate [7]. However, the controversy remains regarding whether they are effective in reversing fibrosis [8]. It is clear, then, that development of new strategies to reverse cholestasis-induced hepatic damage and the concomitant fibrosis is attractive. Recently, Zhong *et al.* have reported that viral gene delivery of superoxide dismutase attenuates experimental cholestasis-induced liver fibrosis in the rat [9].

1525-0016/$30.00

Nonetheless, the nature of the experimental design would preclude the generalized utility of this treatment in patients with biliary obstruction. Our experience in the field has rendered information that one single injection of an adenoviral vector bearing a modified cDNA coding for a nonsecreted form of human urokinase-plasminogen activator (AdHuPA) efficiently reverts CCl_4-induced liver cirrhosis, which resembles human alcoholic cirrhosis [10].

Here, we have combined a surgical procedure to accomplish biliary decompression with AdHuPA-targeted liver delivery to improve the outcome of experimental SBC. Contrary to data obtained from cirrhotic animals treated with BDA plus AdGFP gene delivery, the combined therapy using AdHuPA instead resulted in enhanced liver fibrosis reversion, disappearance of collagen-making cells, and stimulation of hepatocyte cell regeneration. Livers from AdHuPA-injected animals experienced clear-cut expression of human corresponding protein detected by immunohistochemistry. This cascade of events resulted in up-regulated expression of specific collagen-degrading enzymes (metalloproteinases) like MMP-3, MMP-9, and MMP-2. We believe these latter enzymes as accountable for enhanced hepatic fibrosis reversion. Biochemical parameters, specifically bilirubin determinations, as well as functional measurements (ascites, gastric varices) were also down-regulated with a tendency to normalize.

Results and Discussion

Application of gene therapy strategies in cooperation with standard medical practices seem promising and plausible therapeutic measures for a number of pathophysiologic conditions. Thus, *in vivo* surgical resection plus adjuvant gene therapy protocols have been devised for the treatment of experimental mammary and prostate cancer [16]. Along the same rationale, an enhanced therapeutic effect of herpes simplex virus thymidine kinase gene plus ganciclovir (gene therapy approach) in combination with ionizing radiation for mouse prostate cancer has been reported [17]. A clinical study using this combined strategy is now ongoing. In the field of chronic hepatic diseases, the development of the Kasai portoenterostomy procedure improved the prognosis for children with biliary atresia [18,19]. However, progressive hepatic fibrosis, portal hypertension, and eventual liver failure are common; 70 to 80% of patients eventually require liver transplantation, accounting for 50–60% of all children who undergo liver transplantation [18,19]. Therefore, a need for different therapeutic approaches to alleviate cholestatic disorders resulting in liver cirrhosis becomes evident. Ursodeoxycholic acid is currently the most promising therapy for chronic cholestatic liver diseases; however, it cannot prevent fibrosis [20,21]. Recently, Zhong *et al.* [9] demonstrated that gene delivery of mitochondrial Mn-superoxide dismutase (Mn-SOD) to bile-duct-ligated rats blocks formation

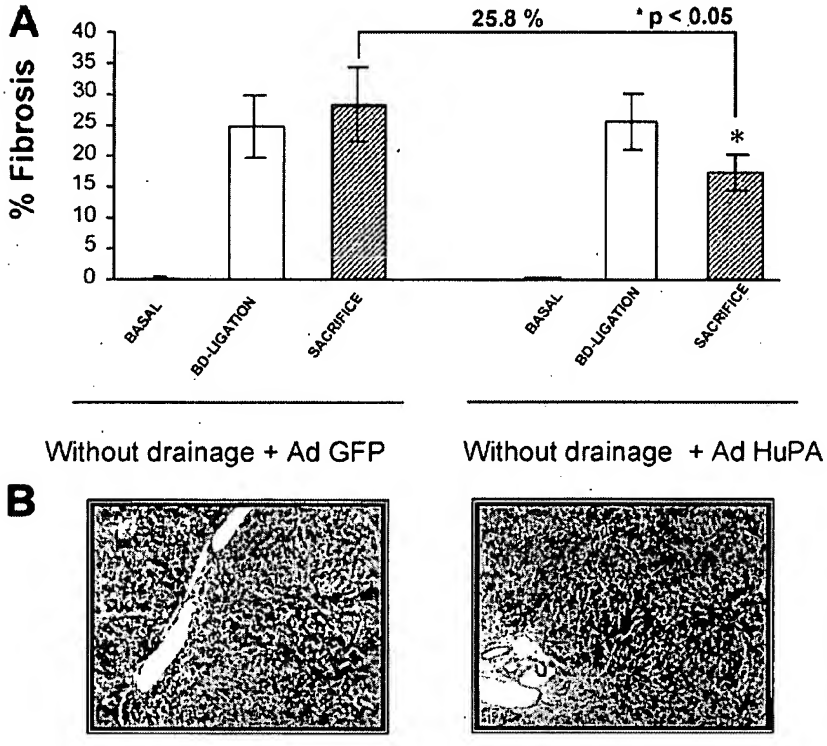

FIG. 1. Histologic analysis of fibrosis in bile duct-ligated (BDL) rats treated with either AdHuPA or AdGFP adenoviral vector. Liver tissue was processed as described under Materials and Methods. (A) Fibrosis index was determined in control rats without bile duct ligation (basal), 4 weeks after BDL, and 7 days later. After this liver biopsy was taken, BDA rats were divided into groups and injected via the iliac vein with either 6×10^{11} vp/kg AdHuPA ($n = 6$) or 6×10^{11} vp/kg control adenoviral vector AdGFP ($n = 6$). Rats were kept under surveillance for 10 more days and then sacrificed. (B) Both animal groups were maintained for 4 weeks after BDL without bile drainage.

doi:10.1016/j.ymthe.2003.09.015

of oxygen radicals and production of toxic cytokines, thereby minimizing liver injury caused by cholestasis. However, their study has a major strategic difference with ours. They had to administer the adenoviral vector containing Mn-SOD 3 days before rat bile-duct ligation took place. Potential translational application of such a strategy to the clinical scenario would be difficult.

Here, we used a biliary common duct ligation (BDL) rat model resembling biliary cirrhosis in humans [22,23]. In this BDL model, extrahepatic cholestasis due to prolonged obstruction of bile flow led to anatomic destruction of the biliary tree and produced a mortality rate of 20–30% at 4 weeks of ligature. In the surviving animals, biochemical and morphological changes with extensive proliferation of bile ducts, enlarged portal tracts, inflammation, necrosis, and formation of periportal fibrosis with pericentral collagen deposition were evident in 4-week BDL cirrhotic animals ($n = 6$) deprived of gene therapy treatment (Fig. 1B). We sacrificed animals 10 days after 4-week BD ligation. On the other hand, a matching lot of cirrhotic rats ($n = 6$) otherwise treated with one single injection of 6×10^{11} viral particles (vp)/kg clinical grade AdHuPA adenoviral vector showed a slight histologic improvement and a significant 25.8% fibrosis index reduction (P 0.05) (Fig. 1A). It is important to make a note of this, since our previous work in rats with CCl_4-induced cirrhosis treated with AdHuPA [10] demonstrated that overexpression of corresponding hepatic human uPA correlated with induction of MMP-2 and almost complete resolution of periportal and centrilobular fibrosis (85%) compared to a progressive fibrosis in controls. The differences found

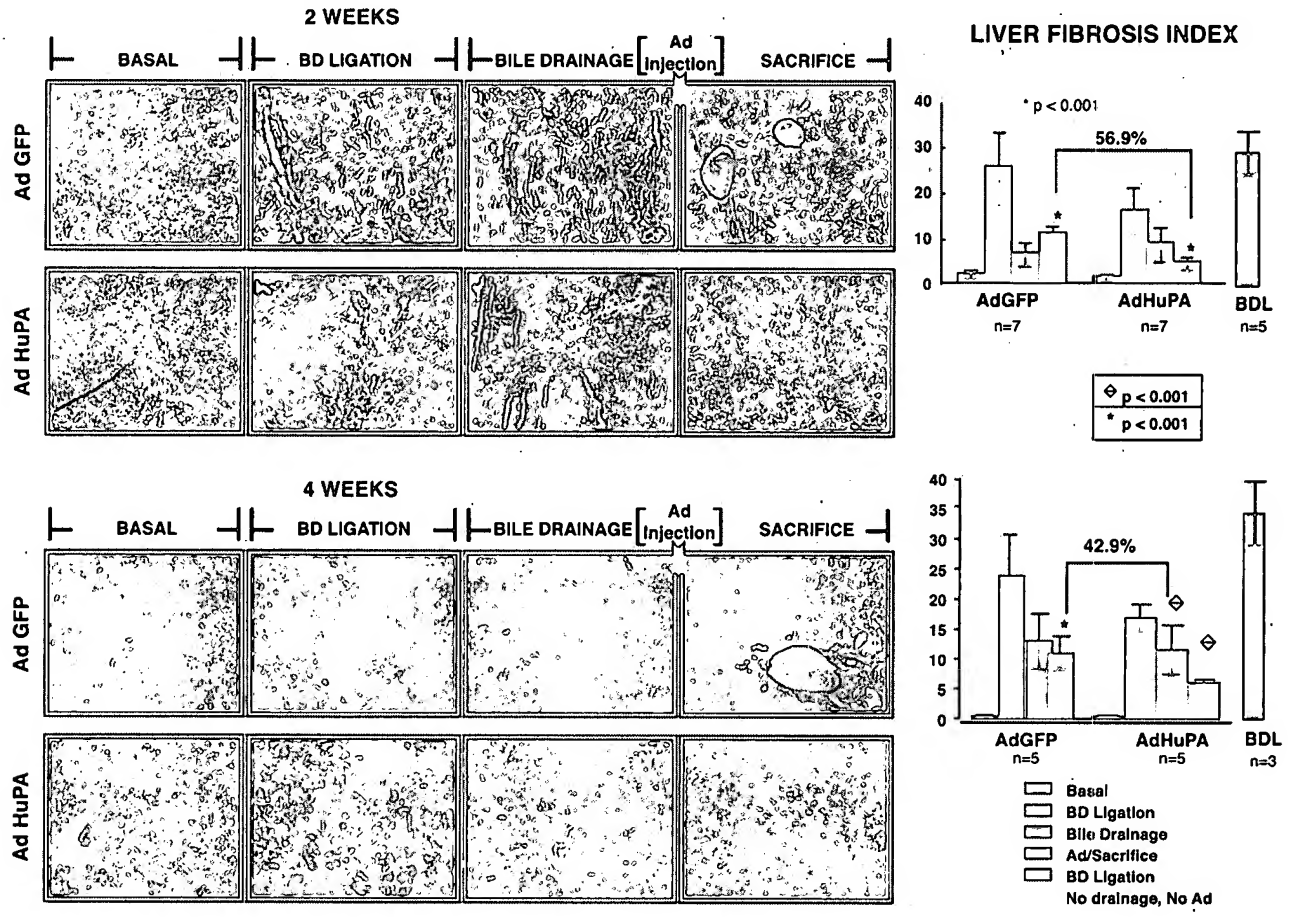

FIG. 2. Positive coadjuvant effect of bile drainage plus AdHuPA adenoviral vector. We compared fibrosis index between AdHuPA and AdGFP adenovirus vector injection and between groups of 2 weeks (top) and 4 weeks (bottom) after BDL. Bile drainage itself improved the fibrosis percentage observed, though a synergistic improvement took place after AdHuPA adenovirus vector injection. Liver fibrosis index decreased 56.9% in cirrhotic rats ligated for 2 weeks ($P < 0.05$) compared with 42.9% in animals with BDL for 4 weeks. A numerical figure of bile-duct-ligated cirrhotic animals that did not receive any adenovector treatment is in the right-hand side. This figure reflects BDL animals ligated for 3 weeks, plus 7 days (with *no* biliodigestive anastomosis), plus 10 days, which equals the time span in animals injected with adenovector. Similarly, in the lower right are shown BDL animals ligated for 4 weeks without biliodigestive anastomosis and no Ad injection and followed up to 17 days until sacrifice.

in this communication regarding percentage of fibrosis reversion may be due to the harshness of the fibrotic process in the BDL model and the different extracellular matrix proteins shaping the scar.

In light of these results, we thought that combination of surgical procedures with AdHuPA gene therapy strategy would result in an enhanced therapeutic effect resulting in relief of the cholestatic disorder, induction of fibrosis reversion, and hepatic cell regeneration.

Therefore, we designed experiments shown in Fig. 2 to evaluate such a combined treatment. Animals showed dramatic elevation of liver enzymes AST, ALT, alkaline phosphatase (AP), and total and direct bilirubins following BDL. We obtained liver biopsies from each rat before BDL and at every step described after ligation. At the end of 2 (Group 1) or 4 (Group 2) weeks all rats had increased liver fibrosis along with histologic and clinical features already described [15]. Then, we subjected all animals in both groups to BDA to induce drainage of the clogged bile. This surgical procedure resembles those performed in humans to ameliorate bile obstruction by discontinuation of the harmful agent and reestablishment of bile flow. We left the rats in this stage for 7 days. Hepatic fibrosis index continued to be elevated to similar extents in all animals. Then, we injected 7 2-week BDL cirrhotic rats via the iliac vein with 6×10^{11} vp/kg AdHuPA and 7 control rats with 6×10^{11} vp/kg irrelevant adenoviral vector AdGFP. These 14 rats constituted Group 1. Similarly, we treated 5 4-week BDL cirrhotic rats with 6×10^{11} vp/kg AdHuPA and 5 parallel rats with 6×10^{11} vp/kg irrelevant adenoviral vector AdGFP. These 10 animals constituted Group 2. We kept all rats under surveillance for 10 more days, monitoring for overall health status, and then sacrificed them. We observed an important and significant 56.9% decrease in fibrosis ratio in Group 1 and 42.9% in Group 2, in rats injected with AdHuPA, but observed no decrease in percentage fibrosis index in animals injected with AdGFP ($P < 0.001$). Moreover, we have included data from animals without any viral transduction nor surgical intervention as control. These data reflect BDL animals ligated for 2 weeks, plus 7 days (with *no* biliodigestive anastomosis), plus 10 days, which equals the time span in animals injected with adenovector. Similarly, Fig. 2 shows in the lower right corner BDL animals ligated for 4 weeks without biliodigestive anastomosis and no Ad injection and followed up to 17 days until sacrifice. These last controls enable us to suggest the specific effect of AdHuPA, but not AdGFP, on induction of collagenous extracellular matrix protein degradation reflected by a statistically significant decreased fibrosis index.

Liver fibrosis index was determined by two different pathologists blinded to the study.

Finally, expression of human uPA (see later in Fig. 5) in cirrhotic livers led to an important resolution of fibrosis and regeneration of functional hepatocytes as determined by immunohistochemical reaction with anti-PCNA antibody (Fig. 3). Multiple mechanisms may account for the induction of hepatocyte regeneration and matrix degradation by activation of the metalloproteinase cascade may lead to remodeling of the distorted architecture and angiogenesis and may free up space for hepatocyte expansion. A potential mechanism for the degradation of fibrotic tissue observed with AdHuPA is through the disengagement of latent metalloproteinase complexes with TIMPs rendering active

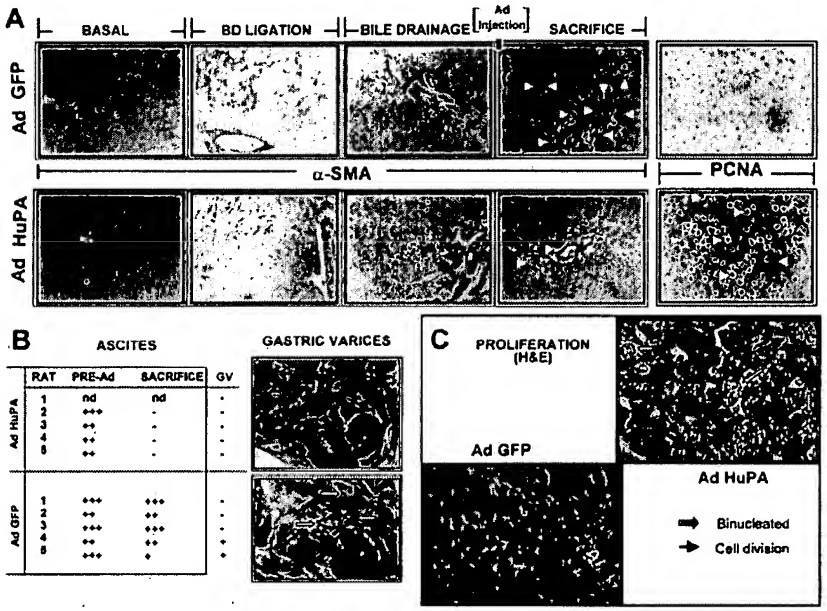

FIG. 3. Liver sections were incubated overnight at room temperature with mouse monoclonal antibody against α-smooth muscle actin diluted 1:50 in PBS. Activated collagen-making cells (hepatic stellate cells) are observed in brown color. HSC activation decreased dramatically in rats treated with AdHuPA (bottom). Hepatocyte regeneration was measured by immunohistochemistry using anti-PCNA antibody. Arrowheads show specific staining. Animals treated with AdGFP (top) showed less cell proliferation compared with animals treated with AdHuPA. Ascites as well gastric varices (GV) improved importantly in rats injected with AdHuPA but not in AdGFP rats. nd, not determined.

doi:10.1016/j.ymthe.2003.09.015

collagen-degrading enzymes (Armendariz-Borunda, unpublished observations).

Hepatic stellate cell (HSC) activation reflects the capacity of these cells to synthesize an increased amount of collagenous proteins. It is clear that we found the specific marker α-smooth muscle actin (α-SMA) in considerably smaller amounts in liver sections from rats treated with AdHuPA. Also, we could observe an augmented number of mitotic figures (PCNA) indicating an active liver cell regeneration as opposed to AdGFP-treated animals. Liver tissue slides stained with hematoxylin and eosin are included in Fig. 3C to demonstrate this mitotic index. Ascites as well gastric varices improved importantly in rats treated with HuPA as opposed to rats treated with irrelevant AdGFP (Fig. 3).

Cirrhotic animals showed dramatic elevation of liver enzymes AST, ALT, AP (data not shown), and total and direct bilirubins followed BDL (Fig. 4). One week after BDA and immediately before adenoviral application, rats showed a significant improvement in biochemical liver enzymes ($P < 0.05$), though the most striking beneficial effect was noted in total bilirubin, specifically direct bilirubin, indicating a clear relief in cholestatic disorder. It is important to point out that we observed this in both groups of animals (2-week BDL and 4-week BDL) injected with the therapeutic adenovector. However, this effect

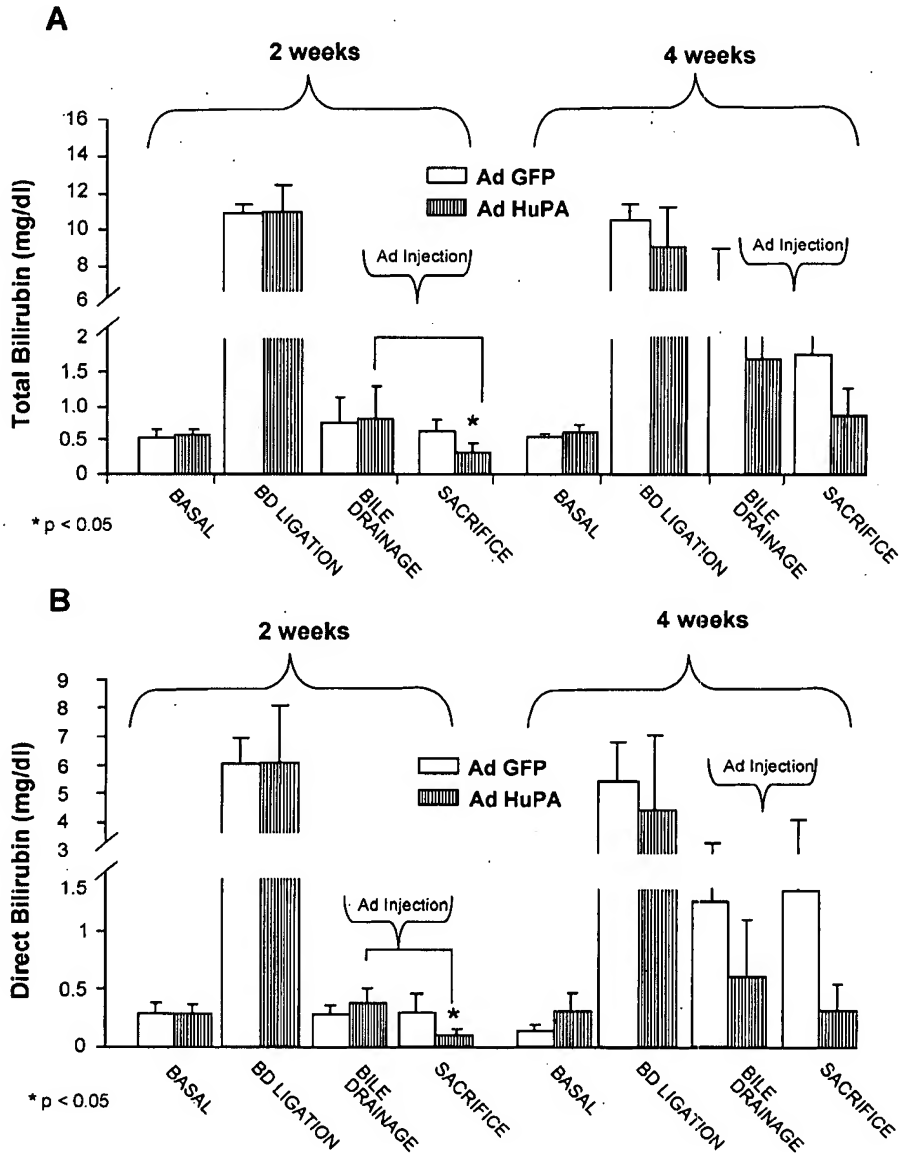

FIG. 4. Total and direct bilirubin improvement.

was statistically significant only in Group 1. These results are relevant since it is well established that the relationship of serum bilirubin concentrations to survival is inversely proportional in most of both adult and pediatric patients with cholestatic disorders who progress to the need for liver transplantation [24]. Higher serum bilirubin values were also clearly associated with much poorer survival in another study [25]. It is clear, then, that in patients with biliary cirrhosis, elevated serum bilirubin values are an independent predictor of poor prognosis [26,27] and bilirubin is one of the most significant variables in the Mayo mathematical model of survival in patients with biliary cirrhosis [24].

In trying to elucidate the mechanisms of action of human uPA protein in the degradation of collagenous extracellular matrix proteins we performed immunohistochemical staining with specific antibodies against human urokinase-plasminogen activator and metalloproteinases like MMP-3, MMP-9, and MMP-2.

Fig. 5 clearly depicts the specific immunostaining in liver from cirrhotic, drained animals injected with either AdHuPA or AdGFP. Livers from AdHuPA-treated animals underwent a cascade of events resulting in specific detection uPA, MMP-3, MMP-9, and MMP-2.

Although we did not run a kinetics curve at different times post-Ad injection, our reasoning, and according to

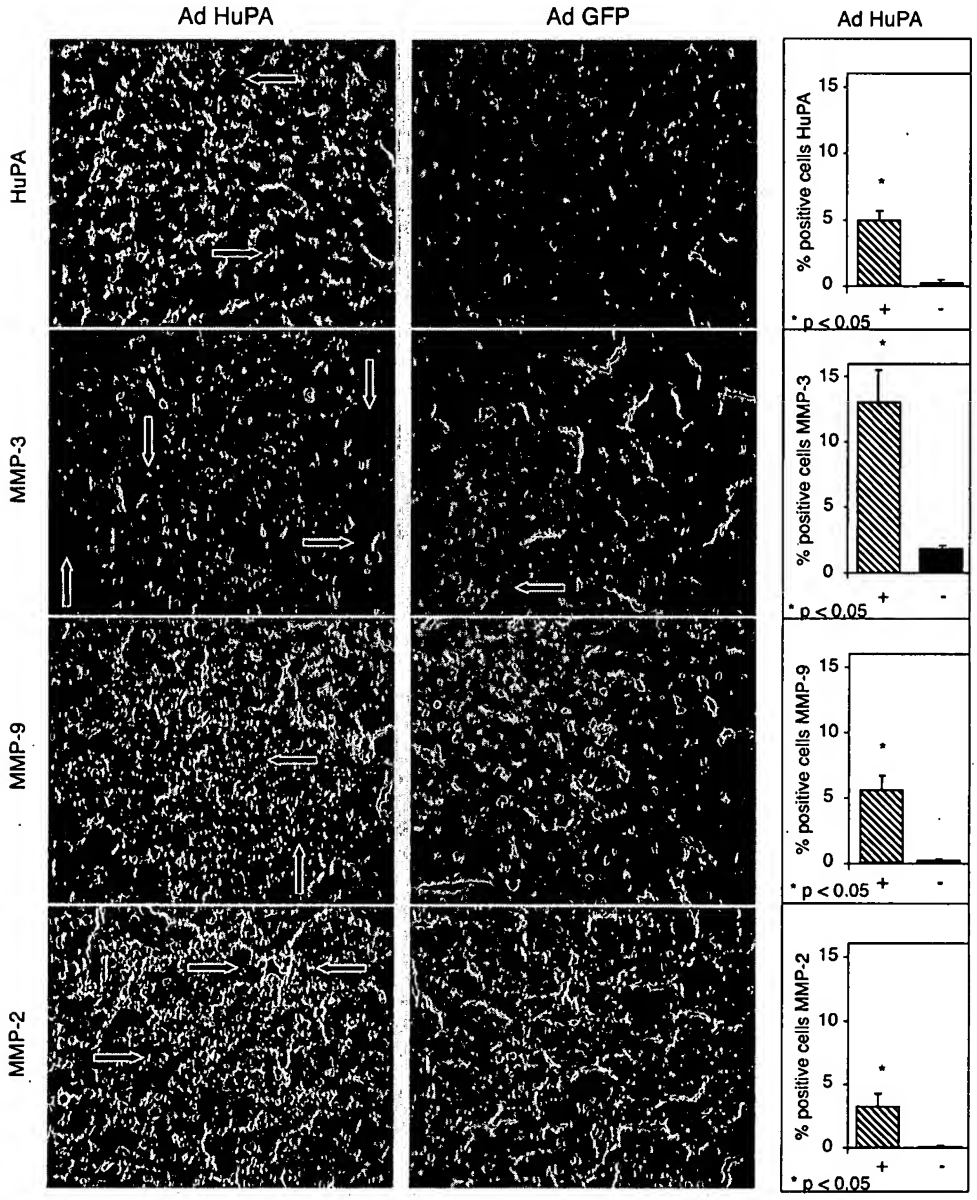

FIG. 5. Liver tissue sections from BDL cirrhotic animals that were ligated for 4 weeks, underwent bile drainage, and then were injected with either AdHuPA or AdGFP. Tissue sections were incubated with corresponding antibodies. The right shows data of positive area for each antibody.

doi:10.1016/j.ymthe.2003.09.015

results shown in other systems, is that uPA activates rat pro-MMP-3 *in situ*, which in turn triggers the initial event of collagen degradation, and also active MMP-3 would induce activation of pro-MMP-9 and MMP-2, degrading in turn collagenous and gelatinous remaining material.

We did not search for MMP-1 action in our system. However, it is possible that initial breakdown of the major constituent of the fibrous scar in these cirrhotic livers, namely collagen type I, is achieved by MMP-1 and/or MMP-3 and then continued by MMP-9 and MMP-2. It has been recently been shown in other systems that degradation of collagen I clearly occurs during recovery from liver fibrosis, and this may not simply promote or facilitate the hepatocyte regenerative response but is also associated with a diminution in hepatic stellate cell number and a decrease in collagen I and α-SMA expression [28,29]. These data correlate with our findings.

The results found in this rodent model of cirrhosis are encouraging and warrant the further development of coadjuvant approaches to heal human secondary biliary cirrhosis.

MATERIALS AND METHODS

Animals and induction of secondary biliary cirrhosis. Wistar female rats were housed in the animal facility of the University of Guadalajara and all animal studies were conducted in accordance with the principles and procedures outlined in the National Institutes of Health's *Guide for the Care and Use of Laboratory Animals*. Rats weighing 200–250 g were fed a standard rat chow diet. Two groups of animals were used: rats ligated for 2 weeks and then subjected to BDA plus either AdGFP (control animals) or AdHuPA constituted Group 1. Animals ligated for 4 weeks and identically managed as before represented Group 2. Thus, animals included in Group 1 (n = 14) underwent BDL for 2 weeks, followed by BDA. Rats were left at this stage for 7 days. Then, rats (n = 7) were injected via the iliac vein with 6×10^{11} vp/kg AdHuPA along with 7 rats injected with 6×10^{11} vp/kg irrelevant adenoviral vector AdGFP used as control. Rats were kept under careful surveillance for 10 days, monitoring for overall health status, and then sacrificed. The procedure involved rats anesthetized at every step with intramuscular dehydrobenzoperidol (400 μg/kg) and ketamine (400 μl/kg) and from which liver biopsies and serum functional hepatic tests were determined at every step. Animals underwent a 2-cm upper-midline abdominal incision below the xifoides appendix, and the suprapancreatic common bile duct was identified and double ligated with 5-O silk (Ethicon; Johnson and Johnson, Mexico City, Mexico) and transected between the ligatures. Subsequently, the abdominal wall was closed in two layers with continuous 5-O silk. BDA was carried out with internal silastic stent (Medicate Grade Tubing 602-205.40; Dow Corning, Midland, MI) between dilated bile duct and duodenum. That procedure was intended to drain the clogged bile and to reestablish bile flow. Group 2 was composed of 10 cirrhotic animals that underwent BDL, BDA was done 4 weeks later, and immediately 5 rats were injected via the iliac vein with 6×10^{11} vp/kg AdHuPA along with 5 rats injected with 6×10^{11} vp/kg irrelevant adenoviral vector AdGFP. The subsequent procedures and tests were performed identically as for Group 1. Rats were kept under careful surveillance for 10 more days, monitored for overall health status, and sacrificed.

Adenovirus vectors. Cloning of the adenoviral plasmid pAd.PGK-ΔNΔC-huPA has been described before [11] and essentially it is a first-generation adenoviral vector bearing a modified cDNA coding for nonsecreted human urokinase plasminogen activator (AdHuPA). The preparations of this Ad vector were monitored for endotoxin and mycoplasm contaminants and were titered as previously described [12]. The rationale for using this vector resided in the advantage of the nonsecreted uPA, which does not cause hypocoagulation and spontaneous bleeding, which represent a main drawback in cirrhotic animals.

The AdGFP vector used here (irrelevant adenovirus) is an E1- and E3-deleted replication-defective adenovirus vector previously described [12]. The vectors were produced under good laboratory practice conditions. The vectors were titered and characterized as described [12,13] and had a vector particle to infection unit ratio of ≤30.

Biochemical assays. Blood (1.5 ml) was drawn from animals when each surgical procedure was performed and serum transaminases, ALT, AST, alkaline phosphatase, and total and direct bilirubins were determined in an automated Sincron-7 analyzer at the Hospital Civil of Guadalajara. Five animals were studied in each group at the indicated steps: basal, 2 or 4 weeks after BDL, 7 days after BDA, and 10 days after 6×10^{11} vp/kg AdHuPA or AdGFP adenovirus vector injection by iliac vein. Results are expressed as means ± SD.

Histological examination of liver sections. Liver biopsies were taken at every step during the experimental design. That is, a piece of liver was obtained from each rat at basal time, either at 14 or at 28 days after BDL (for Groups 1 and 2, respectively), and then at 7 days after BDA and 10 days after adenoviral vector injection. The liver was fixed by immersion in 10% paraformaldehyde diluted in phosphate-buffered saline (PBS), dehydrated in graded ethylic alcohol, and embedded in paraffin. Sections 5 μm thick were stained with hematoxylin/eosin to identify mitotic figures reflecting liver cell regeneration and Masson trichrome to determine the percentage of liver tissue affected by fibrosis, and characteristic proliferation of bile ducts was determined using a computer-assisted automated image analyzer (Image-Pro Plus 4.0) by analyzing 20 random fields per slide and calculating the ratio of connective tissue to the whole area of the liver. Parallel liver slides were stained in 0.1% Picrosirius red solution. Sirius red is a specific dye that has an affinity for collagenous proteins. Then, tissue sections were counterstained with fast green dye, which has an affinity for noncollagenous protein [14,15].

Immunohistochemistry of liver sections. Another set of liver sections was mounted in silane-covered slides and deparaffinized, and the endogenous activity of peroxidase was quenched with 3.0% H_2O_2 in absolute methanol. Liver sections were incubated overnight at room temperature with mouse monoclonal antibodies against PCNA, to determine cell proliferation, and α-smooth muscle actin, to search for hepatic stellate cell activation (Boehringer Mannheim, Germany), diluted 1/20 and 1/50, respectively, in PBS and with goat polyclonal antibodies against human uPA (Chemicon International, USA) diluted 1/400 in PBS. We also used goat polyclonal IgG antibodies against rat collagen-degrading enzymes or metalloproteinases MMP-2, -3, and -9 (Santa Cruz Biotechnology, USA) diluted 1/300 in PBS. For this staining, we used liver slides from animals of 4-week BDL plus drainage and 10 days after injection of adenovirus with HuPA or GFP gene. We included a negative control without primary antibody in each slide.

Bound antibodies were detected with peroxidase-labeled rabbit polyclonal antibodies against mouse or goat immunoglobulins and diaminobenzidine and counterstained with hematoxylin. Histopathology was interpreted by two independent board-certified pathologists who were blinded to the study.

Ascites was considered severe (+++) when ascitic fluid comprised >5% of body weight; moderate (+ or ++) when <5% of body weight. We also determined gravity of gastric varices.

Statistical analyses. Results are expressed as means and SD. Student's t test and Mann–Whitney U test were used. $P < 0.05$ was considered to indicate significant differences between groups.

ACKNOWLEDGMENTS

The authors greatly appreciate the support of personnel at the CUCS Animal Facilities, especially the help of Dr. Pedro Díaz. The authors are also indebted to Mario Cárdenas and Rosa Lina Torres-Rodríguez for their invaluable technical help and Ing. Rogelio Troyo for his support in carrying statistic analysis. This work was supported in part by a Grant from CONACyT, No. 28832-M, to J.A.B. and by PIHCSA Medica.

RECEIVED FOR PUBLICATION FEBRUARY 19, 2003; ACCEPTED SEPTEMBER 26, 2003.

REFERENCES

1. Starzl, T. E., Demetris, A. J., and Van Thiel, D. (1989). Liver transplantation (1). *N. Engl. J. Med.* **321:** 1014–1022.
2. Whitington, P. F., and Balistreri, W. F. (1991). Liver transplantation in pediatrics: Indications, contraindications, and pretransplant management. *J. Pediatr.* **118:** 169–177.
3. Poupon, R., Chazouilleres, O., and Poupon, R. E. (2000). Chronic cholestatic diseases. *J. Hepatol.* **32**(Suppl. 1)**:** 129–140.
4. Friedman, S. L. (1993). The cellular basis of hepatic fibrosis: Mechanisms and treatment strategies. *N. Engl. J. Med.* **328:** 1828–1835.
5. Rossi, R. L., and Tsao, J. L. (1994). Biliary reconstruction. *Surg. Clin. North Am.* **74:** 825–844.
6. Poupon, R. E., Balkau, B., Eschwege, E., and Poupon, R. (1991). A multicenter, controlled trial of ursodiol for the treatment of primary biliary cirrhosis. UDCA-PBC Study Group. *N. Engl. J. Med.* **324:** 1548–1554.
7. Kaplan, M. M., DeLellis, R. A., and Wolfe, H. J. (1997). Sustained biochemical and histologic remission of primary biliary cirrhosis in response to medical treatment. *Ann. Intern. Med.* **126:** 682–688.
8. Zimmerman, H., Reichen, J., Zimmermann, A., Sagesser, H., Thenisch, B., and Hoflin, F. (1992). Reversibility of secondary biliary fibrosis by biliodigestive anastomosis in the rat. *Gastroenterology* **103:** 579–589.
9. Zhong, Z., Froh, M., Wheeler, M. D., Smutney, O., Lehmann, T. G., and Thurman, R. G. (2002). Viral gene delivery of superoxide dismutase attenuates experimental cholestasis-induced liver fibrosis in the rat. *Gene Ther.* **9:** 183–191.
10. Salgado, S., *et al.* (2000). Liver cirrhosis is reverted by urokinase-type plasminogen activator gene therapy. *Mol. Ther.* **2:** 545–551.
11. Lieber, A., Peeters, M. J., Gown, A., Perkins, J., and Kay, M. A. (1995). A modified urokinase plasminogen activator induces liver regeneration without bleeding. *Hum. Gene Ther.* **6:** 1029–1037.
12. Nyberg-Hoffman, C., Shabram, P., Li, W., Giroux, D., and Aguilar-Cordova, E. (1997). Sensitivity and reproducibility in adenoviral infectious titer determination. *Nat. Med.* **3:** 808–811.
13. García-Bañuelos, J., Siller-López, F., Miranda, A., Aguilar, L. K., Aguilar-Córdova, E., and Armendáriz-Borunda, J. (2002). Cirrhotic rat livers with extensive fibrosis can be safely transduced with clinical-grade adenoviral vectors: Evidence of cirrhosis reversion. *Gene Ther.* **9:** 127–134.
14. Lopez-De Leon, A., and Rojkind, M. (1985). A simple micromethod for collagen and total protein determination in formalin-fixed paraffin-embedded section. *J. Histochem. Cytochem.* **33:** 737–743.
15. Bueno, M. R., Daneri, A., and Armendáriz-Borunda, J. (2000). Cholestasis-induced fibrosis is reduced by interferon alpha-2a and is associated with elevated liver metalloprotease activity. *J. Hepatol.* **33:** 915–925.
16. Sukin, S. W., *et al.* (2001). In vivo surgical resection plus adjuvant gene therapy in the treatment of mammary and prostate cancer. *Mol. Ther.* **3:** 500–506.
17. Chhikara, M., *et al.* (2001). Enhanced therapeutic effect of HSV-tk + GCV gene therapy and ionizing radiation for prostate cancer. *Mol. Ther.* **3:** 536–542.
18. Kasai, M. (1974). Treatment of biliary atresia with special reference to hepatic portoenterostomy and its modifications. *Prog. Pediatr. Surg.* **6:** 5–52.
19. Karrer, F. M., *et al.* (1996). Long-term results with the Kasai operation for biliary atresia. *Arch. Surg.* **131:** 493–496.
20. Stiehl, A., *et al.* (1990). Ursodeoxycholic acid-induced changes of plasma and urinary bile acids in patients with primary biliary cirrhosis. *Hepatology* **12:** 492–497.
21. Skulina, D., *et al.* (1999). The influence of ursodeoxycholic acid on some biochemical, immunologic and histopathologic parameters in patients with primary biliary cirrhosis. *Przegl Lek.* **56:** 201–204.
22. Murr, M., Gigot, J. F., Nagorney, D. M., Harmsen, W. S., Ilstrup, D. M., and Farnell, M. B. (1999). Long-term results of biliary reconstruction after laparoscopic bile duct injuries. *Arch. Surg.* **134:** 604–610.
23. Pickleman, J., Marsan, R., and Borge, M. (2000). Portoenterostomy: An old treatment for a new disease. *Arch. Surg.* **135:** 811–817.
24. Dickson, E. R., Grambsch, P. M., Fleming, T. R., Fisher, L. D., and Langoworthy, A. (1989). Prognosis in primary biliary cirrhosis: Model for decision making. *Hepatology* **10:** 1–7.
25. Miga, D., Sokol, R. J., Mackenzie, T., Narkewicz, M. R., Smith, D., and Karrer, F. M. (2001). Survival after first esophageal variceal hemorrhage in patients with biliary atresia. *J. Pediatr.* **139:** 291–296.
26. Bonnand, A. M., Heathcote, E. J., Lindor, K. D., and Poupon, R. E. (1999). Clinical significance of serum bilirubin levels under ursodeoxycholic acid therapy in patients with primary biliary cirrhosis. *Hepatology* **29:** 39–43.
27. Shapiro, J. M., Smith, H., and Schaffner, F. (1979). Serum bilirubin: a prognostic factor in primary biliary cirrhosis. *Gut* **20:** 137–140.
28. Issa, R., *et al.* (2003). Mutation in collagen-I that confers resistance to the action of collagenase results in failure of recovery from CCl_4-induced in liver fibrosis, persistence of activated hepatic stellate cells, and diminished hepatocyte regeneration. *FASEB J.* **17:** 47–49.
29. Iimuro, Y., *et al.* (2003). Delivery of matrix metalloproteinase-1 attenuates established liver fibrosis in the rat. *Gastroenterology* **124:** 445–458.

Gene Therapy (2002) 9, 127–134

www.nature.com/gt

RESEARCH ARTICLE

Cirrhotic rat livers with extensive fibrosis can be safely transduced with clinical-grade adenoviral vectors. Evidence of cirrhosis reversion

J Garcia-Bañuelos[1], F Siller-Lopez[1], A Miranda, LK Aguilar[2], E Aguilar-Cordova[3] and J Armendariz-Borunda[1]

[1]*Institute of Molecular Biology in Medicine and Gene Therapy, CUCS, University of Guadalajara, Guadalajara, Mexico;* [2]*Advantagene, Inc., San Diego, CA, USA; and* [3]*Harvard Gene Therapy Initiative, Boston, MA, USA*

Adenoviral vectors efficiently target normal liver cells; however, a clear-cut description of the safety boundaries for using adenovectors in hepatic cirrhosis has not been settled. With this in mind, we used a first-generation, replication-deficient adenoviral vector carrying the E. coli lacZ gene (Ad5βGal) to monitor therapeutic range, biodistribution, toxicity and transduction efficiency in Wistar rats made cirrhotic by two different experimental approaches resembling alcoholic cirrhosis and biliary cirrhosis in humans. Further, we show proof of concept on fibrosis reversion by a 'therapeutic' Ad-vector (AdMMP8) carrying a gene coding for a collagen-degrading enzyme. Dose–response experiments with Ad5βGal ranging from 1×10^9–3×10^{12} viral particles (vp) per rat (250 g), demonstrated that adenovirus-mediated gene transfer via iliac vein at 3×10^{11} vp/rat, resulted in an approximately 40% transduction in livers of rats made cirrhotic by chronic intoxication with carbon tetrachloride, compared with approximately 80% in control non-cirrhotic livers. In rats made cirrhotic by bile-duct obstruction only, 10% efficiency of transduction was observed. Biodistribution analyses showed that vector expression was detected primarily in liver and at a low level in spleen and kidney. Although there was an important increase in liver enzymes between the first 48 h after adenovirus injection in cirrhotic animals compared to non-transduced cirrhotic rats, this hepatic damage was resolved after 72–96 h. Then, the cDNA for neutrophil collagenase, also known as Matrix Metalloproteinase 8 (MMP8), was cloned in an Ad-vector and delivered to cirrhotic rat livers being able to reverse fibrosis in 44%. This study demonstrates the potential use of adenoviral vectors in safe transient gene therapy strategies for human liver cirrhosis.

Gene Therapy (2002) **9**, 127–134. DOI: 10.1038/sj/gt/3301647

Keywords: *cirrhosis; gene transfer; safety; fibrosis reversion*

Introduction

Liver cirrhosis is a worldwide health problem. Cirrhosis is a major liver disease for which there are no completely satisfactory therapies. Cirrhotic livers are characterized by extensive fibrosis throughout the entire hepatic parenchyma, especially around central and portal veins. The deposition of excessive fibrous or collagenous proteins in the subendothelial space or Space of Disse results in decreased free exchange flow between hepatocytes and sinusoidal blood. The cellular effects of these collagenous materials and other non-collagenous components, especially on hepatocytes, cause synthetic and metabolic dysfunction characteristic of advanced liver disease.[1,2] Removing the fibrous septa might result in benefit for subjects undergoing liver fibrosis due to the functional re-establishment of the hepatocyte–sinusoid flow exchange. Thus, delivery of genes coding for collagen-degrading enzymes may represent a novel therapy strategy for liver cirrhosis.

Various vector types have been shown to be efficient at delivering genes to normal livers.[3–7] Similarly, the use of viral and nonviral vectors for gene delivery to functionally compromised livers has been instrumental to establish 'proof of concept' in several experimental models. Various strategies involving adenoviral vectors have been used.[8,9] However, a key issue concerning toxicology, biodistribution and safety when using adenoviral vectors in cirrhotic animals, remains unresolved. Part of this study was designed to evaluate biodistribution, liver toxicity and efficiency of transduction of a reporter gene in hepatic cells of cirrhotic Wistar rats. We also wanted to delimit the 'therapeutic window' for potential and safe use of these vectors in a given clinical setting. Adenoviral vectors were chosen because they have been shown to be efficient vehicles for delivering genes to the liver and their distribution has been extensively analyzed in healthy animals. However, the potential toxicity of these vectors, especially to the liver, was a major concern. Animals with decreased liver function may have increased sensitivity to hepatotoxic effects of adenoviral vector administration. Therefore, we analyzed liver enzyme profiles of

Correspondence: J Armendariz-Borunda, Institute of Molecular Biology in Medicine and Gene Therapy, CUCS, University of Guadalajara, Apdo Postal 2-123, Guadalajara, Jal, Mexico 44281
Received 1 May 2001; accepted 20 November 2001

cirrhotic rats after intravenous adenoviral delivery with gene expression in the liver. Another part of this study was designed to determine proof of concept when using a neutrophil collagenase cDNA, cloned in an adenoviral vector (AdMMP8). Here, it is clearly shown that a 'safe dose' (3×10^{11} vp/kg) of adenoviral particles, induces a vigorous and fast degradation of excessive collagenous material deposited in livers of experimental animals resembling secondary biliary cirrhosis in humans. This effect resulted in marked improvement of functional hepatic tests (alanine transaminase or ALT, aspartate transaminase or AST and bilirubins) and ascitis. Importantly, our results are supported by recent publications showing that systemic administration of adenoviral vectors can effectively target diseased livers.[10,11]

Results and discussion

Two rat cirrhosis models were used: carbon tetrachloride (CCl_4-treatment) induced experimental cirrhosis that resembles alcoholic human disease, as well as cirrhosis post-chronic infection with hepatitis C virus and the biliary duct ligation model (BDL) mimics biliary cirrhosis in humans.[12,13] Doses of Ad5βGal ranging from 1×10^8–3×10^{12} viral particles (vp) per rat (weighing approximately 250 g) were delivered systemically through the iliac vein and a total of five rats per dose were tested. The goal of these experiments was to establish the toxicity window of adenovector dosage. The dose level of 1×10^{12} (4×10^{12} vp/kg) resulted in high mortality (100% in cirrhotic animals and approximately 60% in normal rats). A 3×10^{12} vp (1.2×10^{13} vp/kg) dose killed all cirrhotic animals and 80% of healthy animals, whereas 3×10^{11} total vp (1.2×10^{12} vp/kg) was reasonably tolerated in normal and cirrhotic rats with an optimal degree of efficiency of liver transduction (Figure 1). The threshold between dosages is quite narrow. However, recent data obtained in our laboratory using 6×10^{11} vp/kg of a therapeutic Ad vector which efficiently reverses experimental liver fibrosis,[8] provides confidence and warrants further investigation on the use of Ad vectors on liver fibrosis. In a previous paper,[8] we used a first generation, clinical-grade adenovector bearing the cDNA for urokinase-plasminogen activator capable of reversing liver cirrhosis in an efficient manner with no further complications.[8] The dose used was 6.6-fold and 20-fold lower than 4×10^{12} and 1.2×10^{13} vp/kg toxic doses respectively, reported in this paper. Transduction was assessed by X-gal staining of tissue sections 72 h after vector administration.

Morphometric analyses of multiple tissue sections revealed a transduction efficiency of approximately 40% in animals transduced with 3×10^{11} Ad5βGal virus particles after CCl_4-treatment for 5 weeks and decreasing only slightly to 38% after 8 weeks of intoxication (Figure 2). Ad5βGal was internalized mostly by hepatocytes, though sinusoidal cells were also shown slightly permissive to the Ad vector. Decreased β-gal transduction efficiency in CCl_4 animals as measured by internalization of Ad5βGal, might not be mediated through $\alpha_v\beta_5$ integrin, since we did not find significant differences in specific staining between CCl_4-injured animals and normal rats (data not shown). We speculate that such a transduction efficiency difference could be due to decreased expression of coxsackie/adenovirus receptor (CAR) or to

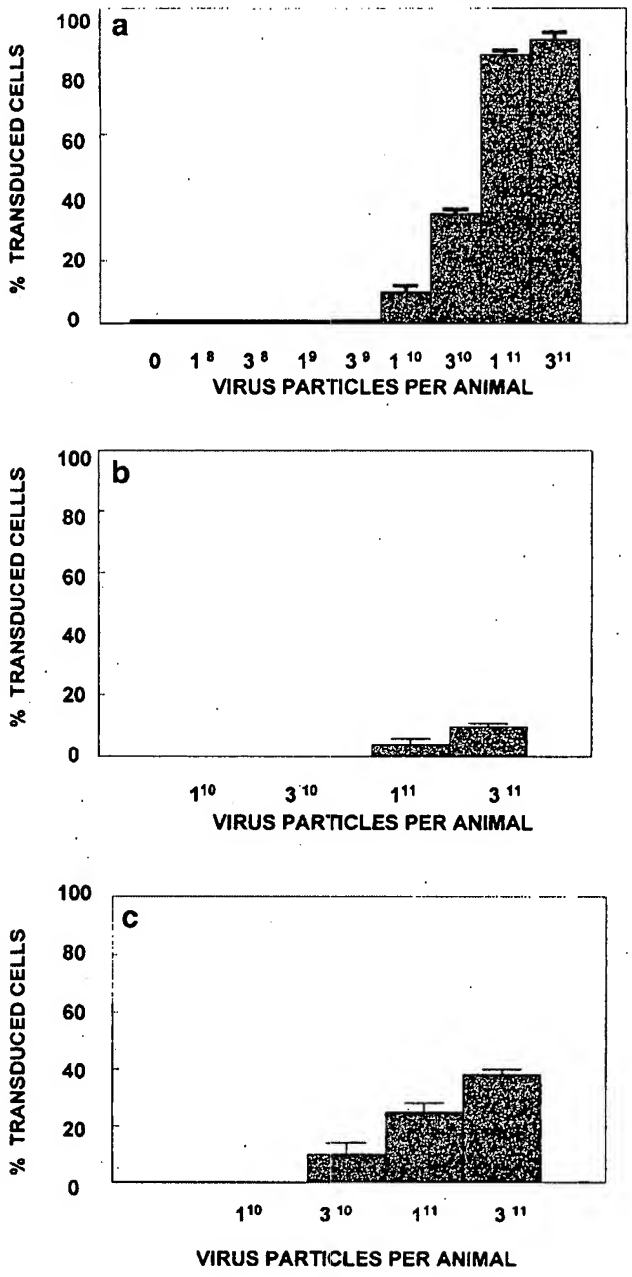

Figure 1 Efficiency of transduction of cirrhotic rat livers compared with normal livers. Doses of Ad5βGal vector ranging from 1×10^8–3×10^{12} virus particles (vp) were injected into the iliac vein of non-cirrhotic (a), bile duct ligated (BDL)- (b) and CCl_4-treated animals (c). β-Gal staining was determined 72 h after injection. Five animals were tested per dose. The percentage of transduced area was quantitatively monitored by computer-assisted morphometric analysis of tissue sections. The doses of 1×10^{12} and 3×10^{12} were fatal and therefore could not be analyzed.

an impediment in hepatocyte exposure to adenoviral vectors due to hemodynamic alterations, ie shunting of blood circulation in the severely damaged liver.

In the BDL model, extrahepatic cholestasis due to prolonged obstruction of bile flow resulted in even more extensive morphological and biochemical changes. This included an extensive proliferation of bile ducts in enlarged portal tracts, with inflammation and necrosis, and the formation of periportal fibrosis, as well as peri-

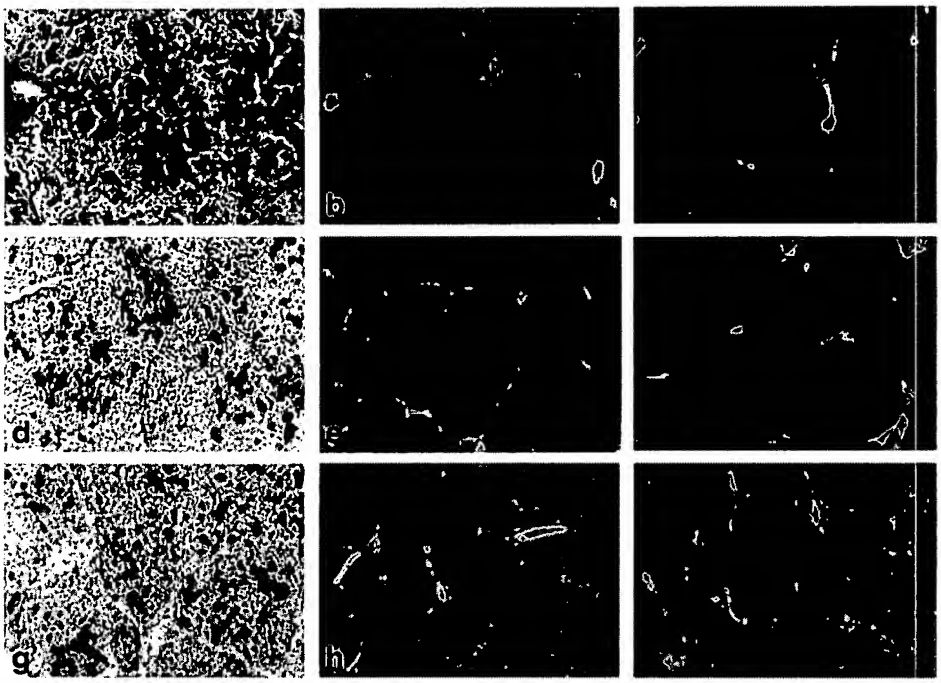

Figure 2 Histologic analysis of transduction and fibrosis in livers from normal rats (a–c) and rats treated with CCl_4 for 5 weeks (d–f) or 8 weeks (g–i). (a, d and g) β-Galactosidase staining 72 h after infusion of 3×10^{11} vp of Ad5βGal via the iliac vein (magnification, ×200). (b, e and h) Staining for collagenous protein using Sirius Red on paraffin sections (magnification, ×100). (c, f and I) Same as b, e and h, respectively, but stained with Masson's trichromic staining (magnification, ×100). Note the increase in collagenous material and distortion of liver architecture which is apparent by 5 weeks (e and f) and complete cirrhosis by 8 weeks (h and i) with characteristic bridging septa of collagen between central veins and portal tracts.

central collagen deposition (Figure 3). The degree of transduction with 3×10^{11} vp in animals after 2 or 4 weeks of biliary obstruction was about 10% (Figure 3). In spite of the evolution of the fibrotic process from 2 to 4 weeks of bile duct ligation, this percentage did not change considerably. The relatively low transduced area correlates with an increased degree of fibrosis, which may be, at least in part, explained by the fact that fewer cells were available in a given area to be transduced due to space-occupying extracellular fibrous tissue. In the bile duct ligation model, the main extracellular matrix components deposited are basement membrane collagen type IV, laminin and collagen type III, although collagen type I is also increased. These macromolecules form a continuous layer,[14] setting a barrier against the free adenoviral diffusion from the sinusoid into the surrounding hepatocytes. This may explain, in part, the differential distribution of ß-gal activity in liver tissue from non-cirrhotic animals (mainly around the central veins) and cirrhotic livers (mostly concentrated in midzonal regions) (compare Figure 2 panels d and g with a; and 3d and g with a). The level of transduction observed in these cirrhotic rat liver models might be significant since it has been shown for other diseases that there is a substantial resolution of the pathology when just a low percentage of targeted cells are successfully transduced[12,15] (see Figure 6).

The use of adenoviral vectors for gene therapy in liver cirrhosis will partly depend on successful delivery of vector to target tissue while minimizing leakage to extrahepatic tissues. The distribution of β-gal expression after peripheral vein injection was primarily to the liver in cirrhotic and in normal rats (Figure 4). The analyses of vector expression showed no β-gal staining in brain, heart, lung, testis or ileum in any of the experimental animals. However, β-gal expression was detected at low levels in the spleen and kidney of two of five cirrhotic animals. Previous studies in rodents have shown that approximately 90% of systemic vector is found in the liver of animals with normal function.[16,17] However, it was important to demonstrate that the distribution would not be significantly different in cirrhotic animals. Recently, and contrary to what is reported here, Nakamura *et al*[18] have demonstrated that adenovirus-mediated *Lac*Z gene expression was preferentially shown in septal cells, rather than hepatocytes in cirrhotic rats. However, they used only one dose of the vector (1.5×10^9 p.f.u.) and delivered it through the tail vein,[18] facts that might account for such a difference. On the other hand, a recent study by Nakatani *et al*[11] using 2×10^8 p.f.u./ml of Adex1C*alac*Z adenovirus as a reporter vector, demonstrated that 80% of cells in cirrhotic livers expressed the *LacZ* gene as compared with 40% in normal livers. Differences with our work might be accounted for by the fact that they used a different route of administration and cirrhosis was induced with thioacetamide. Concerning these issues, the lack of standardization to establish comparable dosages of vectors makes it extremely difficult to reach comparative conclusions on toxicity and efficacy. Recently, we have addressed this question[19] and conclude that it is almost impossible to compare dosages from study to study, as different researchers measure vector titers in different ways. This is true not only for adenoviral vectors, but also for any of the vectors in current use.

In this study, we used adenovectors prepared in a Good Manufacturing Practices (GMP) facility and the cer-

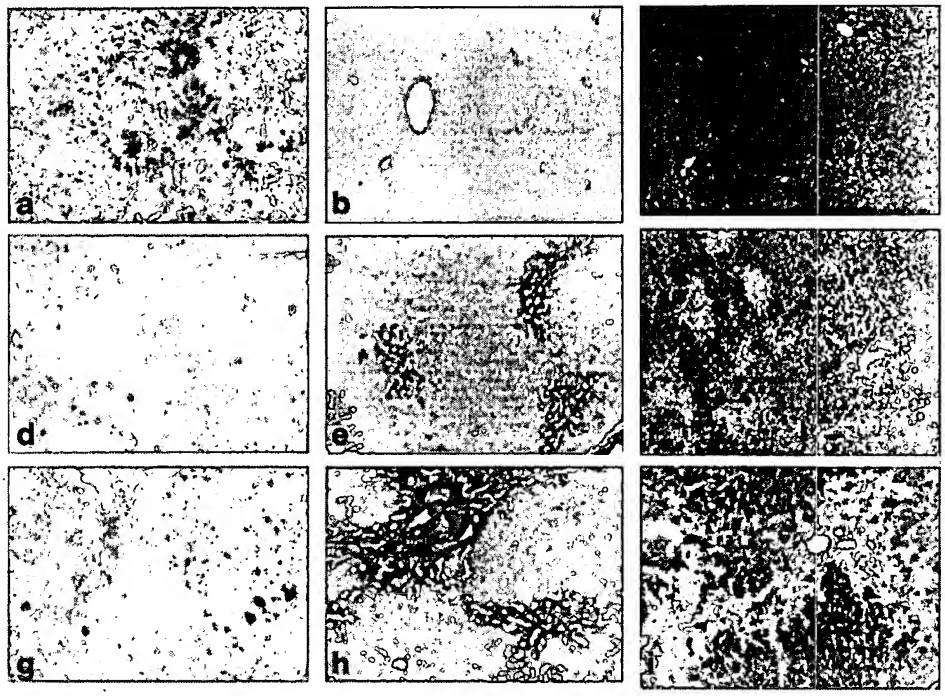

Figure 3 Histologic analysis of transduction and fibrosis in livers from normal rats (a–c) and rats treated by bile duct ligation for 2 weeks (d–f) or 4 weeks (g–i). (a, d and g) β-Galactosidase staining 72 h after infusion of 3 × 10^{11} vp of Ad5βGal via the iliac vein (magnification, ×200). (b, e and h) Staining for collagenous protein using Sirius Red on paraffin sections (magnification, ×200). (c, f and I) Represent the same as b, e and h, respectively, but stained with Masson's trichromic staining (magnification, ×100). Note the increase in collagenous material and distortion of liver architecture which is apparent by 2 weeks (e and f) and complete cirrhosis by 4 weeks (h and i) with characteristic bridging septa of collagen between central veins and portal tracts. Note the increase in collagenous material and bile duct proliferation in e and f, which is even more extensive in h and i.

tified quality of our Ad preparations was assured. Besides, we chose the iliac vein because it was the most efficient method, as compared with tail vein and intraperitoneal injection (data not shown). Also, and this is particularly important in cirrhosis, delivery via more invasive procedures such as to the portal vasculature, would be difficult in cirrhotic patients due to coagulopathy and poor wound healing making a more invasive procedure particularly dangerous. This approach is further supported by a recent report, which showed liver-directed gene transfer in non-human primates via the saphenous vein with nearly the same level of transduction in the liver as compared with portal vein infusion.[20]

Cirrhotic animals had elevated liver enzymes and these levels increased significantly during the first 48 h after adenoviral administration. Nonetheless, and concomitantly with evidence of significant exposure of the liver to adenovirus, these liver enzymes dropped between 72 to 96 h (Figure 5).

Although high mortality was observed at the 10^{12}–10^{13} dose levels, none of the animals died in either experimental model at the 10^{11} dose level despite efficient transduction at this level.

To determine whether this system could be useful in improving liver cirrhosis in an experimental model, we selected neutrophil collagenase (Matrix Metalloproteinase 8; MMP8) as a potential therapeutic reagent,[21] due to the fact that this enzyme preferentially hydrolyzes collagens faster than hepatic fibroblast collagenase. In human cirrhosis, collagen I is the most prominent extracellular protein and its abundant synthesis and deposition is responsible for alterations in hepatic architecture and consequent hemodynamic dysfunctions.

Here, we establish an experimental model of human secondary biliary cirrhosis by ligating and sectioning the common bile duct (BDL) in Wistar rats (n = 10). Liver biopsies were obtained from each rat before BDL ligation and at every step described after ligation. At the end of BDL (4 weeks) all rats had dramatic increases in liver fibrosis as compared with basal fibrosis (Figure 6) and were subjected to a bilio-digestive anastomosis to drain the clogged bile. This is a surgical procedure that imitates those performed in humans to alleviate bile-obstructive disorders by discontinuation of the harmful agent and re-establishment of bile flow. However, it is important to state that this procedure is therapeutically effective only in a small number of patients. Rats were left at this stage for 7 days. Hepatic fibrosis index and hepatic functional tests, however, continued to be elevated to similar extents in all animals. Then, five rats were injected via the iliac vein with 3 × 10^{11} vp/kg of AdMMP-8 along with five rats injected with a 3 × 10^{11} v/kg of irrelevant adenoviral vector (Ad-GFP) used as controls. The 10 rats were kept under careful surveillance for 10 more days, monitoring for overall health status and then killed. Levels of MMP8 protein expression in AdGFP and AdMMP8-transduced cirrhotic animals were quantified by ELISA using a polyclonal antibody against human neutrophil MMP8 that does not crossreact with MMP-1, -2, -3, -7, -9, -13 or MT1-MMP. Liver extracts from AdMMP8-transduced cirrhotic animals averaged 2.7 ng MMP8/ml. AdGFP-cirrhotic livers showed no detectable levels of recombinant MMP8.

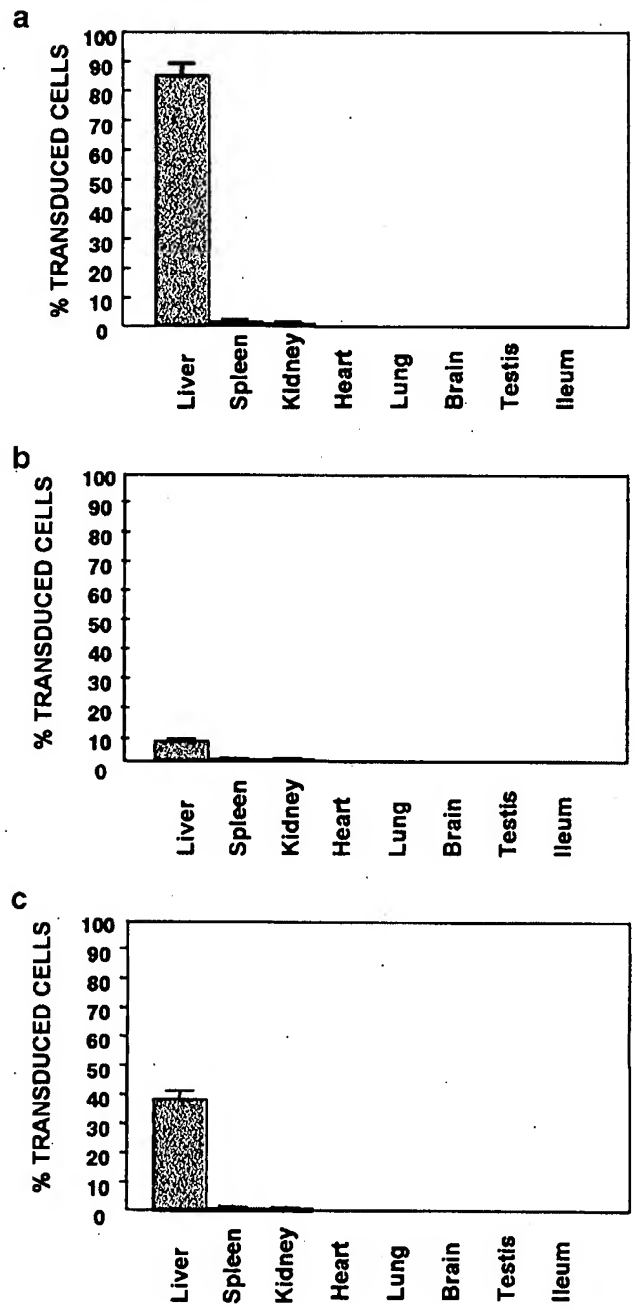

Figure 4 Biodistribution of the vector Ad5βGal 72 h after administration to rats in which cirrhosis was induced by bile duct ligation (BDL) (b), or chronic CCl_4 treatment (c). Five animals were studied in each model and each received 3×10^{11} total vp injected via the iliac vein. Transduction was detected by β-gal staining. (a) Normal animals.

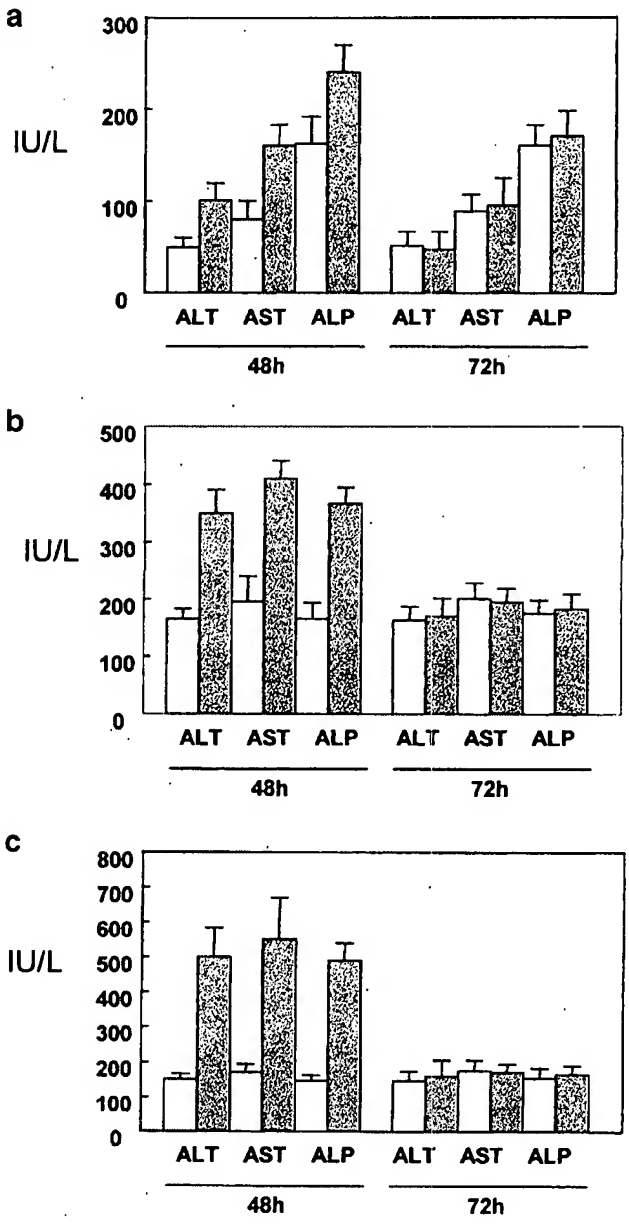

Figure 5 Comparison of HFTs in normal rats (a), with the BDL (b) or CCl_4 cirrhotic animals (c) , before □, and after ■, injection of Ad5βGal. Five animals were studied in each group. Blood was drawn from all animals and HFTs were performed. Then, vector dose (3×10^{11} total vp) was injected via the iliac vein and blood analysis was performed 48 and 72 h after comparing with previous HFTs from the same animal.

Importantly, a statistically significant decrease in fibrosis (43.9%; $P < 0.05$) was noted in rats injected with AdMMP8, but no decrease in the percentage fibrosis index was observed in the five animals injected with AdGFP. Also, an important decrease in total and direct bilirubins was noted, although ALT and AST did not diminished at the same extent. Ascitis decreased in AdMMP8-injected animals as well. Furthermore, extrahepatic cholestasis due to prolonged obstruction of bile flow in bile duct-ligated rats, resulted in important morphological and biochemical changes. They included an extensive proliferation of bile ducts in enlarged and dilated portal tracts, with inflammation and necrosis. Nonetheless, a salient improvement in these pathological changes was observed at the end of AdMMP8-treatment as determined by observations made by two different pathologists blinded to the study. It is clear then that the resulting extracellular turnover is facilitating recovery of hepatic lobule function.

The level of transduction achieved in the two rat cirrhosis models is encouraging for the further development of gene therapy approaches for human cirrhosis. Of particular importance, is the demonstration that cirrhotic ani-

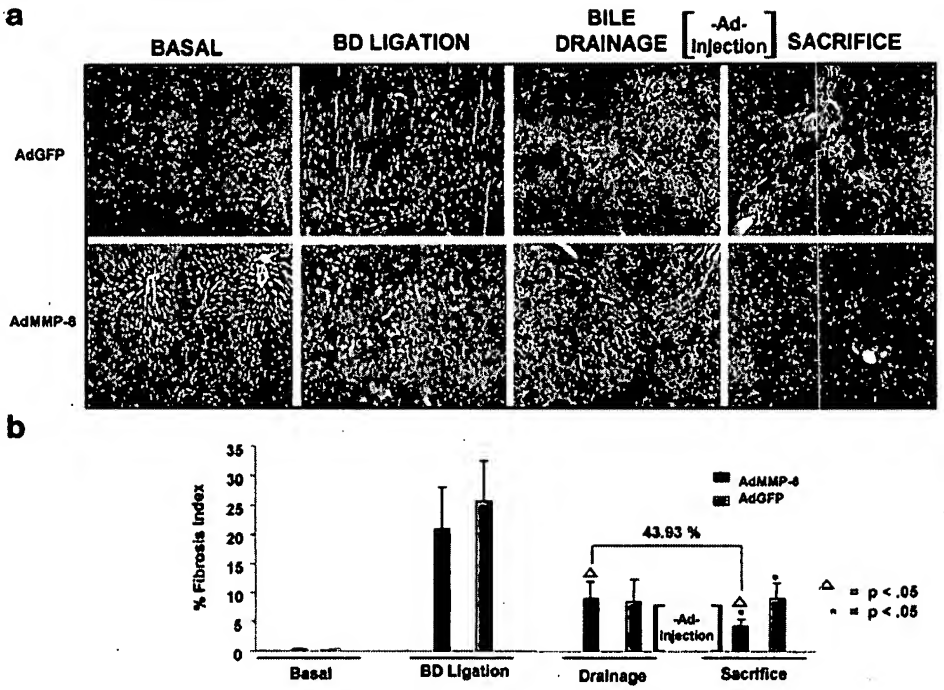

Figure 6 Proof of concept showing reversion of fibrosis by AdMMP8 in experimental secondary biliary cirrhosis. (a) Liver sections of cirrhotic rats after bile-duct ligation, bile drainage by biliodigestive anastomosis and AdMMP8 or AdGFP adenoviral vector injection. Masson trichromic staining (×100) showing cirrhotic nodules surrounded by thick fibrotic bands (in blue color) even at the end of treatment with AdGFP. On the other hand, animals treated with AdMMP8 show only thin fibrous bands consisting of connective tissue proteins. (b) Percentages of fibrous tissue deposition at every step and after AdGFP or AdMMP8 adenoviral vector infusion. Determinations of fibrous tissue were done in 20 random fields by an automated image analyzer. Values are presented as means ± standard deviation.

mals can tolerate doses of adenoviral vector necessary to achieve significant transduction efficiency in the absence of life-threatening liver toxicity. Although adenovectors may not be ideal for treatment of human liver disease, they may provide important tools for the evaluation of gene therapy strategies in rodent models of cirrhosis.

Materials and methods

Experimental models of liver cirrhosis

Wistar rats were housed and cared for according to National Institutes of Health guidelines in the animal facility of University of Guadalajara. For the first experimental model of cirrhosis, five rats per group were used. Rats weighing 150–200 g were anesthetized with ethylether and the common bile duct was exposed and ligated to induce fibrosis by total biliary obstruction (BDL rats) according to the method of Lee *et al.*[22] Briefly, animals underwent a 2-cm upper-midline abdominal incision below the xifoides appendix, the extrapancreatic common bile duct was identified and double ligated with 4/0 silk (Ethicon; Johnson and Johnson, Mexico City, Mexico) and transected between the ligatures. Subsequently, the abdomen was closed in one layer with continuous 4/0 silk. These rats were kept for 4 weeks and they were given free access to food and water throughout the experimental period. Five rats were sham operated at the same time and used as controls. For the experiments which aimed to show proof of concept on fibrosis revertion, at least five rats were used for experiment. That is, 10 rats were ligated as described before for 4 weeks and a liver biopsy was obtained from each animal before and after the surgical procedure. Then, a biliodigestive anastomosis was performed on each animal to drain the clogged bile and re-establish bile flow in order to eliminate the injurious fibrogenic cause. Animals were left at this stage for 7 days and liver biopsy was also taken. At this point, five animals received either 3×10^{11} vp/kg of AdMMP8 or AdGFP and 10 days later were killed obtaining the fourth and final liver biopsy for each animal. Fibrosis index in multiple liver biopsies from animals at different stages were then carried out. Similarly, blood was obtained from each rat to carry out hepatic functional tests.

The second experimental model consisted of animals undergoing chronic intoxication with CCl_4.[23] Briefly, animals weighing 50–80 g received three doses a week via i.p. of a mixture 1:6 of CCl_4-mineral oil for the first week, the 2nd week the ratio was 1:5, 3rd week 1:4, and 4th–8th week the ratio was 1:3. Control rats were pair fed and injected similarly with vehicle only.

Adenoviral vectors

The Ad5βGal vector used here is a first generation E1- and E3-deleted replication-defective adenovirus vector previously described.[24] The vector was produced at the Baylor College of Medicine Gene Vector Laboratory under Good Laboratory Practice conditions, checked for general sterility and was free of contaminants such as endotoxin, mycoplasma, *in vitro* adventitious virus and replication-competent adenovirus (RCA). Thus, the vector was titered (1×10^{13} vp/ml from lot No. 01496AbgalA) and characterized as described[24] and had a vector particle (v.p.) to infectious unit (IU) ratio of ≤10 which makes it

suitable for controlled trials. Escalating doses were injected via iliac vein diluted in 250 μl of 10 mM Tris-HCl, pH 8.0, 2 mM, $MgCl_2$ and 4% sucrose. All rats used in both experimental cirrhosis models weighed approximately 250 g at the time of Ad5βGal injection. For the experiments to check for fibrosis revertion, AdMMP8 was generated as described before by our group.[21] Briefly, pAdHM2-MMP8 was transfected into 293 cells. pAdHM2-MMP8 was constructed by an *in vitro* ligation method of the MMP-8 cDNA in a replication-defective dE1, dE3 adenoviral plasmid.[25] This and AdGFP were also titered and characterized as described above.

In situ β-gal assay in whole tissue preparations

The β-gal activity was determined 72 h after Ad5βGal injection. To monitor the degree of transduction of different organs, liver, brain, heart, ileum, testis, lung, kidney and spleen were obtained and immediately cut in thin slices using a sterile scalpel. These manipulations were quickly performed on ice and the tissue slices were placed in 24-well tissue culture plates and washed three times with cold PBS and fixed for 15 min with 10% buffered-formalin at 4°C. After fixation, tissue slices were washed twice with cold PBS and X-gal staining was performed. All reactions were carried out at pH 8.5 to avoid endogenous galactosidase activity. X-gal reaction solutions contained 1 mg/ml X-gal, 100 mM $K_3Fe(CN)_6$, 100 mM $K_4Fe(CN)_6$, 1 M $MgCl_2$, 2% NP-40 and 1% sodium desoxicholate. Exposure of tissues was performed in the dark at 4°C for 16–18 h and then tissues were carefully washed with PBS and preserved in 10% buffered-formalin. For histological analyses, tissues were embedded in paraffin, sectioned and mounted on glass slides.[26]

Evaluation of β-gal *activity in tissue section preparations*

Tissues were cut in 5–6-mm^3 squares and embedded in Tissue-Tek OCT compound (Miles, Elkhart, IN, USA), frozen at –30°C and cut in a cryostat to obtain 8-μm thin sections. These sections were placed on methacrylxypropyl-trimethoxisilane-treated glass slides and fixed with 10% buffered-formalin at room temperature for 15–30 min. After this, sections were processed as described above. Slides were subsequently washed in PBS, counterstained with Neutral Red and coverslipped with organic mounting media after standard dehydration in alcohol.

The average number of transduced cells was obtained by evaluating 50 different microscopic areas per rat liver at a magnification of ×200 by computer-assisted morphometric analysis using a Leica Quantimet Q570 image processor (Cambridge Instruments, Cambridge, MA, USA).

Histological staining for fibrous tissue and immunohistochemistry

To monitor the evolution and reversion of the fibrotic process taking place in the liver of cirrhotic animals, liver tissue blocks were fixed in 10% buffered-paraformaldehyde and embedded in paraffin. Sections (10 μm) were cut and stained with Picrosirius red solution at pH 4.0. Sirius red is a specific dye for collagenous proteins.[27] The same tissue sections were counterstained with Fast green dye which has affinity for non-collagenous protein. Parallel tissue sections were stained with Masson's trichromic staining to visualize collagen deposits and characteristic proliferation of bile ducts in the bile duct-ligated rats. Evaluation of tissue area occupied by fibrosis was performed using the same image analysis procedure described above.

For immunohistochemistry, liver sections were mounted in silane covered slides, deparaffinized and endogenous activity of peroxidase was quenched with 3% H_2O_2 in absolute methanol. Liver sections were incubated overnight at room temperature with mouse antibodies against human $\alpha_v\beta_5$ integrin (GIBCO-BRL, Rockville, MD, USA) diluted 1/600 in PBS. Bound antibodies were detected with peroxidase-labeled rabbit polyclonal antibodies against mouse immunoglobulins and diaminobenzidine, and counterstained with hematoxylin. For quantification, 10 random fields of intralobular and periportal areas were evaluated at ×320 magnification. Immunohistochemical-positive and -negative cells were counted by an automated image analyzer (Qwin; Leica).

Quantification of MMP8 secretion by ELISA

Liver homogenates were obtained as previously described[8] and total MMP8 was quantified using a Biotrak ELISA assay according to the manufacturer's instructions. Anti-human MMP8 Biotrak ELISA system was obtained from Amersham Pharmacia Biotech (Piscataway, NJ, USA).

Hepatic function tests (HFTs)

Blood was drawn from animals before and after adenovirus administration and serum transaminases ALT, AST, bilirubins and alkaline phosphatase were determinated in an automated Sincron-7 machine at Hospital Civil de Guadalajara.

Statistical analyses

Results are expressed as mean ± s.d. Student's *t* test was used. $P < 0.05$ was considered to indicate a significant difference between groups.

Acknowledgements

This work was supported in part by a grant from CONACyT No. 28832-M to Juan Armendariz-Borunda. The authors are indebted to Dr Guillermo Grijalva and Jose M Vera for their invaluable assistance.

References

1 Olaso E, Friedman SL. Molecular regulation of hepatic fibrogenesis. *J Hepatol* 1998; **29**: 836–847.
2 Armendariz-Borunda J, Seyer JM, Kang AH, Raghow R. Regulation of TGFβ gene expression in rat liver intoxicated with carbon tetrachloride. *FASEB J* 1990; **4**: 215–221.
3 Terao R *et al*. Supression of proliferation cholangitis in a rat model with direct adenovirus-mediated retinoblastoma gene transfer to the biliary tract. *Hepatology* 1998; **28**: 605–612.
4 Lusky M *et al*. *In vitro* and *in vivo* biology of recombinant adenovirus vectors with E1, E1/E2A, or E1/E4 deleted. *J Virol* 1998; **72**: 2022–2032.
5 Worgall S, Wolff G, Falck-Pedersen E, Crystal RG. Innate immune mechanisms dominate elimination of adenoviral vectors following *in vivo* administration. *Hum Gene Ther* 1997; **8**: 37–44.
6 Drazan KE *et al*. Hepatic function is preserved following liver-directed, adenovirus-mediated gene transfer. *J Surg Res* 1995; **59**: 299–304.
7 Lieber A *et al*. The role of Kupffer cell activation and viral gene

expression in early liver toxicity after infusion of recombinant adenovirus vectors. *J Virol* 1997; **71**: 8798–8807.
8 Salgado S *et al.* Liver cirrhosis is reverted by urokinase-type plasminogen activator gene therapy. *Mol Ther* 2000; **2**: 545–551.
9 Rudolph KL *et al.* Inhibition of experimental liver cirrhosis in mice by telomerase gene delivery. *Science* 2000; **287**: 1253–1258.
10 Hecht N *et al.* Hyper-IL-6 gene therapy reverses fulminant hepatic failure. *Mol Ther* 2001; **3**: 683–687.
11 Nakatani T *et al.* Assessment of efficiency and safety of adenovirus-mediated gene transfer into normal and damaged murine livers. *Gut* 2000; **47**: 563–570.
12 Ramm GA *et al.* Contribution of hepatic parenchymal and nonparnchymal cells to hepatic fibrogenesis in biliary atresia. *Am J Pathol* 1998; **153**: 527–535.
13 Kossakowska AE *et al.* Altered balance between matrix metalloproteinases and their inhibitors in experimental biliary fibrosis. *Am J Pathol* 1998; **53**: 1895–1902.
14 Desmouliere A *et al.* Extracellular matrix deposition, lysyl oxidase expression and myofibroblastic differentiation during the initial stages of cholestatic fibrosis in rat. *Lab Invest* 1997; **76**: 765–778.
15 Zern MA, Kresina TF. Hepatic drug delivery and gene therapy. *Hepatology* 1997; **25**: 484–491.
16 de Roos WK *et al.* Isolated-organ perfusion for local gene delivery: efficient adenovirus-mediated gene transfer into the liver. *Gene Therapy* 1997; **71**: 55–62.
17 Ferry N, Heard JM. Liver-directed gene transfer vectors. *Hum Gene Ther* 1998; **9**: 1975–1981.
18 Nakamura T, Akiyoshi H, Saito I, Sato K. Adenovirus-mediated gene expression in the septal cells of cirrhotic rat livers. *J Hepatol* 1999; **30**: 101–106.
19 Aguilar LK *et al.* A prescription for gene therapy. *Mol Ther* 2000; **1**: 385–388.
20 Sullivan DE *et al.* Liver-directed gene transfer in non-human primates. *Hum Gene Ther* 1997; **8**: 1195–1206.
21 Siller-Lopez F *et al.* Truncated active matrix metalloproteinase-8 gene expression in HepG2 cells is active against native type I collagen. *J Hepatol* 2000; **33**: 758–763.
22 Lee SS *et al.* Hemodynamic characterization of chronic bile duct-ligated rats: effect of pentobarbital sodium. *Am J Physiol* 1986; **251**: 176–180.
23 Armendariz-Borunda J, Katayama K, Seyer JM. Transcriptional mechanisms of type I collagen gene expression are differentially regulated by IL-1β TNF-α and TGFβ in Ito cells. *J Biol Chem* 1992; **267**: 14316–14321.
24 Nyberg-Hoffman C *et al.* Sensitivity and reproducibility in adenoviral infectious titer determination. *Nat Med* 1997; **3**: 808–811.
25 Mizuguchi H, Kay MA. Efficient construction of a recombinant adenovirus vector by an improved *in vitro* ligation method. *Hum Gene Ther* 198; **9**: 2577–2583.
26 Weiss DJ, Liggitt D, Clark JG. *In situ* histochemical detection of β-galactosidase activity in lung: assessment of X-gal reagent in distinguishing *lacZ* gene expression and endogenus β-galactosidase activity. *Hum Gene Ther* 1997; **8**: 1545–1554.
27 Lopez-De Leon A, Rojkind M. A simple micromethod for collagen and total protein determination in formalin-fixed paraffin-ambedded sections. *J Histochem Cytochem* 1985; **33**: 737–743.